

AN ALTERNATIVE PROCESS INCLUDING SAND CASTING, FORGING AND
HEAT TREATMENT OF 30MM DIAMETER X48CrMoV8-1 TOOL STEEL

A THESIS SUBMITTED TO
THE GRADUATE SCHOOL OF NATURAL AND APPLIED SCIENCES
OF
MIDDLE EAST TECHNICAL UNIVERSITY

BY

İHSAN ALP AĞACIK

IN PARTIAL FULFILLMENT OF THE REQUIREMENTS
FOR
THE DEGREE OF MASTER OF SCIENCE
IN
MECHANICAL ENGINEERING

SEPTEMBER 2012

Approval of the thesis:

**AN ALTERNATIVE PROCESS INCLUDING SAND CASTING FORGING
AND HEAT TREATMENT OF 30MM DIAMETER X48CrMoV8-1 TOOL
STEEL**

submitted by **İHSAN ALP AĞACIK** in partial fulfillment of the requirements for
the degree of **Master of Science in Mechanical Engineering Department, Middle
East Technical University** by,

Prof. Dr. Canan ÖZGEN
Dean, Graduate School of **Natural and Applied Science**

Prof. Dr. Süha ORAL
Head of Department, **Mechanical Engineering**

Prof. Dr. Mustafa İlhan GÖKLER
Supervisor, **Mechanical Engineering Dept.**

Prof. Dr. Ali KALKANLI
Co-Supervisor, **Metallurgical and Materials Engineering Dept.**

Examining Committee Members:

Prof. Dr. Metin AKKÖK
Mechanical Engineering Dept.

Prof. Dr. Mustafa İlhan GÖKLER
Mechanical Engineering Dept.

Prof. Dr. Ali KALKANLI
Metallurgical and Materials Engineering Dept.

Prof. Dr. Can COĞUN
Mechanical Engineering Dept.

Prof. Dr. Haluk DARENDELİLER
Mechanical Engineering Dept.

Date: 13.09.2012

I hereby declare that all information in this document has been obtained and presented in accordance with academic rules and ethical conduct. I also declare that, as required by these rules and conduct, I have fully cited and referenced all materials and results that are not original to this work.

Name, Last Name : İHSAN ALP AĞACIK

Signature :

ABSTRACT

AN ALTERNATIVE PROCESS INCLUDING SAND CASTING, FORGING AND HEAT TREATMENT OF 30MM DIAMETER X48CrMoV8-1 TOOL STEEL

AĞACIK, İhsan Alp

M.Sc., Department Mechanical Engineering

Supervisor: Prof. Dr. Mustafa İlhan GÖKLER

Co-Supervisor: Prof. Dr. Ali KALKANLI

September 2012, Pages 119

Shear blades are mostly made of cold-work tool steels and manufactured by rolling process. Rolling process is performed not only for forming the tool but also for improving the mechanical properties.

In this study, an alternative method, involving sand casting, hot forging and heat treatment processes to manufacture the shear blades, has been proposed. In the proposed method, plastic deformation will be carried out by means of forging instead of rolling. The material has been selected as X48CrMoV8-1. For both of casting and forging processes, simulations have been conducted by using Computer Aided Engineering Software. According to the results of casting process simulation, the billets have been poured. These billets have been soft annealed first and then taken as the initial raw material for the forging process. After the forging process, quenching and tempering processes have been applied.

The specimens have been taken as cast, as forged and as tempered and the microstructural analysis and mechanical tests have been performed on these. The same tests and analysis have been repeated for a commercially available shear blade sample which is manufactured by rolling. All these investigations have shown that the properties of the forged shear blade are very similar to the rolled shear blade. Therefore, the new proposed method has been verified to be used as an alternative manufacturing method for the cold-work tool steel shear blades.

Key words: Forging, Sand Casting, Shear Blade, Tool Steel

ÖZ

30 MM ÇAPINDAKİ X48CrMoV8-1 TAKIM ÇELİĞİNİN KUM DÖKÜM, DÖVME VE ISIL İŞLEM İÇEREN ALTERNATİF ÜRETİM YÖNTEMİ

AĞACIK, İhsan Alp

Yüksek Lisans, Makine Mühendisliği Bölümü

Tez Yöneticisi: Prof. Dr. Mustafa İlhan GÖKLER

Ortak Tez Yöneticisi: Prof. Dr. Ali KALKANLI

Eylül 2012, Pages 119

Kesici bıçaklarının üretiminde genellikle soğuk iş takım çelikleri kullanılır ve bu bıçaklar çoğunlukla hadde mamulu olurlar. Haddelenme işlemi, takım çeliği kesici bıçaklarda sadece şekillenmek için değil, aynı zamanda mekanik özelliklerin iyileştirilmesi yönünde de çok etkilidir.

Bu çalışmada, kesici bıçaklarının üretilmesinde kuma döküm, dövme ve ısıl işlemi içeren alternatif bir yöntemi önerilmiştir. Bu önerilen yöntem ile, şekillendirme haddelenmek yerine dövülerek gerçekleştirilmektedir. Bu yöntemde kullanılacak olan soğuk iş takım çeliğinin kompozisyonu X48CrMoV8-1 olarak seçilmiştir. Döküm ve dövme işlemleri için sırasıyla Sonlu Eleman ve Sonlu Hacim Metodları kullanılarak benzetim yapılmıştır. Benzetim sonuçlarından yararlanılarak, öncelikle kütükler dökülmüştür. Sonrasında, kütükler dövme işlemine hazır hale getirilmek için tavlanmıştır. Tavlanmış olan kütükler tekrar ısıtılarak, sıcak dövülmüştür. En son yağda su verilerek temperlenmiştir.

Üretim sırasında, kaba döküm, dövülmüş ve temperlenmiş olarak alınan numuneler üzerinde mikroyapı incelemesi ve mekanik testler gerçekleştirilmiştir. Bu incelemeler ve testler, endüstride kullanılan hadde mamülü aynı kompozisyondaki soğuk iş takım çeliği için de gerçekleştirilmiştir. İncelemelerin ve karşılaştırmaların sonucu olarak, dövülerek üretilen kesici bıçakların, hadde mamülü olanlarla

neredeysi aynı özelliklere sahip olduđunu görölmüştür. Sonuç olarak, kesici bıcağların üretiminde önerilen yeni yöntem başarılı olmuştur.

Anahtar Sözcükler: Dövme, Kumda Döküm, Kesici Bıçak, Takım Çeliđi

To my mother,

ACKNOWLEDGEMENTS

First of all I would like to imply my deepest appreciation to my supervisor Prof. Dr. Mustafa İlhan GÖKLER and to my co-supervisor Ali Kalkanlı for precious encouragement, guidance and insight throughout the research.

Another important academic support given by Dr. Önder ORHANER should be specified gratefully, especially for practicable ideas and consults about the experiments.

Necdet AKDAŞ, who is head of the AKDAS Foundry, is appreciated with deepest thanks for assists and advices for experiments.

I would also like to express my thanks to my friends who are Simge Altındemir, Kutay Gürtürk, Umut Afşar, Ümit Akçaoğlu and Onur Demirel for morale and courage given by them.

Special thanks go to my colleagues, Apak Aysal, Nilüfer Çağlayık, Gülsüm Çakır, Seda Erkıılıç and Haydar Recep.

Finally, the biggest and the most sincere gratitude should be expressed to my mother and sister for every success in my life.

TABLE OF CONTENTS

ABSTRACT	iv
ACKNOWLEDGEMENTS	viii
TABLE OF CONTENTS	ix
LIST OF FIGURES	xii
LIST OF TABLES	iii
CHAPTERS1	
1. INTRODUCTION	1
1.1. Shearing Process and Types of Shears	1
1.2. Shear Blades	3
1.3. Tool Steels	3
1.4. Production of Tool Steel	5
1.5. Some Previous Previous Studies.....	5
1.6. Scope of the Thesis	6
2. CASTING AND FORGING PROCESSES	8
2.1. Casting Process	8
2.1.1. Types of Casting Processes	8
2.1.2. Casting Process Selection	9
2.1.3. The Operations of Sand Casting	10
2.1.4. Heat Transfer in Sand Mold.....	11
2.1.5. Estimation of the Solidification time	11
2.1.6. Solidification and Microstructure of Tool Steel.....	14
2.2. Tool Steel Forging	17
2.2.1. Forging Process	17
2.2.2. Classification of Forging Process	17
3. DESIGN AND ANALYSIS OF SAND CASTING OF TOOL STEEL SHEAR BLADE SAMPLE.....	22

3.1. Introduction.....	22
3.2. Alloy Composition Selection.....	23
3.3. Methodology and Finite Volume Analysis of Sand Casting	25
3.3.1. Modeling the Billet and the Gating System	25
3.3.2. Defining the Sand Mold, Importing the Billets and the Gating System Geometries	27
3.3.3. Assigning the Material Properties.....	27
3.3.4. Finite Volume Simulation for Casting	29
3.4. Discussion on the Simulation Results for Casting.....	34
4. THE EXPERIMENTAL STUDY OF SAND CASTING.....	35
4.1. Molding.....	35
4.2. Melting and Pouring	40
4.3. Shake Out and Cleaning	43
4.4. Initial Heat Treatment.....	45
5. DESIGN AND ANALYSIS OF FORGING OF TOOL STEEL SHEAR BLADE SAMPLE.....	46
5.1. Introduction.....	46
5.2. Billet Design	46
5.3. Simulation Process Parameters for Finite Element Method	51
5.3.1. Defining the Process Type, Importing Forging Dies and Modeling of Billet.....	51
5.3.2. Assigning the Material Properties of Dies and Billet.....	51
5.3.3. Initial Temperature of Billet and Dies	53
5.3.4. Defining the Coefficient of Friction.....	53
5.3.5. Defining the Press in Finite Element Program.....	53
5.4. Analysis of Tool Steel Forging Process by Finite Element Method.....	55
5.5. Simulation Results of Forging	56
6. MANUFACTURING OF TOOL STEEL SHEAR BLADE SPECIMENS AND FORGING PROCESS.....	76
6.1. Introduction.....	76
6.2. Preparation for the Forging Operation.....	76
6.3. Experimentation of the Tool Steel Forging Process	79

6.4. Results of the Experiments	83
6.5. Quenching and Tempering of the Billets	85
7. MECHANICAL TESTS AND MICROSTRUCTURAL ANALYSIS	89
7.1. Mechanical Tests	89
7.1.1. Hardness Test	89
7.1.2. Charpy Impact Test	92
7.2. Microstructural Analysis.....	95
7.2.1. As Annealed Microstructure	95
7.2.2. As Forged Microstructure	97
7.2.3. As Quenched and Tempered Microstructure	100
8. CONCLUSIONS AND FUTURE WORK	103
8.1. General Conclusions	103
8.2. Future Works	104
REFERENCES.....	106
APPENDICES	109
A. TECHNICAL INFORMATION OF 10 MN (1000 TON) SMERAL MECHANICAL PRESS.....	109
B. TECHNICAL DRAWING OF THE PATTERN	111
C. TECHNICAL DRAWINGS OF THE DIE SET	113

LIST OF FIGURES

FIGURES:

Figure 1.1 Bench Shear	2
Figure 1.2 Guillotine	2
Figure 1.3 Shear Blade Samples	3
Figure 2.1 Classification of Casting Processes According to Type of Molding.....	9
Figure 2.2 Flow of a typical sand casting process	10
Figure 2.3 Three Zones of Freezing in a Casting.....	15
Figure 2.4 The block segregation on a hot work tool steel.	16
Figure 2.5 Schematic of a Mechanical Forging with Eccentric Drive.....	19
Figure 2.6 Schematic of a Hydraulic Press	20
Figure 2.7 Schematic of Open Die Forging	20
Figure 2.8 Schematic of Close Die Forging	21
Figure 3.1 Flowchart of the Progress in Chapter 3	22
Figure 3.2 Isometric and Top View of the 3D Model of the Pattern	26
Figure 3.4 Variation of the Fraction of Solid with Temperature for X48CrMoV8-1	27
Figure 3.3 Variation of Density with Temperature for X48CrMoV8-1	28
Figure 3.5 Variation of Specific Heat Capacity with Temperature for X48CrMoV8-1	28
Figure 3.6 Variation of Yield Strength with Temperature for X48CrMoV8-1	29
Figure 3.7 Dimensions of Sand Mold	29
Figure 3.8 Meshing of the Billets and the Gating System	30
Figure 3.9 Velocity of Molten Metal in the Mold.....	31

Figure 3.10 Fraction Liquid with the Elapsed Time during Solidification	32
Figure 3.11 Simulation Result for the Porosity.....	33
Figure 4.1 The Pattern of the Gating System in Lowest Flask	36
Figure 4.2 The Filling of the Drag with Sand	36
Figure 4.3 The Patterns of the Billets Placed in the Middle Flask.....	37
Figure 4.4 Molding of Cope (First Stage).....	37
Figure 4.5 Formation of the Gas Release Holes	38
Figure 4.6 Molding of Cope.....	38
Figure 4.7 Painted Cavity of Gating System (Lowest Flask)	39
Figure 4.8 The view of the Cope after Painting	39
Figure 4.9 The induction furnaces at Akdas Casting	40
Figure 4.10 Emission spectrometer and its analyzing chamber	41
Figure 4.11 Pouring of tool steel into the mold	43
Figure 4.12 Specimens after shakeout	44
Figure 4.13 The Surface Cleaning of the Billets by Grinding	44
Figure 4.14 Electrical Box Type Furnace	45
Figure 5.1 Schematic Views of the Specimens According to Their Aspect Ratios .	47
Figure 5.2 Ram Adjustment Mechanism of the Forging Press	47
Figure 5.3 Configurations of the modular die set	50
Figure 5.4 Illustration of Crank Press Schematic	54
Figure 5.5 Axi-symmetric Problem Set Up for the Finite Element Analysis	54
Figure 5.6 Orientation of the Dies and Billets Prior to Forging	55
Figure 5.7 Variation of Die Force with Respect to Time for Billet Group No:1	58
Figure 5.8 Effective Plastic Strain for Billet Group No:1.....	58
Figure 5.9 Temperature Distribution for Billet Group No:1.....	59

Figure 5.10	Variation of Die Force with Respect to Time for Billet Group No: 2 ...	59
Figure 5.11	Effective Plastic Strain for Billet Group No:2.....	60
Figure 5.12	Temperature distribution for Billet Group No:2.....	60
Figure 5.13	Variation of Die Force with Respect to Time for Billet Group No: 3 ...	61
Figure 5.14	Effective Plastic Strain for Billet Group No:3.....	61
Figure 5.15	Temperature Distribution for Billet Group No:3.....	62
Figure 5.16	Variation of Die Force with Respect to Time for Billet Group No: 4 ...	62
Figure 5.17	Effective Plastic Strain for Billet Group No:4.....	63
Figure 5.18	Temperature Distribution for Billet Group No:4.....	63
Figure 5.19	Variation of Die Force with Respect to Time for Billet Group No: 5 ...	64
Figure 5.20	Effective Plastic Strain for Billet Group No:5.....	64
Figure 5.21	Temperature Distribution for Billet Group No:5.....	65
Figure 5.22	Variation of Die Force with Respect to Time for Billet Group No: 6 ...	65
Figure 5.23	Effective Plastic Strain for Billet Group No:6.....	66
Figure 5.24	Temperature Distribution for Billet Group No:6.....	66
Figure 5.25	Variation of Die Force with Respect to Time for Billet Group No: 7 ...	67
Figure 5.26	Effective Plastic Strain for Billet Group No:7.....	67
Figure 5.27	Temperature Distribution for Billet Group No:7.....	68
Figure 5.28	Variation of Die Force with Respect to Time for Billet Group No: 8 ...	68
Figure 5.29	Effective Plastic Strain for Billet Group No:8.....	69
Figure 5.30	Temperature Distribution for Billet Group No:8.....	69
Figure 5.31	Variation of Die Force with Respect to Time for Billet Group No: 9 ...	70
Figure 5.32	Effective Plastic Strain for Billet Group No:9.....	70
Figure 5.33	Temperature Distribution for Billet Group No:9.....	71
Figure 5.34	Variation of Die Force with Respect to Time for Billet Group No: 10 .	71

Figure 5.35 Effective Plastic Strain for Billet Group No:10.....	72
Figure 5.36 Temperature Distribution for Billet Group No:10.....	72
Figure 5.37 Variation of Die Force with Respect to Time for Billet Group No: 11 .	73
Figure 5.38 Effective Plastic Strain for Billet Group No:11.....	73
Figure 5.39 Temperature Distribution for Billet Group No:11.....	74
Figure 5.40 Variation of Die Force with Respect to Time for Billet Group No: 12.	74
Figure 5.41 Effective Plastic Strain for Billet Group No:12.....	75
Figure 5.42 Temperature Distribution for Billet Group No:12.....	75
Figure 6.1 Turning Operation of the Specimens.....	77
Figure 6.2 Turned Specimens	77
Figure 6.3 Lower Die Assembly of the Forging Press.....	80
Figure 6.4 a) Billet at the Output of Furnace b) The Temperature Measurement of the Billet.....	80
Figure 6.5 a) Preheating of the Dies b) The Temperature Measurement of the Dies	81
Figure 6.6 Billet Just After Forging	82
Figure 6.7 Grouped Billets After Forging.....	82
Figure 6.8 CCT Diagram for X48CrMoV8-1 [24].....	86
Figure 6.9 Oil Quenching of the Forged Billets.....	87
Figure 6.10 Variation of Hardness with Tempering Temperature for X48CrMoV8-1	88
Figure 7.1 Rockwell Hardness Tester	90
Figure 7.2 Positions of the Indentations from the Ground Side of the Billet.....	90
Figure 7.3 V- Notch Geometry	92
Figure 7.4 V- Notch Machining by Electrical Discharge Machining	93
Figure 7.5 Charpy V- Notch Specimen.....	93

Figure 7.6 X48CrMoV8-1, Annealed, 10% Nital, x100	96
Figure 7.7 X48CrMoV8-1, Annealed, 10% Nital, x400	96
Figure 7.8 AISI W4 water-hardening tool steel, annealed, 4% picral. 1000× [34] ..	97
Figure 7.9 X48CrMoV8-1, Forged, 10% Nital, x100	98
Figure 7.10 X48CrMoV8-1, Forged, 10% Nital, x200	99
Figure 7.11 AISI L1, As-Rolled, Containing Pearlite and a Grain-Boundary Cementite Network. Boiling Alkaline Sodium Picrate. X100 [34]	99
Figure 7.12 X48CrMoV8-1, Quenched and Tempered, 15% HCl and then 10% Nital, x50	101
Figure 7.13 X48CrMoV8-1, Quenched and Tempered, 15% HCl and then 10% Nital, x100	101
Figure 7.14 Uddeholm Viking Rolled Sample, As Quenched and Tempered, 15% HCl and then 10% Nital, x400	102
Figure A.1 Smeral 10 MN Mechanical Press in METU-BILTIR Center Forging Research and Application Laboratory	109
Figure B.1 Technical Drawing of the Pattern	109
Figure C.1 Technical Drawing of the Upper Die	114
Figure C.2 Technical Drawing of the Lower Die	115
Figure C.3 Technical Drawing of the Insert with 10 mm Height	116
Figure C.4 Technical Drawing of the Insert with 20 mm Height	117
Figure C.5 Technical Drawing of the Insert with 30 mm Height	118
Figure C.6 Technical Drawing of the Insert with 40 mm Height	119

LIST OF TABLES

TABLES:

Table 1.1 Basic Types of Tool Steel and Corresponding AISI Grades	4
Table 3.1 Some Examples for Cold-Work Tool Steels.....	23
Table 3.2 Chemical Composition of X48CrMoV8-1-1	24
Table 3.3 Some Properties of the Billets and the Gating System	30
Table 4.1 Amount of Ferroalloy Addition During Melting of Tool Steel	42
Table 4.2 Results of the Spectral Analysis at Various Stages	42
Table 5.1 Table of Initial and Final Dimensions of the Specimens.....	48
Table 5.2 Modular Die Set Configurations.....	49
Table 5.3 Some of the Mechanical Properties of X48CrMoV8-1 for Various Hardness Values [24].....	52
Table 5.4 Some Other Physical Properties of X48CrMoV8-1 at Various Temperatures [24].....	52
Table 5.5 Details Regarding the Meshing.....	56
Table 6.1 Billet Dimensions After Turning	78
Table 6.2 Measures of the Forging Process	83
Table 6.2 Measures of the Forging Process (Cont'd)	84
Table 6.3 Approximate Hardness Values Before Tempering of X48CrMoV8-1 for Different Austenitizing Temperatures [24]	86
Table 7.1 Hardness of Billets.....	91
Table 7.2 Hardness of Billets as Annealed Condition	94

CHAPTER 1

INTRODUCTION

1.1. Shearing Process and Types of Shears

Shearing is a process which cuts a material without any chips. Preparing the material for subsequent operation by means of shearing is quite often. It is possible to produce accurate and precise finish product by shearing.

In shearing process the blade goes down and pushes the work piece, the metal starts flowing plastically. The clearance between two tools is so small that the deformation occurs as highly localized shear. Sometimes the upper blade is inclined with respect to lower die. This geometry reduces the risk of wedging between dies [1] .

There are many types of shears used to cut sheet metals. As shown in Figure 1.1, bench shear [2] is used for cutting pieces for small to medium size pieces. However, the expectations from the quality of end product should not be so high. This device is mainly used for rough cutting operations.

Guillotine is a machine which is also called “squaring shear” or “power shear”. As shown in Figure 1.2, moving blade comes down to a fixed blade to shear the material.



Figure 1.1 Bench Shear [2]

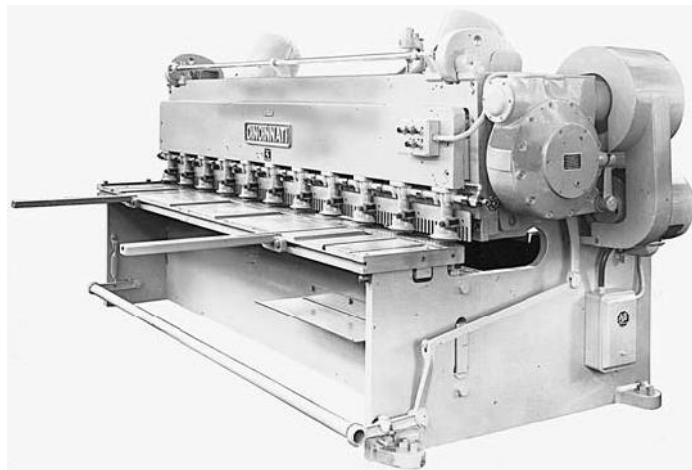


Figure 1.2 Guillotine [1]

1.2. Shear Blades

On the shears, the shear blades are used as the cutting tools. These blades are produced in every conceivable size and shape and can be custom-designed to fit almost any sort of machine or cutting application as shown in Figure 1.3. Shear blades should produce clean, straight cuts each and every time.



Figure 1.3 Shear Blade Samples [3]

1.3. Tool Steels

The types of the steels which are well-suited to be made into tools are called “Tool Steels”. They can be used in applications where an optimization for hardness, toughness, strength and resistance to wear is needed.

Generally, the matrix of hardened microstructure is martensite together with various types of carbides. Actually carbides play an important role to obtain high hardness. To the contrary, the excessive amount of carbide can easily reduce the toughness [4].

There are several classification bases for tool steels, some using chemistry as a basis and others employing hardening method or major mechanical property. The AISI

system uses a letter designation to identify basic features such as quenching method, primary application, special alloy or characteristic or specific industry. Table 1.1 lists seven basic families of tool steels with the corresponding AISI letter grades.

Table 1.1 Basic Types of Tool Steel and Corresponding AISI Grades

Type	AISI Grade	Significant Characteristic
1. Water-Hardening	W	
2. Cold-work	O	Oil-hardening
	A	Air-hardening medium alloy
	D	High-carbon-high-chromium
3. Shock-resisting	S	
4. High-speed	T	Tungsten alloy
	M	Molybdenum alloy
5. Hot-work	H	H1–H19: chromium alloy
		H20–H39: tungsten alloy
		H40–H59: molybdenum alloy
6. Plastic-mold	P	
7. Special-purpose	L	Low alloy
	F	Carbon–tungsten

The shear blades are mainly made of cold-work tool steels. Therefore in this study, the main focus will be on the cold-work tool steels. Cold work tool steels have generally high carbon contents and relatively low amount of tungsten, manganese, chromium and molybdenum.

1.4. Production of Tool Steel

Before the invention of Bessemer Converter (1854), there were mainly two ferrous materials which were wrought iron and steel. Steel was made by means of burning charcoal together with wrought iron. Around 5-8 days the carbon was diffusing to the iron and forming steel. The carbon concentration was around 0,5% to 1%. This type of steel was being used for making tools. Today this composition is still being used with a standard called W1.

In today's world, electric arc furnaces are being used in the steel making plants. Steel scrap is melted in the furnace and depending on the target composition, alloy elements such as manganese, silicon, chromium, vanadium, tungsten and carbon are being introduced into the molten steel.

After degassing the molten steel, it is being poured into the molds. They can be in various geometrical shapes depending on the following procedures.

When the steel solidifies, it is brittle and must be heat treated. This heat treatment process is called annealing. Annealing is a heat treatment process, where the metal is heated around 950°C and hold for a certain time. This treatment refines the microstructure, increases the ductility and relieves the stresses. Hence, its cold-working properties are improved [5].

1.5. Some Previous Previous Studies

Some previous studies have been reviewed regarding the forging of steels with various compositions like stainless, tool and carbon steels.

Forejt, Jopek and Krejci [6] investigated the influence of the strain rate on the microstructure of carbon steel. This study shows the effect of stress by impact force in dependence on impact velocity on the structure of steel.

Johansson, Jervis and Norström [7] have studied the term of toughness for Tool Steels. They have stated that the toughness is a rather complex property. Even the method used to measure can be a source of misinterpretation. They have investigated mainly toughness and ductility, test methods and the fracture models of tool steels.

Karagoz and Yilmaz [8] have studied the carbide formation in tool steel with a very detailed manner. Besides, the influence of niobium addition on cast high speed tool steels is also explained

Switzner, Van Tyne, M.C. Mataya [9] have investigated the effect of forging strain rate and deformation temperature on the mechanical properties of warm-worked 304L stainless steel. During their study, they have used four different type of equipment which are hydraulic press, mechanical press, screw press, and high-energy rate forging to observe the results of different nominal strain rate during deformation. In this study the researcher has come into a conclusion that” Lower strain rates produced lower strength and higher ductility components, but the lower strain rate processes were more sensitive to deformation temperature variation and resulted in more within-part property variation.” [9].

Karagoz, Unal, Kahriman, Demircani [10] have studied the “Segregation in Steels and Their Influence”. In this study several types of segregations are presented together with their effect on crack formation and growth. Furthermore, the concentration gradient is shown in the crystal for the carbide forming elements.

Bicer [11] have performed the Cook and Larke Simple Compression Test on a mechanical press to AISI 1045 to obtain the stress-strain curves. Bicer has found that the experimental results are consistent with the results of commercial finite element analysis software.

1.6. Scope of the Thesis

For different types of shearing operations, shear blades are extensively used in almost all industries. The shear blades are mostly made of cold-work tool steels by employing rolling process as discussed in the previous sections. Due to the high alloy content of tool steels, all stages of the production are very challenging.

The scope of this study is the investigation of feasibility of using hot forging process instead of rolling process to produce the cold-work tool steel shear blades. Additionally, the production steps of the billets by sand casting and series of heat treatment processes are within this scope.

Basic principles of casting and forging are explained in Chapter 2 to provide a basis for the study. Before casting the samples, the pattern should be designed by the help of finite volume analysis software. The filling of the sand mold and the solidification

of the casting are required to be simulated and these are given in Chapter 3. Then, the experiment study of sand casting and initial heat treatment is covered in Chapter 4.

The finite element analysis for hot forging process is presented in Chapter 5. The experimental procedure of forging process is given in Chapter 6.

After the completion of the production processes, the forged shear blade samples should be prepared to be examined in the laboratory. The mechanical tests and microstructural analysis are discussed in Chapter 7. Discussion and conclusion are given in Chapter 8.

CHAPTER 2

CASTING AND FORGING PROCESSES

2.1. Casting Process

2.1.1. Types of Casting Processes

In casting process, the material is melted, heated to proper temperature and if it is necessary the chemical composition is adjusted. When it is ready, depending on the desired geometry, it is poured into a cavity or mold. Casting is a versatile process, in the production of complex shapes, parts having hollow sections or internal cavities, parts that contain irregular curved surfaces.

The selection of the right casting process depends on the type of the material, composition, size of the work piece and dimensional requirements (i.e. geometry, tolerances, surface quality etc.). In some cases the feasibility of machining versus casting should also be investigated. Bearing in mind all of these parameters, Figure 2.1 shows the classification of casting processes [4].

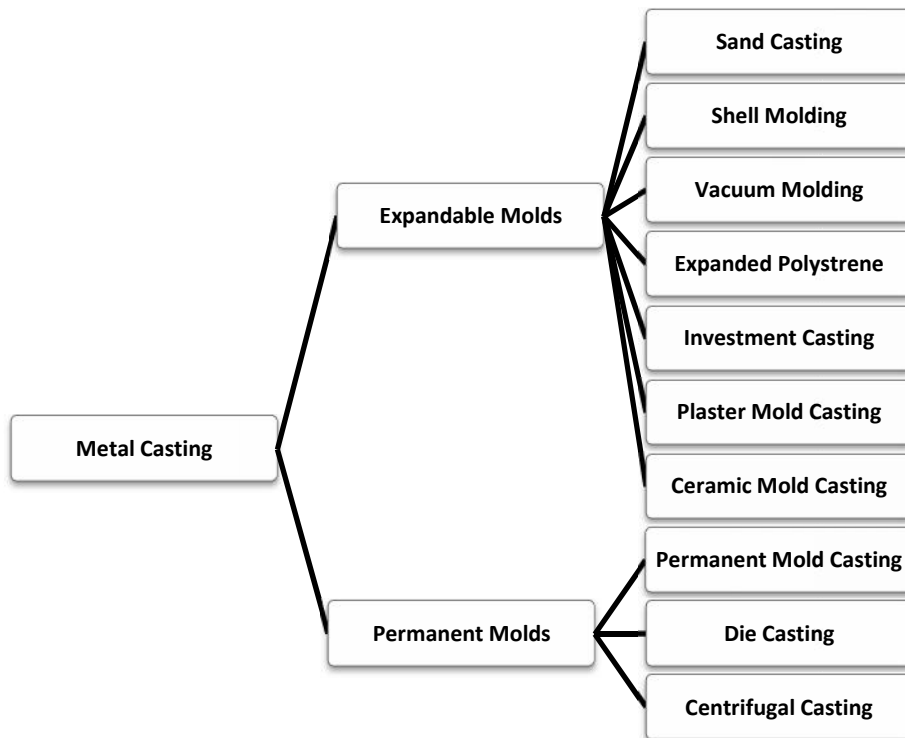


Figure 2.1 Classification of Casting Processes According to Type of Molding [4]

2.1.2. Casting Process Selection

In this study, sand casting is used as casting method, since sand casting is relatively easy and feasible method compared to the others. To the contrary, sand casting has some disadvantages. Poor surface quality and low accuracy on the dimensions are some of these disadvantages. However, in this case, the castings are going to be machined. So there is not any problem neither with the dimensions nor with the surface quality. The flow chart of a typical sand casting process is shown in Figure 2.2.

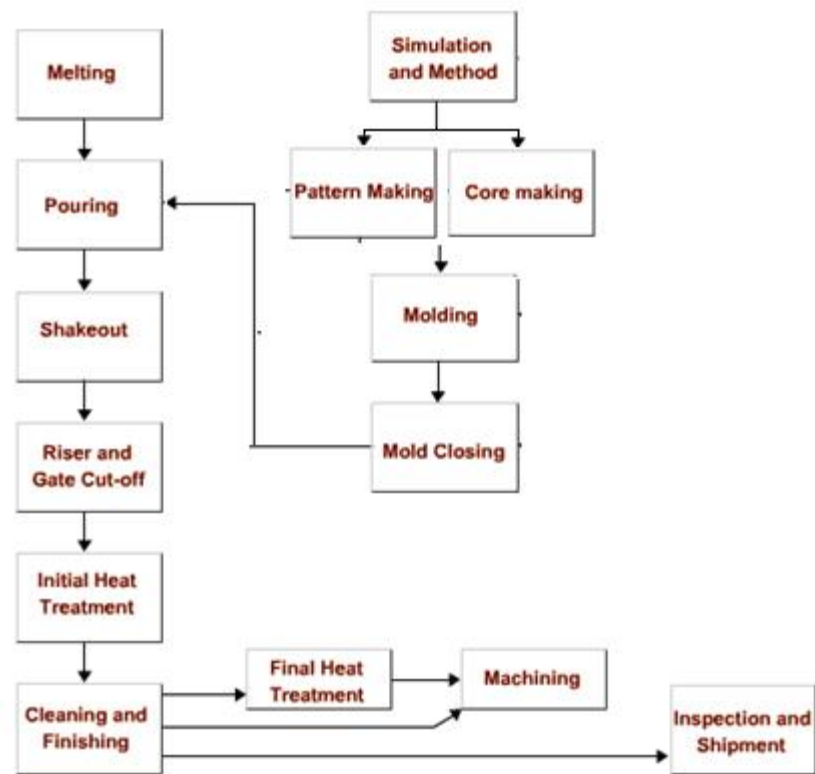


Figure 2.2 Flow of a typical sand casting process

2.1.3. The Operations of Sand Casting

After molding, if there are any cores required, they are placed into the mold carefully. The cope (i.e. upper half of the mold) is placed on the drag (i.e. lower half). They are clamped and supported by some weights to prevent any leakage due the pressure exerted by the gas of liquid metal.

The liquid metal has to flow into the cavity of the pattern properly. The gating system plays an important role at this point. The turbulent flow of the liquid metal in the gating system should be avoided.

The riser design is also important. If the density of the liquid metal is lower that its solid density, it means that it will shrink during solidification. There has to be extra liquid metal reservoir to feed the work piece during solidification. This reservoir is

called riser. The position of the risers in the mold is detrimental. If the positions and the volumes of the risers are not determined carefully, the work piece will become a scrape.

When the piece is shaken out from the sand mold, the surface is fully covered with oxide and/or sand. After cleaning the surface, the risers and gates are cut off. Depending on the type of the metal, it might be necessary to heat treat the piece, to get the desired properties.

2.1.4. Heat Transfer in Sand Mold

During solidification, in addition to the conduction through the solid metal, there is convection within the liquid metal. Conduction from particle to particle in the mold media; gaseous conduction and convection through the air gaps between individual particles of the mold; and radiation from particle to particle through the mold are some of the heat transfer phenomena in the mold. Besides that, the cooling effect of entrapped moisture in the mold, and the influence of the combustion of organic binders should also be kept in mind.

Fleming [12] lists five different regions of thermal resistances to heat transfer from liquid metals being cooled to produce castings:

1. The liquid metal
2. The solidified metal
3. The metal/mold interface
4. The mold
5. The surrounding area around the mold

2.1.5. Estimation of the Solidification time

Modulus of casting, M , is related with the geometry of casting is given in (2.)

$$M = \frac{V}{A} \quad (2,1)$$

Where;

V= Total Volume of Casting

A= Total Surface Area of Casting in Contact with the Mold

Chvorinov [13] found that there is a relationship between M and the time need for the solidification of molten metal, t_f on log-log plot. The equation for this relationship is;

$$t_f = \frac{\pi}{4} \left(\frac{\rho_s H}{T_s - T_0} \right)^2 \left(\frac{1}{k_n \rho_m c_m} \right) (M)^2 \quad (2,2)$$

Where;

T_s : The initial temperature of the molten metal

T_0 : The initial temperature of the mold

ρ_s : The density of solidifying metal

H: The latent heat of fusion of the metal

K_m : The thermal conductivity of the mold

ρ_m : The density of the mold, and C_m is the specific heat of the mold

However, it is obvious that according to Chvorinov's relation, there was no difference between the solidification times of a spherical mold as opposed to a plate mold.

According to Trbizan [14], a plate shape should have slower cooling rate compared to spherical mold. Hence he modified the Chvorinov's relation with a factor which defines the shape of the mold. The equation is as follows;

$$\frac{V}{A} = \frac{2}{\sqrt{\pi}} \left(\frac{T_s - T_0}{\rho_s H} \right) (k_m \rho_m C_m) \sqrt{t_f} + \left(\frac{n K_m t_f}{2r} \right) \quad (2,3)$$

Where; n = 0 for a flat plate, 1 for a cylinder, and 2 for a sphere.

The calculation of the thermal conductivity of the mold is probably the most challenging part of the estimation solidification time.

According to theory developed by Gori and Corasaniti [15], the thermal conductivity, k_e can be calculated as follows;

$$\frac{1}{k_e} = \frac{\alpha - 1}{k_v \alpha} + \frac{\alpha}{k_v \cdot (\alpha^2 - 1) + k_s} \quad (2,4)$$

Where;

K_v : thermal conductivity of the void phase

V_{void} : Volume of the void

V_{cell} : Volume of the cell (void and solid),

For the calculation of α and ϵ (2,5) and (2,6) are to be used;

$$\alpha = \sqrt[3]{\frac{1}{1-\epsilon}} \quad (2,5)$$

$$\epsilon = \frac{V_{void}}{V_{cell}} \quad (2,6)$$

2.1.6. Solidification and Microstructure of Tool Steel

During the solidification of Tool Steels, three different grain structures can conform. The first zone is located on the contact with the mold and called “chill zone”. The second zone comes after the chill zone and called “columnar zone”. The third zone is located at the center of the casting and called “equiaxed zone”. These zones are schematically illustrated in Figure 2.3. The main reason of these different zones is the influence of the cooling rate on the nucleation and growth mechanism.

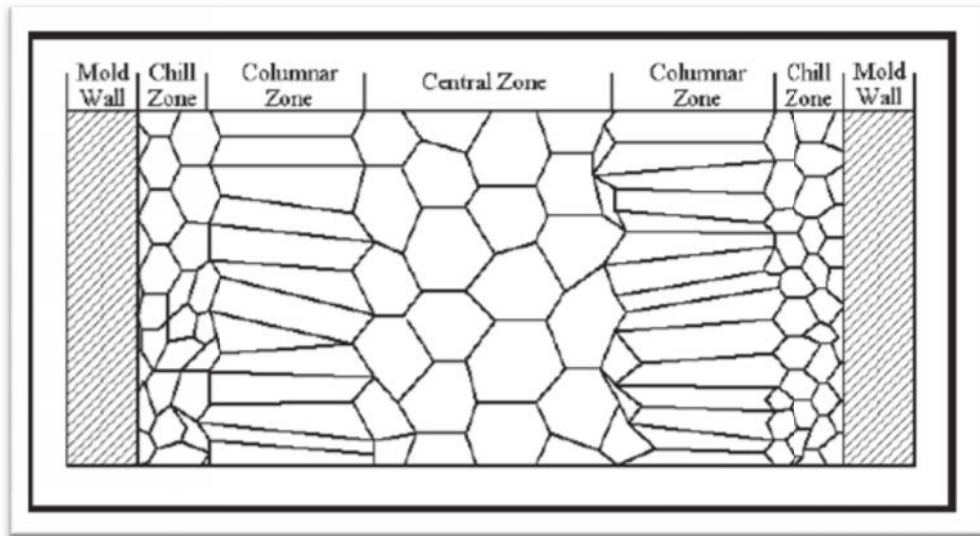


Figure 2.3 Three Zones of Freezing in a Casting [16]

High alloy content and different heat treatment processes are the two main reasons of the complex structures of Tool steels. Addition of alloying elements can influence the austenite to ferrite transformation in three ways. It can change the homogeneity range for a given phase, it can change the nucleation rate of ferrite and the kinetics of the growth of ferrite [35].

All tool steels are alloyed with carbon and some other alloying elements (such as; chromium, molybdenum, vanadium, and tungsten). These elements form various types of carbides. The elements and carbide formation are explained below [34, 35];

Chromium mostly forms carbides of the types $M_{23}C_6$ and some M_7C_3 depending on the chromium content. These carbides dissolve during austenitisation at temperatures exceeding $\sim 900\text{ }^\circ\text{C}$ and are totally dissolved at $\sim 1100\text{ }^\circ\text{C}$.

Molybdenum forms carbides of M_2C type carbides. These carbides become unstable at elevated temperatures, and at $\sim 750\text{ }^\circ\text{C}$ they transform to M_6C type carbides by reaction with Fe.

Vanadium forms carbides of MC . These carbides are thermally stable and very hard. It improves the hardenability and causes grain refinement.

The addition of the elements mentioned above, reduces the martensite formation temperature. As a result, rapid cooling may be required for a full transformation of austine to martensite. However, fast cooling has certain risks like the formation of internal stresses and risk for dimension distortion and cracking.

The mechanical properties of tool steels are directly affected from the microstructure and solidification. Foreign atoms diffuse from the dendrites to interdendritic spaces. This is the mechanism of macro segregation formation as known as ingot/block segregation. Depending on the type of the element which forms the segregation, it has different effects. These foreign atoms can be C, Mn, S etc. For instance, in hot work tool steels, block segregation due to the diffusion of carbon is very common. [8,10]. The microstructure for the macro segregation is given in Figure 2.4.



Figure 2.4 The block segregation on a hot work tool steel. [17]

Besides, segregations can also be observed in the grains, in other words in crystals. In this case, there is a concentration grading from the center of the grain to the

boundary. However this type of segregation can easily be eliminated by annealing [17].

2.2. Tool Steel Forging

2.2.1. Forging Process

Metalworking by means of forging is one of the oldest methods of manufacturing. According to the earliest records, in Middle East (8000 B.C.), the gold and copper were being shaped by hammer. During the industrial revolution, there was a big demand for the metal products; hence the new forging machineries were developed [18].

For the forging process, the input material shall be in a form of rod, billet, or slab. The material is plastically deformed between tools in order to obtain the desired shape. Evidently, tools should have a negative shape of the desired geometry. One of the most important properties of forging, mostly there is little or even no scrap forms during the process. Besides that, forging ensures good surface finish and tolerances in the manufacture of engineering components. Due the formation of grain flow during forging, forged components are more reliable than parts machined from bar stock or plate. Today, forging is used in different industries for the manufacturing of variety parts such as; small bolts, pins as well as gears, cam and crankshafts, connecting rods, valves, landing gear components, etc [19] .

Nowadays, the forging industry is more cost oriented due to the high competition in the market. The trial-and-error method is too expensive to be competitive in today's industry. That's why; engineers are focused on formulations of sophisticated mathematical analyses of forming processes by using Computer Aided Engineering Software. This analyses leads not only to higher efficiency but also to higher quality.

2.2.2. Classification of Forging Process

There are various classifications applied for the forging process. In general,

Forging processes can be classified according to:

- Temperature: Cold Forging, Hot Forging, Semi-Hot Forging
- Type of Machine Used: Hammer, Mechanical Press, Hydraulic Press, etc.
- Type of die: Open die forging, Closed die forging

2.2.2.1. Classification According to Temperature

In cold forging, the material is deformed at or near to the ambient temperature. By means of cold forging, precise geometries shall be obtained. However the force required for the deformation is significantly higher than hot forging operation. Due this force during cold forging, there are high stresses on the tools. As a result forming load and stresses have to be calculated carefully for the machine tools.

In hot forging, the temperature is above the recrystallization temperature. For instance, in steel it is around 1050-1250°C. Above the recrystallization temperature, strain hardening is eliminated. So, the most important advantage is the reduction on the forces. A greater degree of deformation can be carried in a single operation. The scale formation and low dimensional accuracy are some of the disadvantages of hot forging.

In warm forging, the temperature should be around the recrystallization temperature. The forces are lower compared to cold forging. Hence, there is a reduction on the tooling loads and the press loads.

2.2.2.2. Classification According to Type of Machine Used

Forging hammer is the most elementary way of forging. Due to the reasonably low cost of investment, it is the most commonly used way of forging. The machine raises a lever arm that had a hammering tool at one end; it was called a tilt hammer because the arm tilted as the hammering tool was risen. After raising the hammer, the blacksmith let it fall under the force of gravity, thus generating the forging blow. This relatively simple device remained in service for some centuries. These machines are energy restricted.

Mechanical presses are usually used for closed die forging operation. The reciprocating linear motion of the mechanical presses is driven by a slider-crank mechanism. The eccentric shaft is connected through a clutch and brake system

directly to the flywheel. Unlike the impact of the hammers, mechanical presses squeeze the material during deformation. Compared to the forging hammer or hydraulic press, the ram stroke is shorter. These presses are displacement (i.e. stroke) restricted.

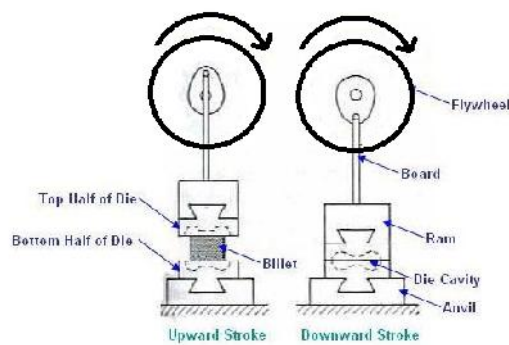


Figure 2.5 Schematic of a Mechanical Forging with Eccentric Drive [20]

A screw press is a type of mechanical press in which the ram is driven up and down by a screw. Flywheel's rotational energy is converted to linear motion by a threaded screw attached to the flywheel on one end and to the ram on the other end. The energy stored in a flywheel, is used for deforming the work piece.

Hydraulic presses can be used both for open and close die forging operations which has a negative shape of the desired part geometry. The hydraulic system has some advantageous. First of all, there are release valves on the hydraulic cylinder to protect the tools and the press from over loading. The maximum press load is constant all through its motion. By means of control systems, it is possible to regulate the ram speed. Hydraulic presses are essentially load restricted machines.

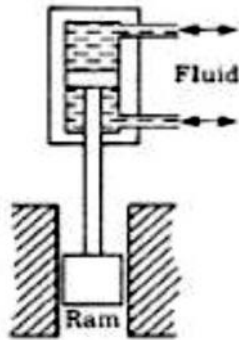


Figure 2.6 Schematic of a Hydraulic Press [18]

2.2.2.3. Classification According to Type of Die Set

Mainly, there are two different types of forging dies, which are open dies and close die sets.

In open die forging, work piece surface deformation occurs freely as shown in Figure 2.7. Hence, this process is less accurate compared closed die forging. The dies are either flat or simple contour dies.

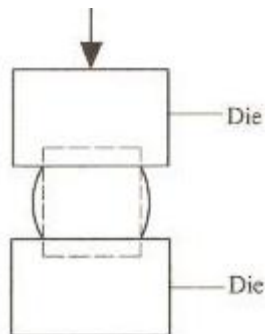


Figure 2.7 Schematic of Open Die Forging

In closed die forging, there is a cavity in the die. As shown in Figure 2.8, during the deformation, the material fills this cavity. If there is an excessive material, it is allowed to escape into the clearance between the dies. The geometry which is formed by this excess material is called flash. One of the most important targets of the die design is minimizing the flash.

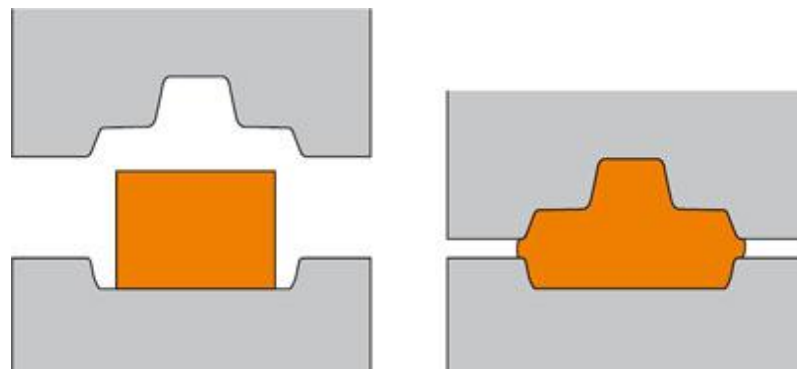


Figure 2.8 Schematic of Close Die Forging [1]

CHAPTER 3

DESIGN AND ANALYSIS OF SAND CASTING OF TOOL STEEL SHEAR BLADE SAMPLE

3.1. Introduction

In this study, the production of the tool steel shear blade starts with the material selection. Then, the design and analysis of sand casting of shear blade will be cover. The Figure 3.1 shows the flowchart of complete progress of shear blade production by sand casting and forging processes

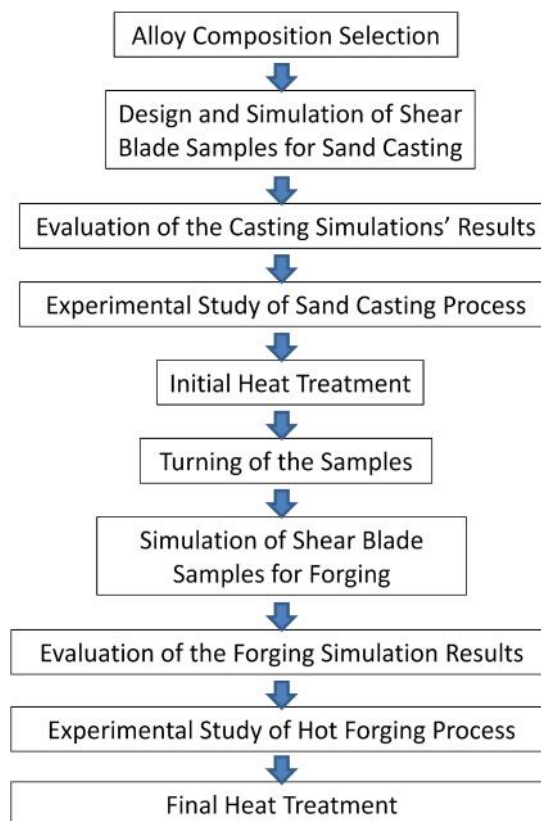


Figure 3.1 Flowchart of the Progress in Chapter 3

3.2. Alloy Composition Selection

Generally, all types of shear blades are exposed to high stresses. Therefore the resistance against wear, impact and bending is very important. Cold-work tool steels are mainly used for these purposes. In industry, there are tool steel materials which are supplied with different trademarks. Some of these cold-work tool steels together with their applications areas are given Table 3.1 [21].

Table 3.1 Some Examples for Cold-Work Tool Steels

GRADE	DESCRIPTION/ APPLICATION
BOHLER K110	High carbon,high chromium Tool steel with high dimensional stability in heat treatment and wear resistance. Cutting and blanking. Wood working. Cold shear blades. Cold forming. Ceramic pressing. Gauges.
UDDEHOLM SLEIPNER	Special steel with very wide properties profile from good general wear resistance, compressive strength and a high resistance to chipping and cracking to good hardenability and good machining properties.
UDDEHOLM CALMAX	Air hardening Cr Mo V alloyed steel with high toughness, good wear resistance and polishability. Cold work - heavy duty blanking & forming rolls, shear blades. Plastic Moulding - for reinforced plastics, compression moulds.
BOHLER K340	Excellent air hardening properties, good dimensional stability, good toughness, high compression strength and wear resistance, very good retention of hardness, excellent nitriding and PVD coating properties. For blanking and punching tools, Cold forming tools ,thread rolling tools.
UDDEHOLM VIKING/CHIPPER	Cr-Mo steel for chipper knives and other knives exposed to high stresses. Has good toughness and wear resistance

In this study, the alloy composition of X48CrMoV8-1 has been selected for the production of the tool steel shear blade. The composition is given in Table 3.2. The versatility of this alloy makes it very common in the industry. The advantages of this alloy can be given as follows (24);

- Good dimensional stability during heat treatment
- Good machinability and grindability
- Excellent combination of toughness and wear resistance
- Normal hardness in the range 52–58 HRC
- Ideal for surface coating

Table 3.2 Chemical Composition of X48CrMoV8-1-1

Element	Min/Max
C	0,45 - 0,50
Si	0,80 – 1,00
Mn	0,35 - 0,45
P	≤0,020
S	≤0,005
Cr	7,30 - 7,80
Mo	1,30 - 1,50
V	0,30 - 0,50

This composition is commonly used for the following applications;

- Shear blades

- Fine blanking
- Deep drawing
- Cold forging
- Swaging dies
- Rolls
- Cold extrusion dies with complicated geometry
- Tools for tube drawing

3.3. Methodology and Finite Volume Analysis of Sand Casting

In today's world, simulation of casting process is the essential tool which lets foundries to obtain reliable and high-quality cast parts. Finite volume analysis leads to efficient processes, reduced cycle times, less down time, and the elimination of rework in Casting Industry. It is possible to predict casting properties for the defined gating system and process parameter combination. In this study, MAGMA 5.2 [22] is used to design system for sand casting of tool steel shear blade samples.

3.3.1. Modeling the Billet and the Gating System

The first is modeling the billets and the gating system by using SolidWorks 2011. The geometry of the billets is cylinder with a diameter of 50mm and the height of 200mm. The pattern is designed in such a way that, 44 billets are cast into the mold simultaneously. The 3D Model of the pattern is shown in Figure 3.2. The technical drawing for the pattern can be found in Appendix B.

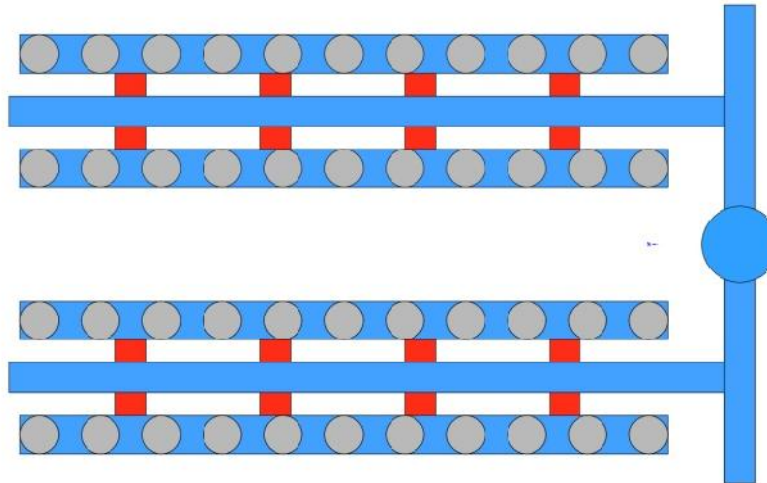
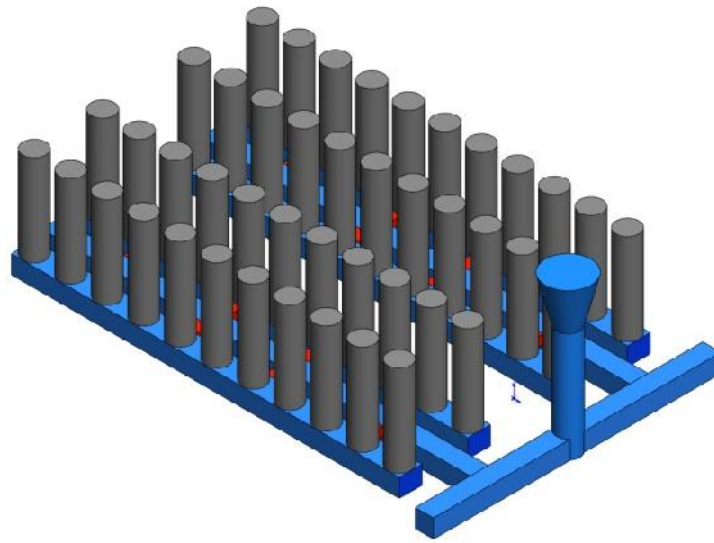


Figure 3.2 Isometric and Top View of the 3D Model of the Pattern

3.3.2. Defining the Sand Mold, Importing the Billets and the Gating System Geometries

The type of the mold is selected as “Sand Mold” in MAGMA Software. The initial temperature of the mold is assigned as 20°C. The physical properties of the sand mold have already been defined by the supplier of the software.

After the definition sand mold, the models of billet and gating system geometries from CAD program are imported to the finite volume program in "stl" (i.e. stereo lithography) format.

3.3.3. Assigning the Material Properties

The next stage is defining the X48CrMoV8-1 from the material database of Magmasoft 5.2. The variation of some of the physical properties with respect to temperature are given in Table 3,3 - 3,6. These properties are critical to define the behavior of X48CrMoV8-1 during solidification.

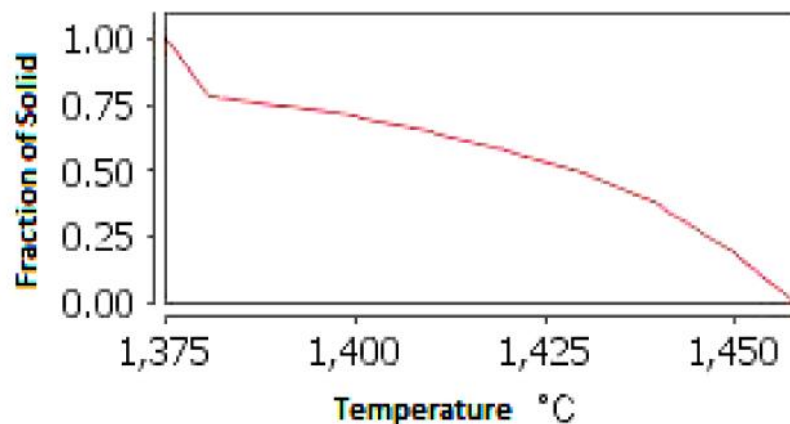


Figure 3.4 Variation of the Fraction of Solid with Temperature for X48CrMoV8-1 [22]

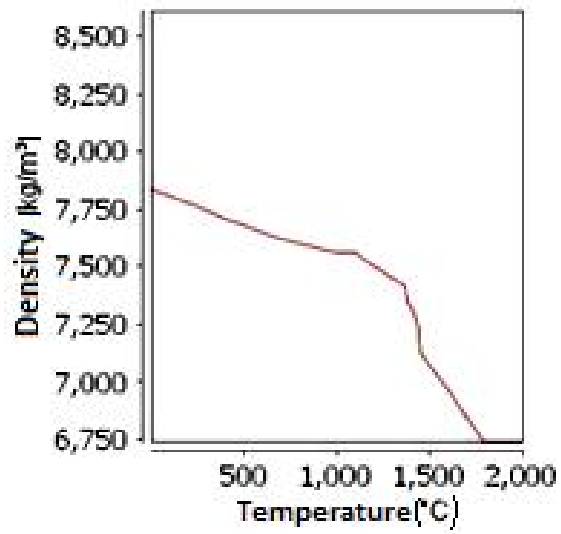


Figure 3.3 Variation of Density with Temperature for X48CrMoV8-1 [22]

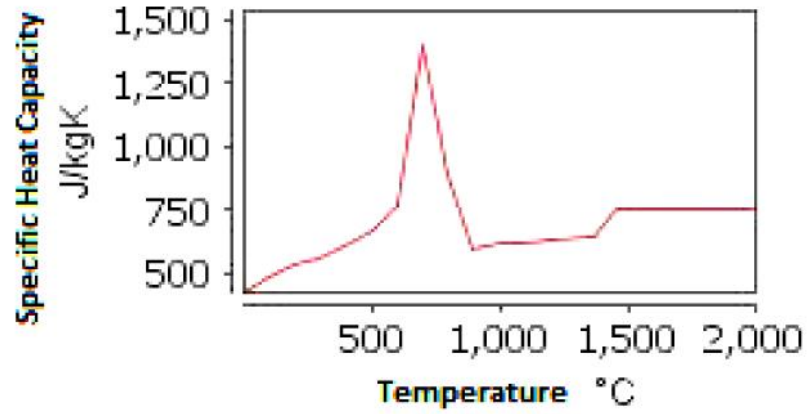


Figure 3.5 Variation of Specific Heat Capacity with Temperature for X48CrMoV8-1 [22]

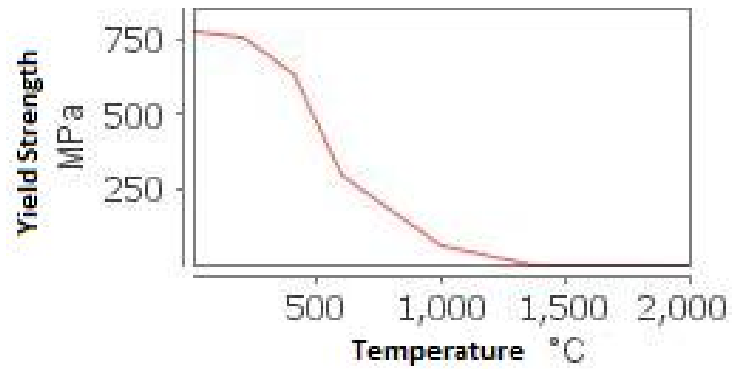


Figure 3.6 Variation of Yield Strength with Temperature for X48CrMoV8-1 [22]

3.3.4. Finite Volume Simulation for Casting

In the simulation, the sand casting of 44pcs of billets with a X48CrMoV8-1 composition is investigated. The initial temperature of the liquid metal is assigned as 1580°C. The position of the casting in the mold and the size of the mold are shown in Figure 3.7.

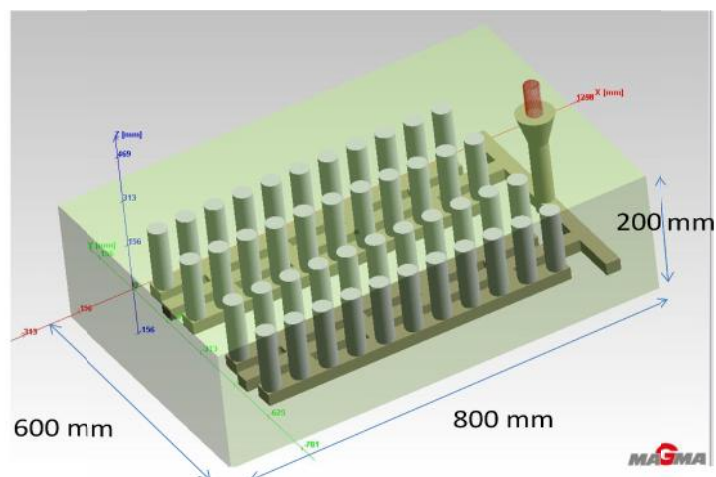


Figure 3.7 Dimensions of Sand Mold

The meshing of the casting is shown in Figure 3.8. In total, there are 871416 cells. 85955 cells are for the gating system and the billets. The rest is for the sand mold.

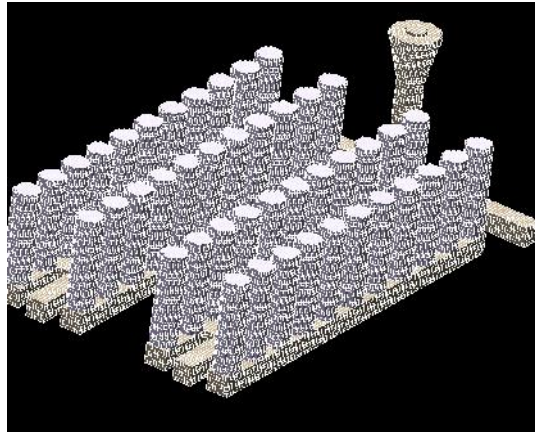


Figure 3.8 Meshing of the Billets and the Gating System

The total volume of the gating system and the billets are given in Table 3.3. From this table, it is understood that the total amount of liquid metal to be poured is around 124 kg. Besides that, since the modulus of the gating system is much lower than the billets, gating system will solidify earlier than billets.

Table 3.3 Some Properties of the Billets and the Gating System

	Total Volume (cm³)	Total Surface Area (cm²)	Modulus (cm)	Mass (kg)
Billets	17278,00	15550,88	1,11	116,63
Gating System	1127,00	11267,71	0,10	7,61

The first design parameter of gating system is avoiding the turbulent flow of the molten metal. The turbulent flow decreases the quality of steel significantly due to re-oxidation. Re-oxidation causes the formation of oxides which is a form of casting defect. Moreover, as the speed of the molten metal increases, the more erosion occurred in the mold. The eroded sand goes into the casting, causes the formation of sand-defects. In Figure 3.9, it is shown that the velocity of the molten metal is mostly below the critical level.

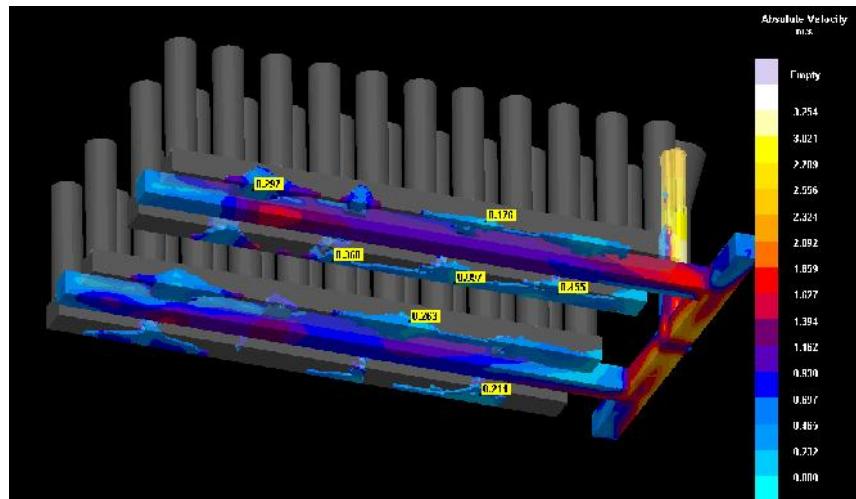


Figure 3.9 Velocity of Molten Metal in the Mold

The second design parameter is filling the billets simultaneously. If the filling is completed concurrently then the solidification will start at the same time. Consequently, the billets should have almost the same properties. This is crucial for the further experiments. It is found that all of the billets are solidifying around 757 seconds. The timeline of solidification is given in Figure 3.10

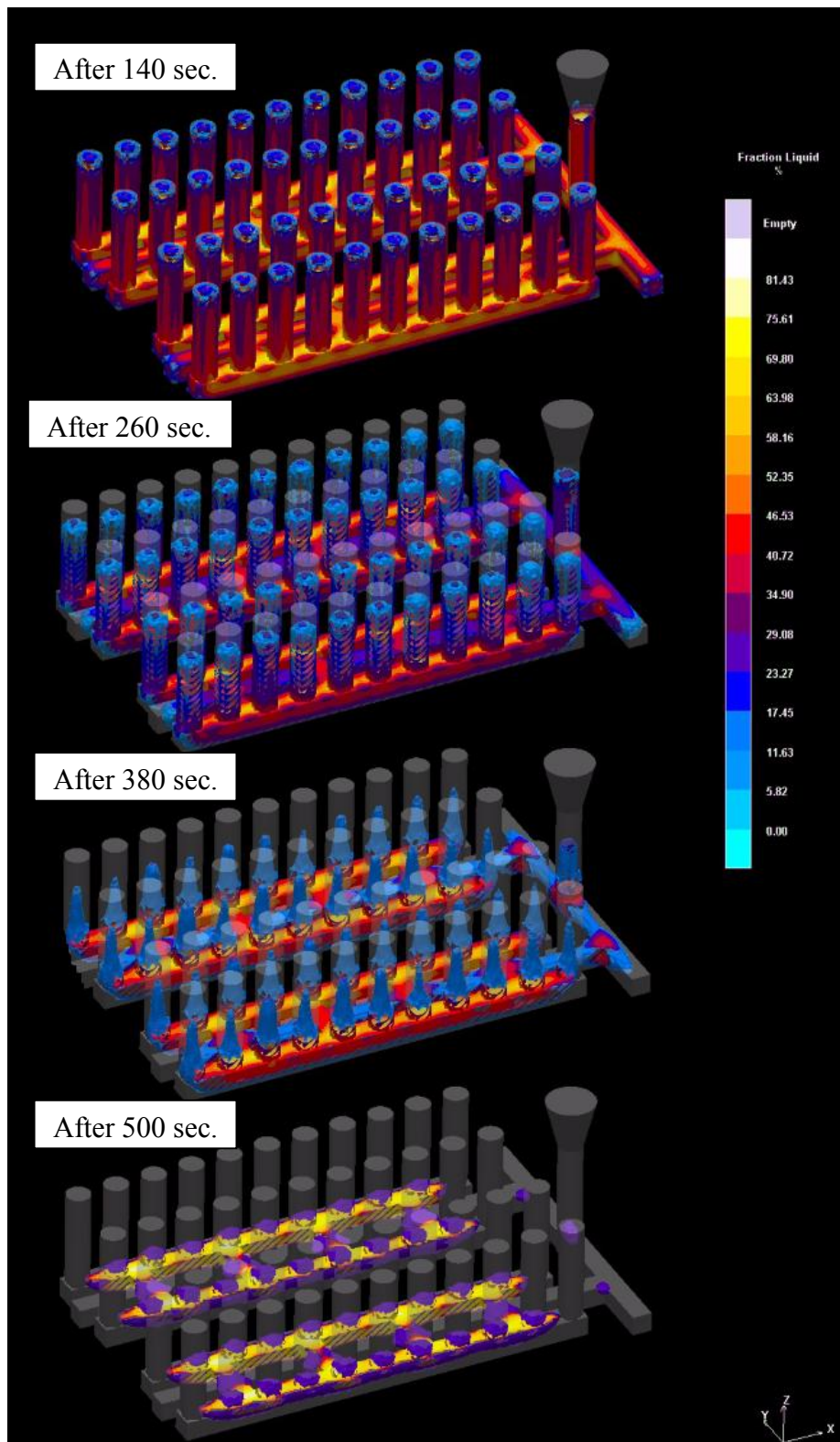


Figure 3.10 Fraction Liquid with the Elapsed Time during Solidification

The third design parameter is the examination of shrinkage and porosity criteria. The rate of solidification is critical for the microstructure of the tool steel. As the cooling rate increases the size of the carbides get smaller. As a result the mechanical properties of the cast tool steel are improved.

Risers are used to prevent the defect formation in the casting. To the contrary, risers decrease the rate of cooling and result with carbide coarsening of alloyed steels such as tool steels. Therefore the billets are designed as riserless.

Due to the riserless design, the formation of defects at the top of the billets is inevitable. Besides that, the gating system is solidifying earlier than the billets. Therefore, the billets are acting as a riser for the gating system. Due to these reasons, there are some potential defects which are shown in Figure 3.11.

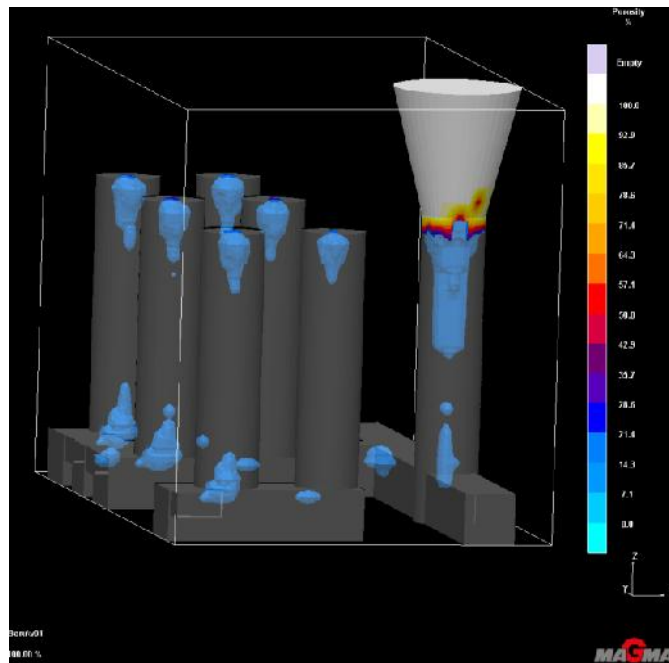


Figure 3.11 Simulation Result for the Porosity

3.4. Discussion on the Simulation Results for Casting

The calculated time of pouring is around 10 seconds. Firstly the gating system solidified in 520 seconds and the solidification is completed nearly in 757 seconds. It is found that the actual design of the gating system works well during filling.

Gating system causes the formation of porosities and shrinkages at the lowest part of the billet during solidification. The modulus difference between the billets and the gating system is the main reason for these defects. Due to the riserless design, extra height is left on the top. It should be noted that these defects are not detrimental. The results of the simulation have shown that the defects are allocated around 40 mm from the top and 35mm from the bottom. During the further stages of preparation, high risk zones are removed by means of turning

CHAPTER 4

THE EXPERIMENTAL STUDY OF SAND CASTING

Design of the gating system and the positions of the billets have been described in Chapter 3. By means of the simulations, it has been found that the current design is suitable for obtaining sound casting. The experimental sand casting of the billets which is the initial stage of the production of the tool steel shear blade sample is presented.

4.1. Molding

According to the results of the simulation, the pattern was produced. The material of the pattern is polystyrene (i.e. Styrofoam) which is feasible and easy to shape.

For the experiment sand mold consists of three parts. Firstly, the lowest flask was molded. The gating system was placed carefully and supported by weights as shown in Figure 4.1, against the movement. Then the flask was filled with sand as shown in Figure 4.2. After the filling the lowest the flask with sand, it was flipped over and molding of the middle flask begins. The cylindrical Styrofoam pieces which were placed on gating system as shown in Figure 4.3. Then, the flask was filled with sand as shown in Figure 4.4. By simple tools, holes were formed on top flask as shown in Figure 4.5. These holes are important to release the entrapped gas out of the mold. Afterwards, the last flask was filled with sand as shown in Figure 4.6. The mold was left for a while for the curing of the resin bonded sand. It should be noted that this process is not a full mold casting. The pattern was taken out of the mold. As shown in Figure 4.7 and Figure 4.8, In order to prevent the sintered sand formation and to increase the surface quality of the pieces, all surfaces were painted.



Figure 4.1 The Pattern of the Gating System in Lowest Flask



Figure 4.2 The Filling of the Drag with Sand



Figure 4.3 The Patterns of the Billets Placed in the Middle Flask



Figure 4.4 Molding of Cope (First Stage)



Figure 4.5 Formation of the Gas Release Holes



Figure 4.6 Molding of Cope



Figure 4.7 Painted Cavity of Gating System (Lowest Flask)



Figure 4.8 The view of the Cope after Painting

4.2. Melting and Pouring

In this study, electromagnetic induction was used for melting the metal. Induction heating is a non-contact heating process where high frequency electricity is passed through a coil. The coil generates a rapidly changing magnetic field inside of the coil. By means induction, eddy currents are generated within the metal. Due to the resistance of metal, the heat is generated. The furnace, used in this study is shown in Figure 4.9 .



Figure 4.9 The induction furnaces at Akdas Casting

Emission Spectrometer is used to measure and adjust the chemical composition of molten metal while it is being prepared for casting as shown in Figure 4.10.



a) Spectrometer



b) Analyzing Chamber

Figure 4.10 Emission spectrometer and its analyzing chamber

To prepare the X48CrMoV8-1-1 alloy, firstly low carbon steel scrap was melted in an Inductotherm induction furnace. 400kg is the minimum capacity of the furnace. Therefore 400kg of scrap was heated to 1600°C and the alloying elements, such as FeCr, FeSi, FeMn, FeMo, FeV, were introduced into the melt.

The ferro alloy addition was carried out in three stages. The first two stages were done into the furnace. The last one was done in the ladle. The quantity of the ferro alloy addition in each stage is shown in Table 4.1. For each stage, the influences of these additions were measured via spectrometer and the results are given in Table 4.2.

Finally the composition of the liquid metal was in accordance with the standards of X48CrMoV8-1. The final composition prior to casting is shown in the third column of Table 4.2.

At this stage the molten metal was ready to be poured. Hence it was taken into the ladle and poured into the mold as shown in Figure 4.11.

Table 4.1 Amount of Ferroalloy Addition During Melting of Tool Steel

Ferro Alloys	Amount of Ferro Alloying (kg)		
	Initial Alloying (In Furnace)	Secondary Alloying (In Furnace)	Third Alloying (In Ladle)
FeSi	-	8	1
FeMn	-	3	-
FeCr (High Carbon)	25	18	-
FeCr (Low Carbon)	20	18	-
FeMo	10	3	-
FeV	3,5	0,5	-

Table 4.2 Results of the Spectral Analysis at Various Stages

Elements	Results of Spectral Analysis (%)		
	First Furnace Analysis	Second Furnace Analysis	Ladle Analysis
C	0,37	0,49	0,50
Si	0,10	0,76	1,03
Mn	0,16	0,41	0,56
Cr	5,62	8,40	8,52
Ni	0,08	0,11	0,11
Mo	1,36	1,39	1,52
V	0,48	0,58	0,57
W	0,01	0,01	0,01
Al	0,00	0,01	0,06
Cu	0,03	0,04	0,09
Mg	0,00	0,00	0,00
Ti	0,04	0,07	0,07
P	0,01	0,01	0,02
S	0,01	0,01	0,01
N	0,01	0,00	0,02



Figure 4.11 Pouring of tool steel into the mold

4.3. Shake Out and Cleaning

After the solidification, the casting was shaken out from the sand mold. Figure 4.12 shows the billets and the gating system. Firstly billets were cut and then the surfaces of the billets were cleaned by grinding as shown in Figure 4.13.



Figure 4.12 Specimens after shakeout



Figure 4.13 The Surface Cleaning of the Billets by Grinding

4.4. Initial Heat Treatment

At this stage, the casting should to be heat treated to homogenize and to soften the casting. This type of heat treatment is known as soft annealing. In soft annealed tool steels, most of the alloying elements form carbides. For some elements, which do not have a tendency towards carbide formation such as cobalt and nickel, they dissolve in the matrix. It is also effective in eliminating element segregation between dendrite arms in as cast microstructure.

Soft annealing is especially useful for high alloy steels such as tool steels. During austenization, the residual carbides agglomerate. As a consequence, coarser carbides reduce the toughness and results in edge fragmentation of the tools in service condition. In this study, soft annealing was carried out at 880°C for 3 hours by and electrical box type furnace as shown in Figure 4.14.



Figure 4.14 Electrical Box Type Furnace

CHAPTER 5

DESIGN AND ANALYSIS OF FORGING OF TOOL STEEL SHEAR BLADE SAMPLE

5.1. Introduction

The second step of the production of the tool steel shear blade sample is the plastic deformation of castings by means of forging process. The die sets should be in such a way that the billets can be deformed with different reduction reductions. By this way, the influence of deformation on the mechanical and the microstructural properties can be investigated.

5.2. Billet Design

In this study, billets with aspect ratios, d_0/h_0 of 2, 1 and 0,5 are selected to be used to investigate the influence of the amount of deformation. During the tests, the same reduction ratios will be tested on billets with different aspect ratios. In Figure 5.1, the types of the billets with different aspect ratios are shown. During forging operation, the height of the billets will be reduced by 10%, 20% , 30% and 40%.

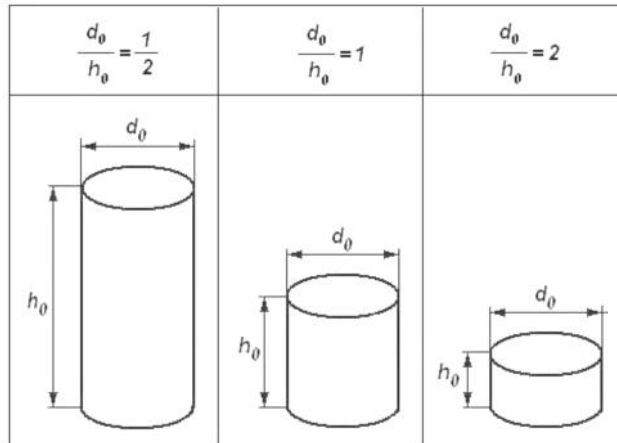


Figure 5.1 Schematic Views of the Specimens According to Their Aspect Ratios [11]

The distance between the ram and the anvil is 200 mms when the ram is at its bottom dead center. By means of the hydraulic system on the Ram, the height can be adjusted by 10 mms. This mechanism is shown in Figure 5.2 schematically.

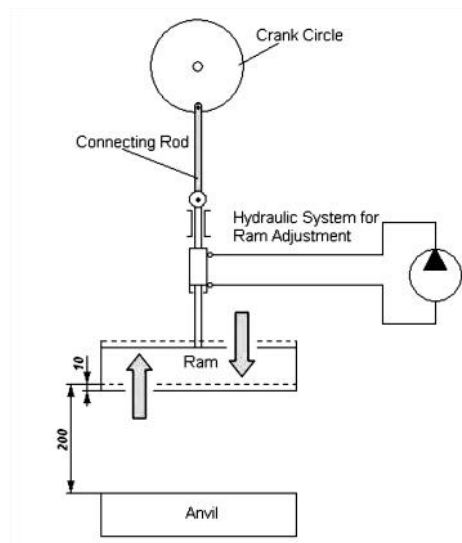


Figure 5.2 Ram Adjustment Mechanism of the Forging Press [11]

Depending on the final height of the billet, the insert configuration and the position of the ram should be calculated. In total 12 different types of forging operations are designed.

For each billet, the final height is calculated according to the decided reduction ratios in advance. The initial and the final dimensions are given in Table 5.1.

Table 5.1 Table of Initial and Final Dimensions of the Specimens

Billet					
Group No	d_0 (mm)	h_0 (mm)	d_0/h_0	r (%)	h (mm)
1	30.00	15.00	2.00	40.00	9.00
2	30.00	15.00	2.00	30.00	10.50
3	30.00	15.00	2.00	20.00	12.00
4	30.00	15.00	2.00	10.00	13.50
5	30.00	30.00	1.00	40.00	18.00
6	30.00	30.00	1.00	30.00	21.00
7	30.00	30.00	1.00	20.00	24.00
8	30.00	30.00	1.00	10.00	27.00
9	30.00	60.00	0.50	40.00	36.00
10	30.00	60.00	0.50	30.00	42.00
11	30.00	60.00	0.50	20.00	48.00
12	30.00	60.00	0.50	10.00	54.00

There is a modular die set in METU-BILTIR Center Forging Research and Application Laboratory. The dimension for the modular die set is given in Appendix C. By means of changing the configuration of the modular dies and using the ram adjustment feature of the press, it is possible to reach the desired dimensions. The modular die set configuration for each billet group is shown in Table 5.2. In this table, used inserts are indicated by “+” for each billet group.

Table 5.2 Modular Die Set Configurations

Specimen Group No	Die Set Configuration	Ram Adj. (mm)	Insert (mm)			
1	Figure 5.3 (a)	7	40	30	20	10
2	Figure 5.3 (b)	5,5	+	+		+
3	Figure 5.3 (c)	4	+	+		+
4	Figure 5.3 (d)	2,5	+	+		+
5	Figure 5.3 (e)	8	+	+		+
6	Figure 5.3 (f)	5	+	+		
7	Figure 5.3 (g)	2	+	+		
8	Figure 5.3 (h)	8,5	+		+	
9	Figure 5.3 (i)	10	+			+
10	Figure 5.3 (j)	4	+			+
11	Figure 5.3 (k)	8	+			
12	Figure 5.3 (l)	2	+			

In accordance with Table 5.2, the modular die set designs are illustrated in Figure 5.3.

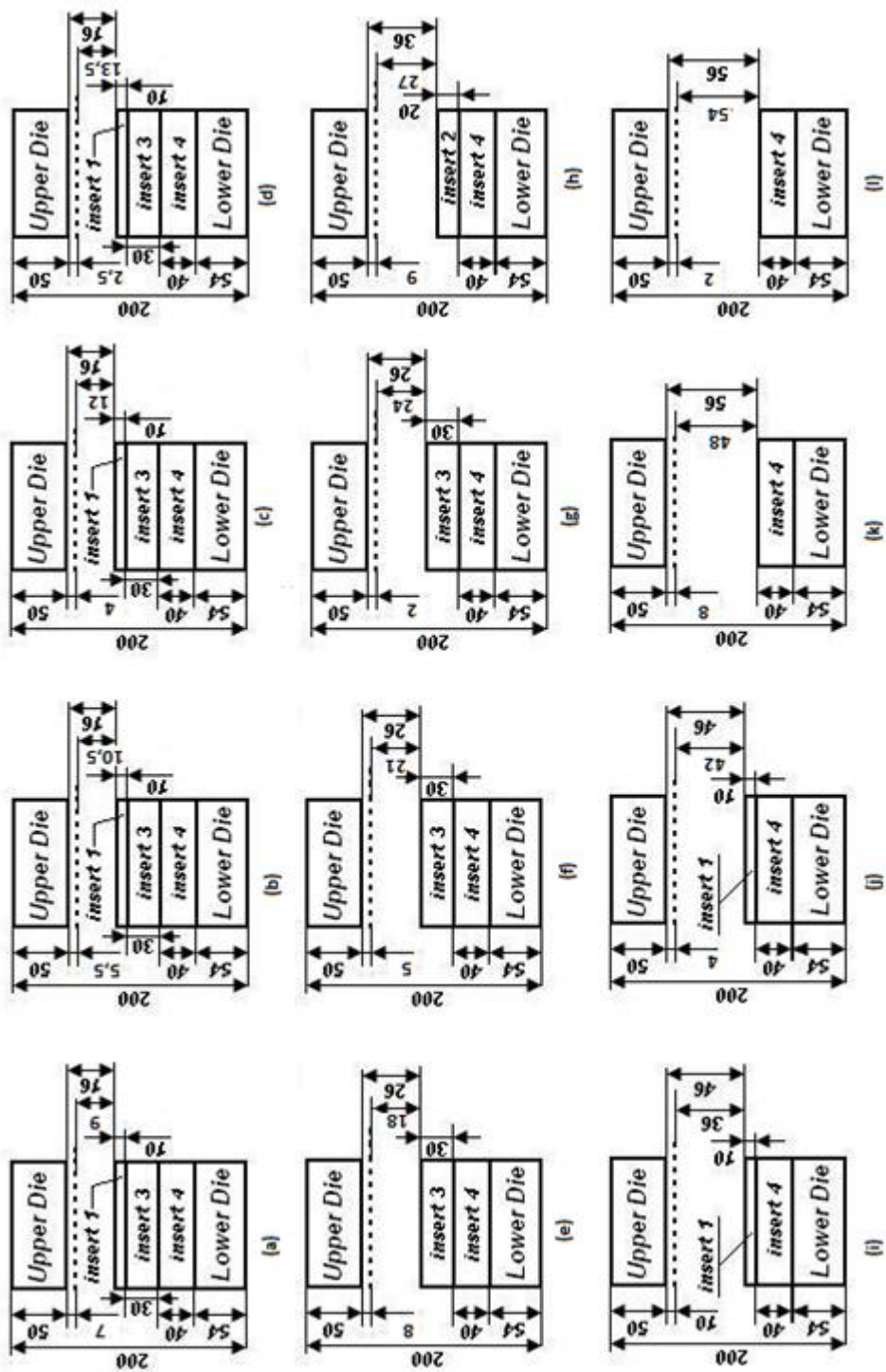


Figure 5.3 Configurations of the modular die set

5.3. Simulation Process Parameters for Finite Element Method

To analyze the metal flow, finite volume method has been used extensively. In the recent years, by means of some computer simulation programs like SuperForge, it is possible to simulate the metals at solid state. In the finite element analysis with SfForming 10.0 module of Simufact 3.0 [23], prior to execution, some simulation parameters should be defined.

5.3.1. Defining the Process Type, Importing Forging Dies and Modeling of Billet

Process type is selected as "upsetting". After selecting process type, forging process is defined as "hot forging", simulation is 2-D and the used solver is finite element.

"Auto Shape" function of the program can be used for the simple parts like billet or simple dies. However, initially the dimensions should be specified. The billet dimensions and modular die configurations are selected according to the Table 5.2.

5.3.2. Assigning the Material Properties of Dies and Billet

In this analysis, the dies are considered as rigid die with heat conduction. Because of this reason, the die material is not defined although different types of die material data exist in the material library of SfForming 10.0 [23].

Tensile yield strength and ultimate tensile and compressive strength of X48CrMoV8-1 are given in Table 5.3. The tensile strength figures are to be considered as typical values only. All samples were taken in the rolling direction from a round bar with the diameter of 35 mm. The samples have been hardened in oil at $1010 \pm 10^\circ\text{C}$ and tempered twice to the hardness indicated. [24]

Some other physical properties are given in Table 5.4. The given figures are for a billet hardened and tempered to 58 HRC.

Table 5.3 Some of the Mechanical Properties of X48CrMoV8-1 for Various Hardness Values [24]

	Hardness HRC		
	58	55	50
Tensile strength R_m N/mm ²	1 960	1 860	1 620
Yield point $R_{p0.2}$ N/mm ²	1 715	1 620	1 470
Reduction of area, Z %	15	28	35
Elongation, A5 %	6	7	8
Compressive strength R_m N/mm ²	2 745	2 450	2 060
Compressive strength $R_{p0.2}$ N/mm ²	2 110	2 060	1715

Table 5.4 Some Other Physical Properties of X48CrMoV8-1 at Various Temperatures [24]

Temperature	20°C	200°C	400°C
Density kg/m ³	7 750	7 700	7 650
Coefficient of thermal expansion per °C from 20°C	–	11,6 x 10 ⁻⁶	11,3 x 10 ⁻⁶
Modulus of elasticity N/mm ²	190 000	185 000	170 000
Thermal conductivity W/m°C	26,1	27,1	28,6
Specific heat J/kg °C	460	–	–

5.3.3. Initial Temperature of Billet and Dies

The initial temperature of the billet is taken as 1050°C. The dies are preheated to 200°C. The rest of the parameters used for the analysis are given below;

Ambient temperature: 25°C

Emissivity for heat radiation to ambient: 0.25

Heat transfer coefficient to ambient: 50 W/m².K

Heat transfer coefficient to work piece: 6000 W/m².K

5.3.4. Defining the Coefficient of Friction

The definition of the friction between the billet and the die plays an important role on the analysis. The shear force due to the friction between the billet and the die, restricts motion of the billet.

From the previous studies [11, 25, 31], the friction coefficient is ranged from 0.06 to 0.24. In this study, the friction coefficient is taken as 0.2.

5.3.5. Defining the Press in Finite Element Program

The mechanical forging press in METU-BILTIR Center Forging Research and Application Laboratory is defined with Crank Radius, R, of 110mm, Rod Length, L, of 750 and Revolution Speed, REV, of 100 rpm. This parameters are schematically shown in Figure 5.4.

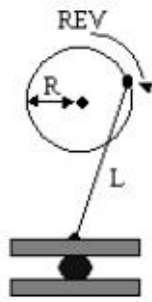


Figure 5.4 Illustration of Crank Press Schematic [23]

Since the billets are axi-symmetric, axi-symmetric elements are used. The element type is four-node rectangular finite element as shown in Figure 5.5 .

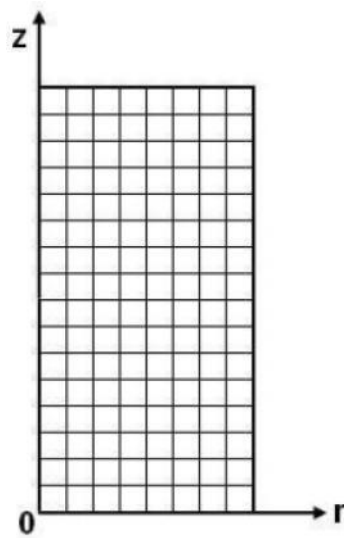


Figure 5.5 Axi-symmetric Problem Set Up for the Finite Element Analysis [22]

5.4. Analysis of Tool Steel Forging Process by Finite Element Method

In this part of the study, 12 different forging operations are simulated. The sizes of the billets and the percentage reduction have already been defined in Table 5.1. For all operations, the billets and the dies are arranged to be in contact as an initial condition. In other words, as soon as the upper die moves down the deformation begins immediately. This orientation of the billet and the dies is shown in Figure 5.6.

The mesh quantity and size are defined. In total, there are three different billets prior to forging operation, so three different meshing operations have been conducted by the software. The results are given in Table 5.5.

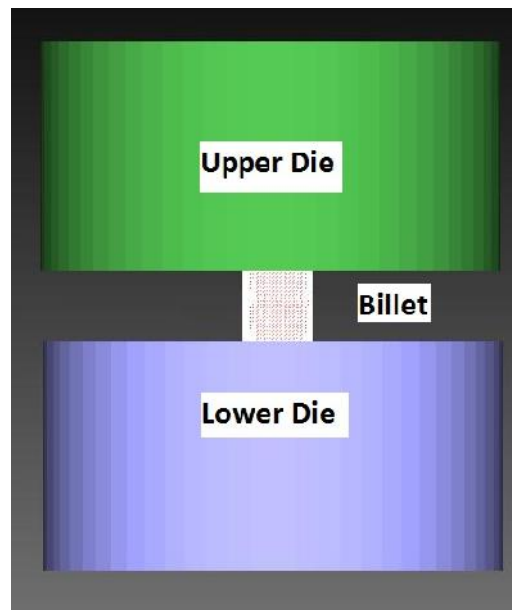


Figure 5.6 Orientation of the Dies and Billets Prior to Forging

Table 5.5 Details Regarding the Meshing

Height of the Billet (mm)	Total Amount of Mesh	The Size of Mesh (mm)
15	441	0,721
30	882	0,721
60	1743	0,721

5.5. Simulation Results of Forging

After simulation of the forging operation, the force requirement, stress values and strain are obtained by the finite element program. As stated previously, 12 different simulations have been made with an initial temperature of 1050°C. The results are given in Figure 5.7-5.42.

In the effective plastic strain distribution figures, the red color always represents the effective plastic strain values and the blue the lowest values. For all groups, the maximum effective plastic strain occurs on surface and at the middle of the billet.

In the temperature distribution figures, the white color always represents the maximum temperature distribution values and the gray the lowest values. For all groups, the maximum temperature distribution occurs at the center of the specimen and on the edge.

In the die force diagrams, the forces are given as a function of time. In each diagram, there are two symmetrical curves, the blue curve is for the upper die and red curve is for the lower die. The results are tabulated in Table 5.6. The maximum die force has been found for Billet Group No 12, which has the highest reduction ratio (i.e. 40%) and smallest (i.e. 15mm)

Table 5.6 Maximum Die Forces for Each Billet Group

Billet Group No.	Maximum Die Force (KN)
1	1530
2	1210
3	1020
4	938
5	1245
6	1060
7	924
8	810
9	1160
10	1010
11	913
12	808

Even the maximum force, which is 1,53MN, is far below the capacity of SMERAL mechanical press in METU-BILTIR Center Forging Research and Application Laboratory, which is 10MN. Therefore, the billets will be safely forged on the SMERAL mechanical press.

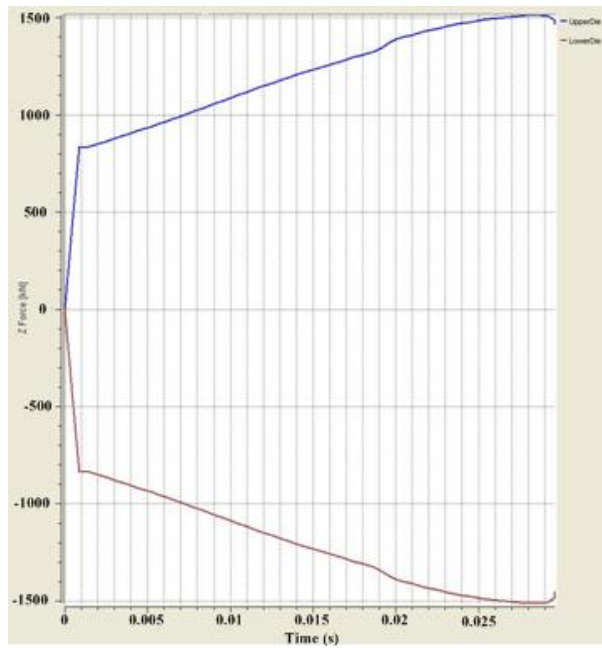


Figure 5.7 Variation of Die Force with Respect to Time for Billet Group No:1

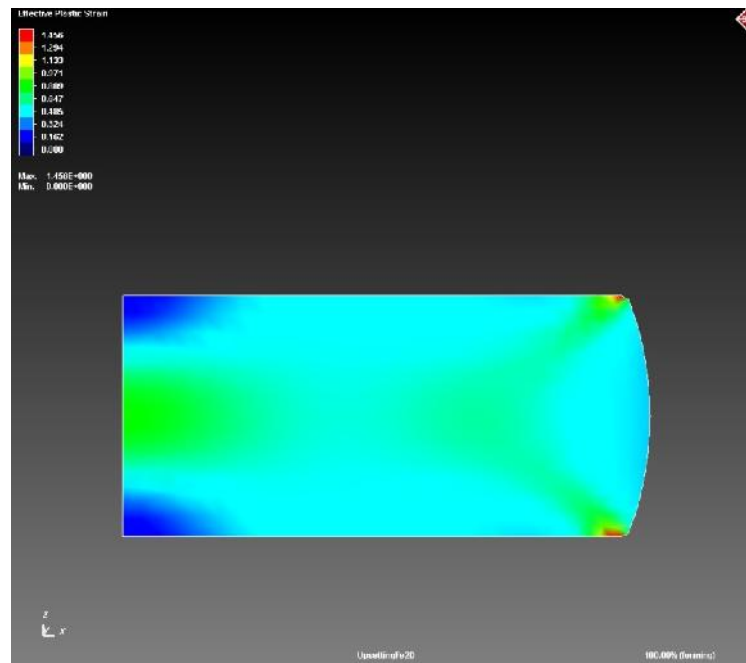


Figure 5.8 Effective Plastic Strain for Billet Group No:1

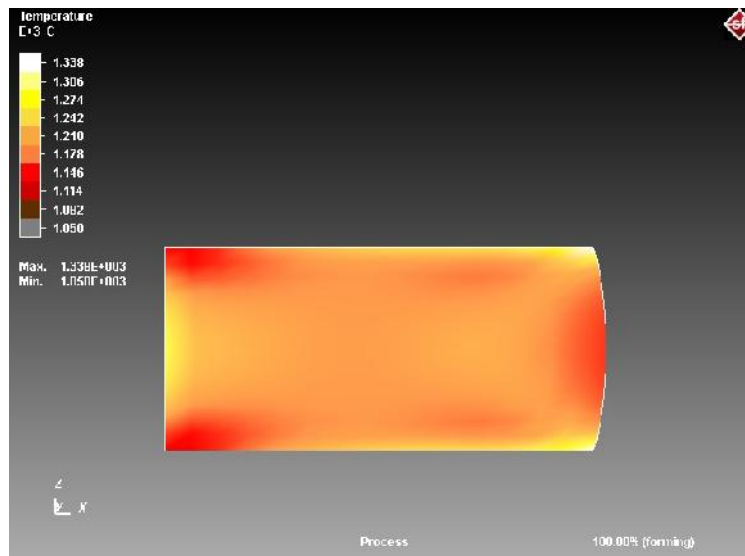


Figure 5.9 Temperature Distribution for Billet Group No:1

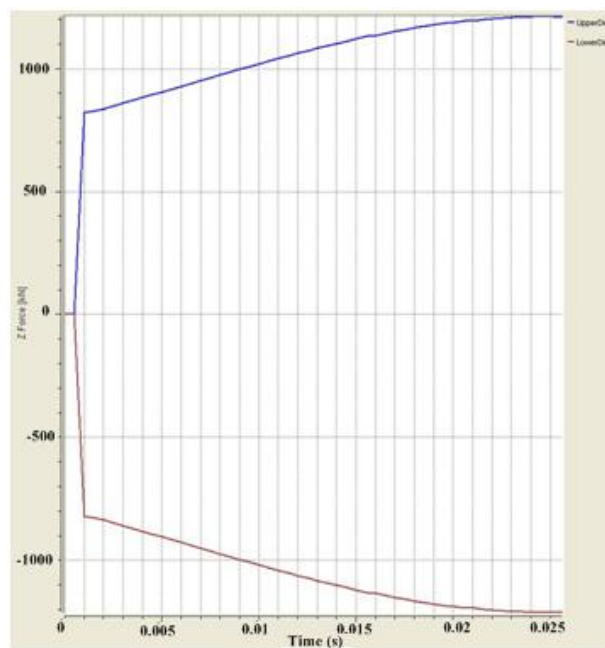


Figure 5.10 Variation of Die Force with Respect to Time for Billet Group No: 2

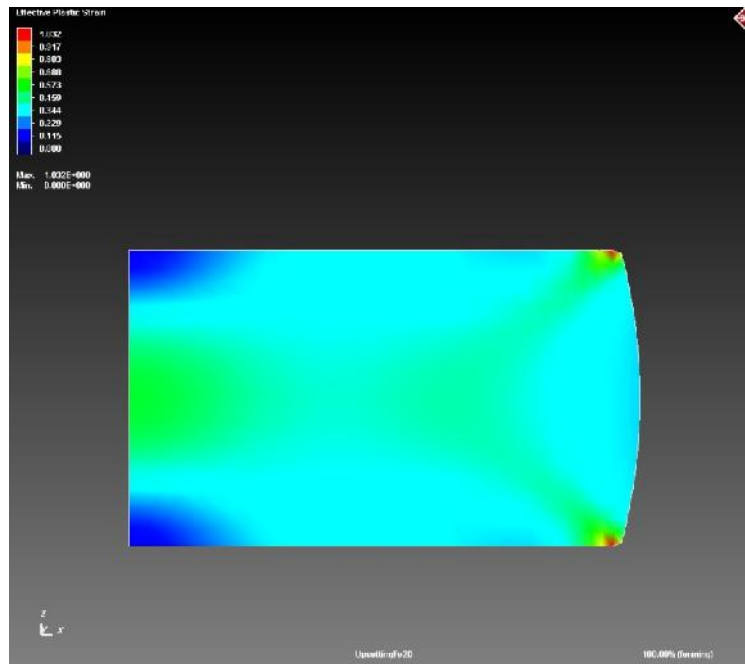


Figure 5.11 Effective Plastic Strain for Billet Group No:2

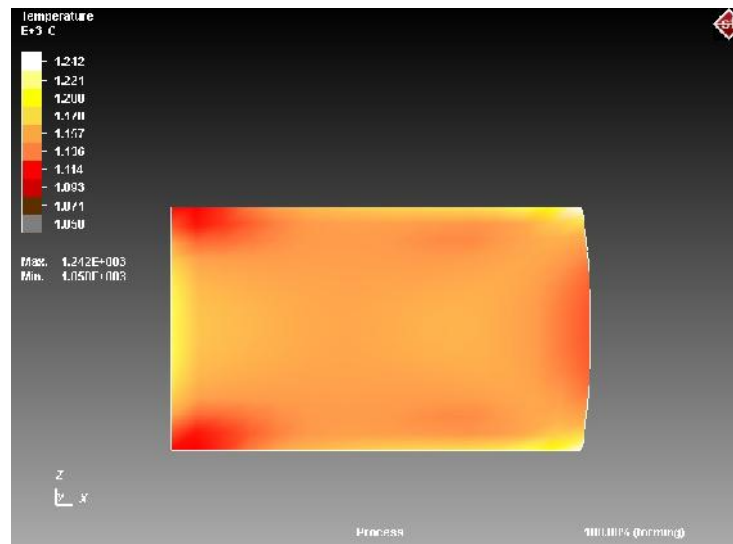


Figure 5.12 Temperature distribution for Billet Group No:2

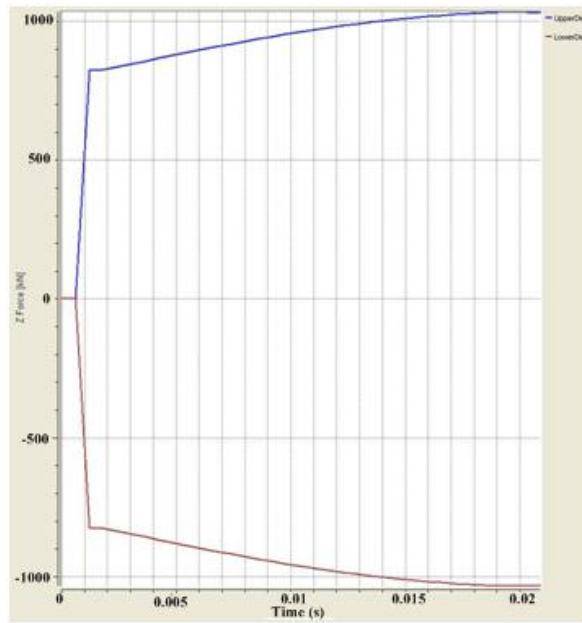


Figure 5.13 Variation of Die Force with Respect to Time for Billet Group No: 3

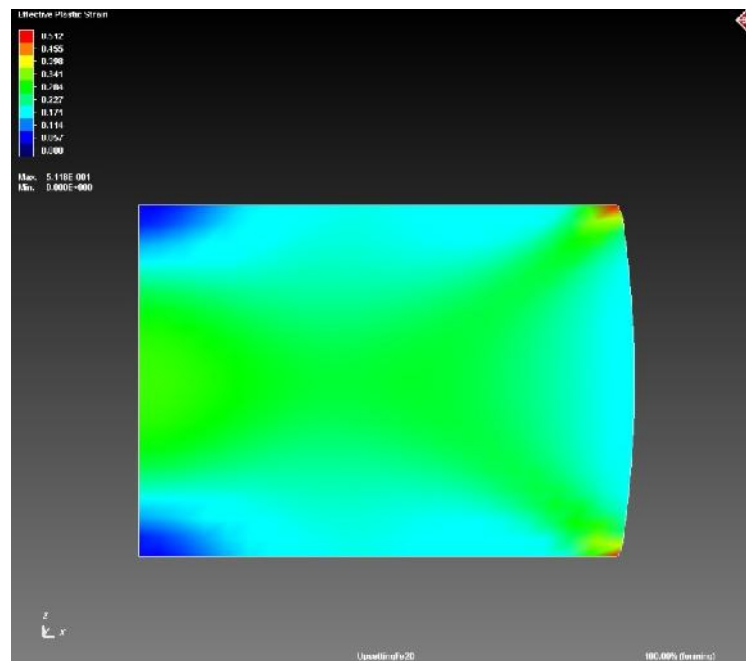


Figure 5.14 Effective Plastic Strain for Billet Group No:3

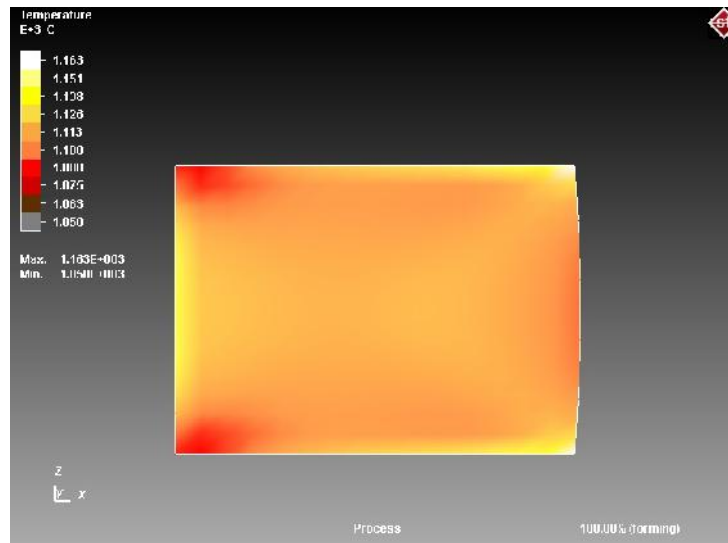


Figure 5.15 Temperature Distribution for Billet Group No:3

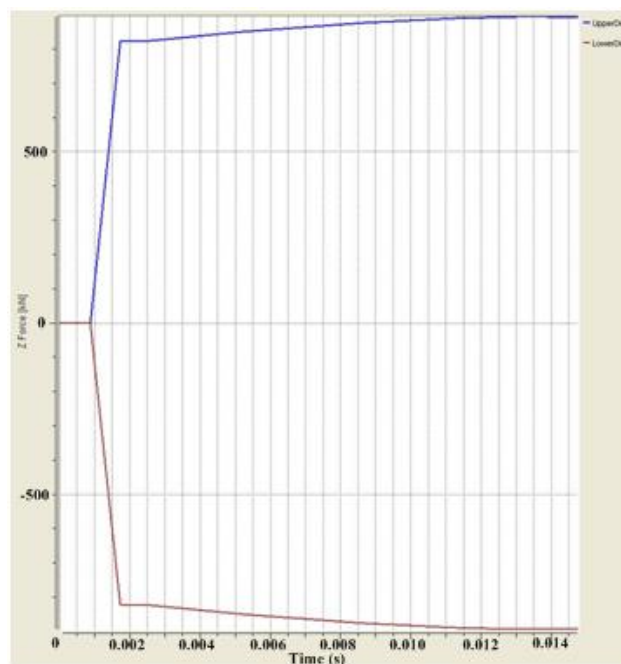


Figure 5.16 Variation of Die Force with Respect to Time for Billet Group No: 4

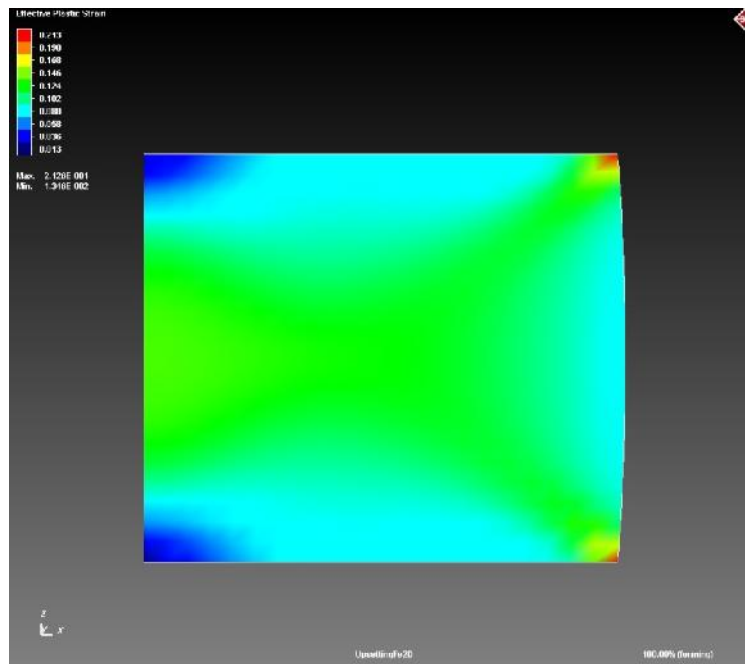


Figure 5.17 Effective Plastic Strain for Billet Group No:4

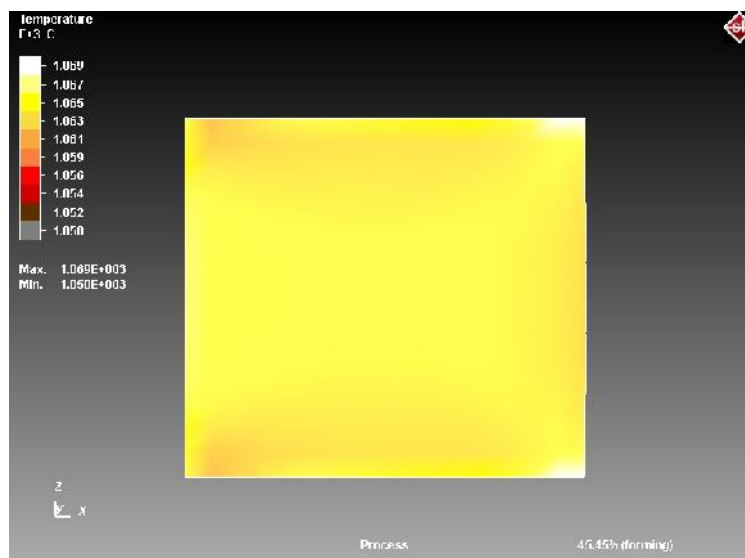


Figure 5.18 Temperature Distribution for Billet Group No:4

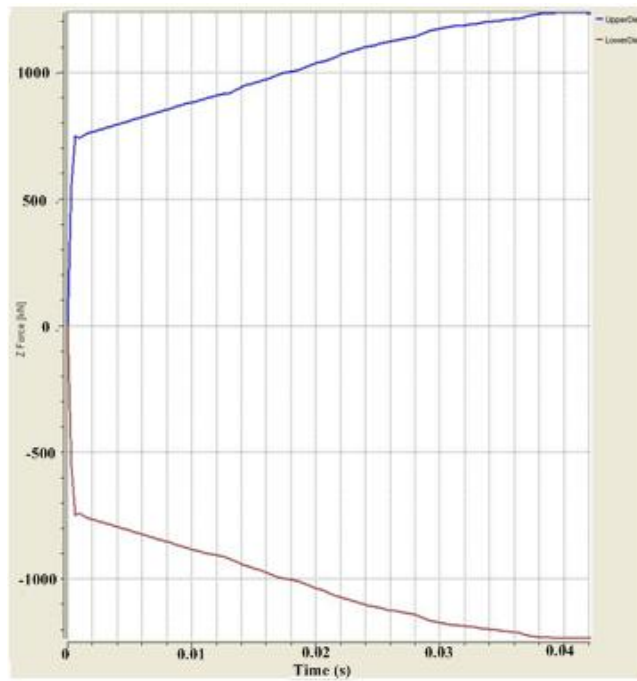


Figure 5.19 Variation of Die Force with Respect to Time for Billet Group No: 5

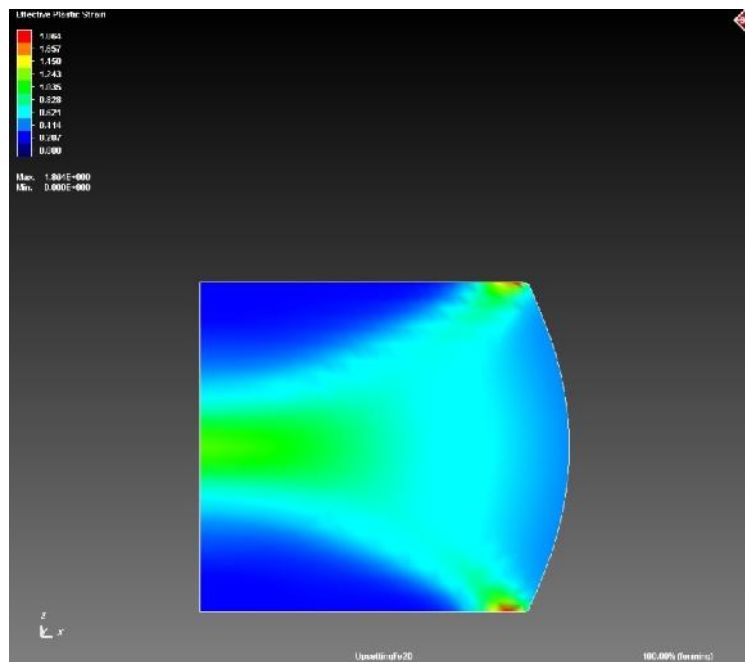


Figure 5.20 Effective Plastic Strain for Billet Group No:5

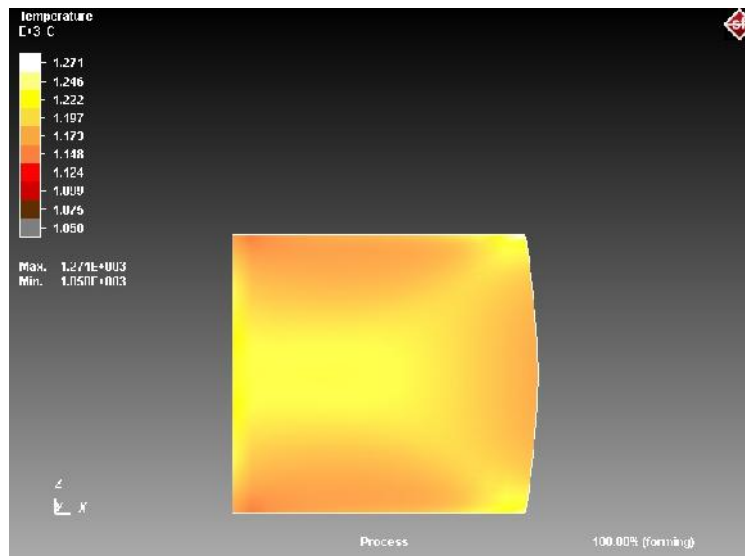


Figure 5.21 Temperature Distribution for Billet Group No:5

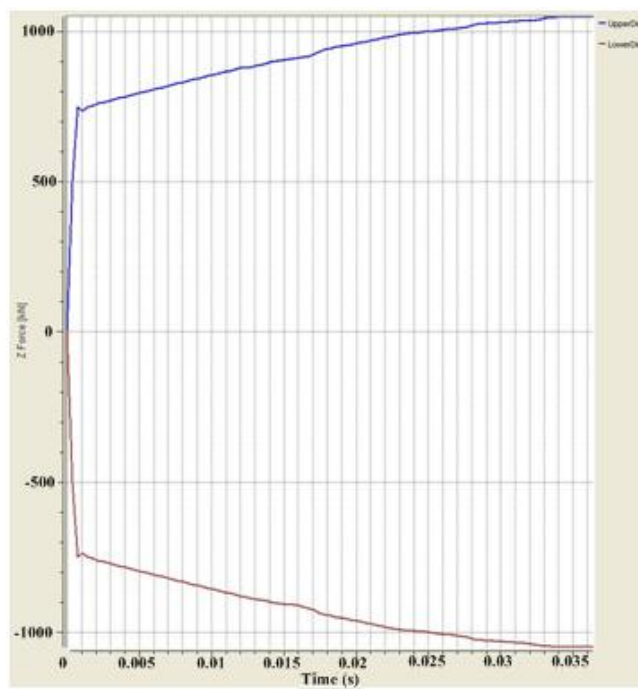


Figure 5.22 Variation of Die Force with Respect to Time for Billet Group No: 6

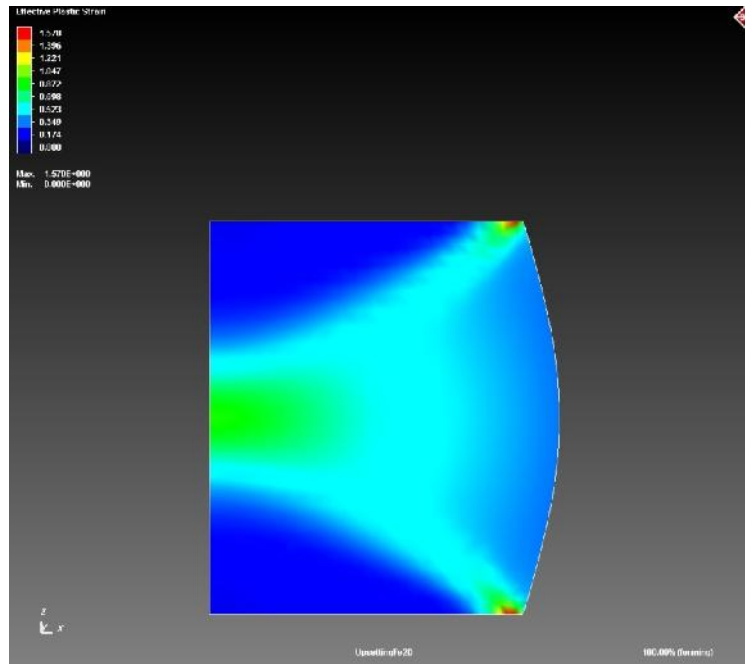


Figure 5.23 Effective Plastic Strain for Billet Group No:6

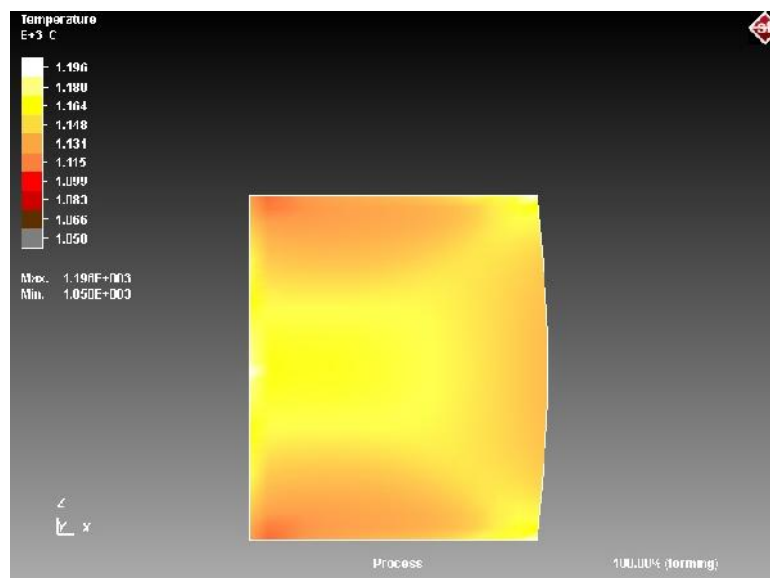


Figure 5.24 Temperature Distribution for Billet Group No:6

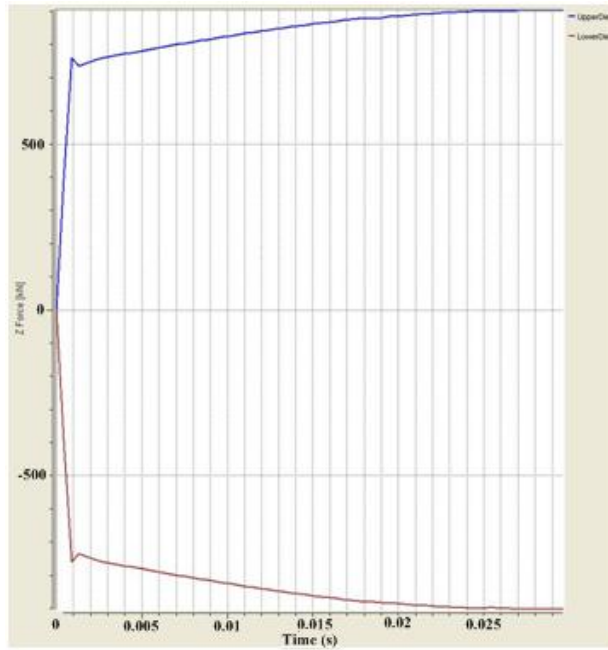


Figure 5.25 Variation of Die Force with Respect to Time for Billet Group No: 7

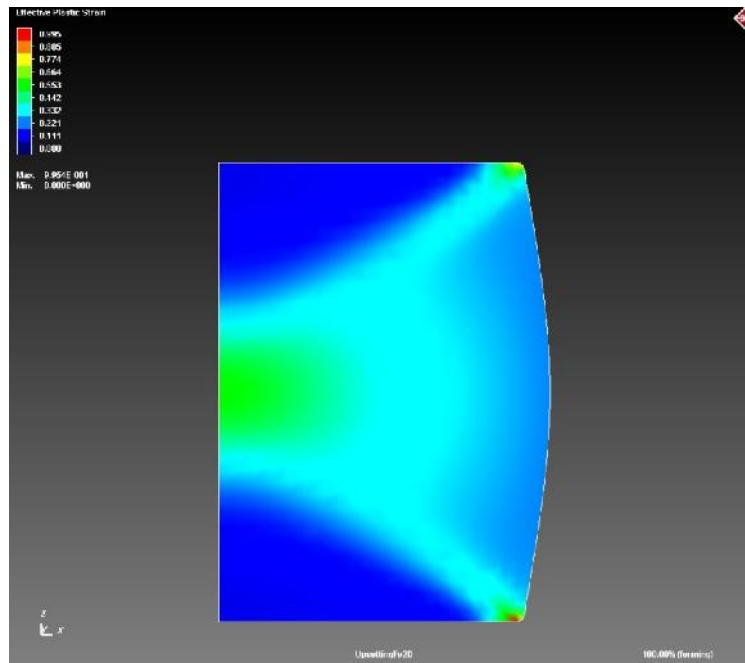


Figure 5.26 Effective Plastic Strain for Billet Group No:7

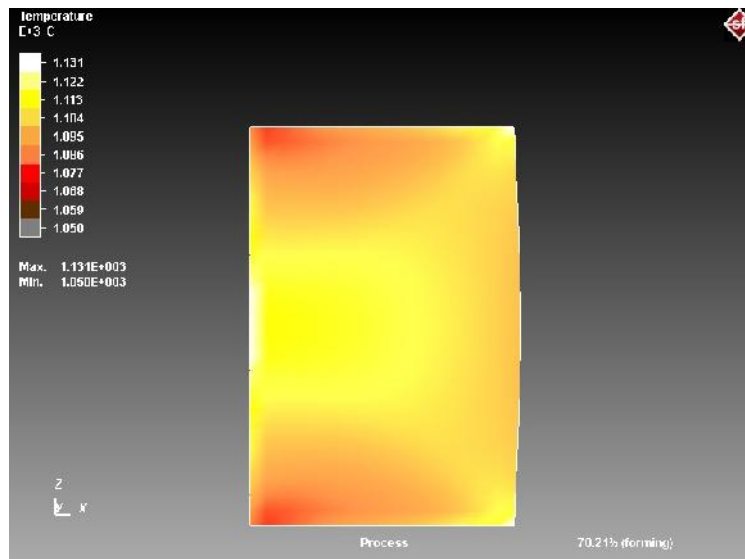


Figure 5.27 Temperature Distribution for Billet Group No:7

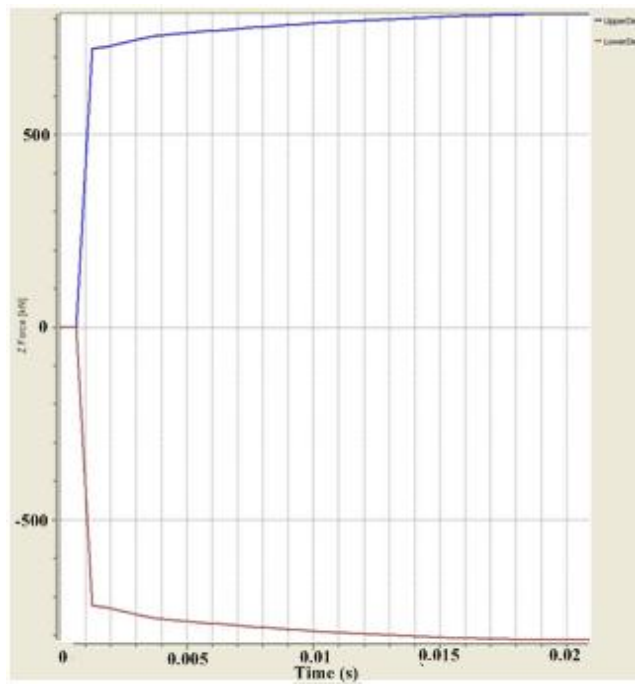


Figure 5.28 Variation of Die Force with Respect to Time for Billet Group No: 8

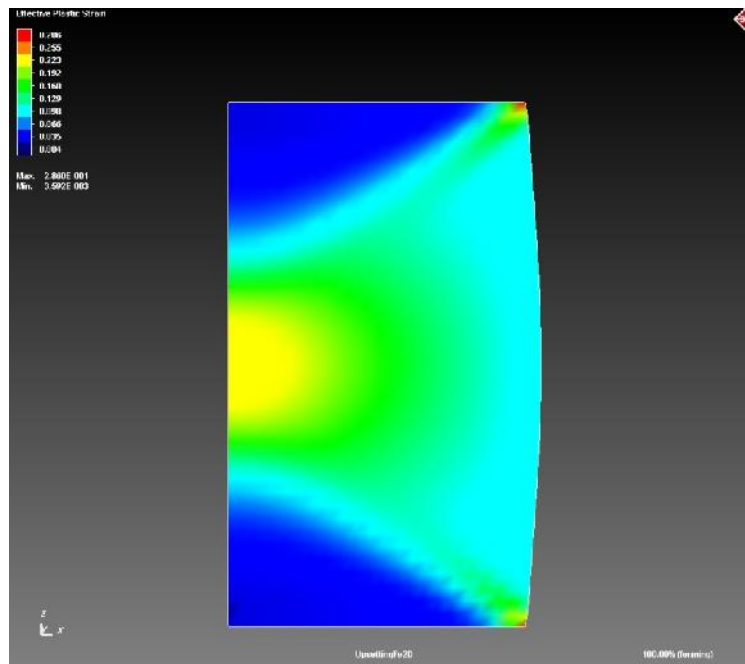


Figure 5.29 Effective Plastic Strain for Billet Group No:8

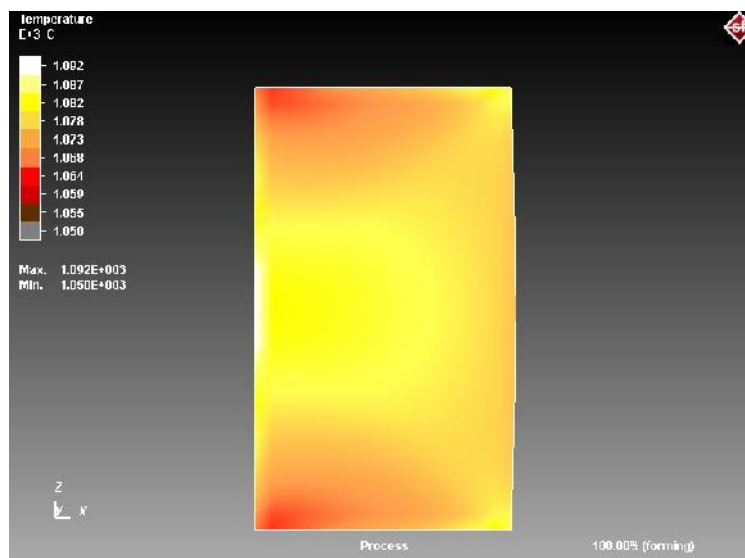


Figure 5.30 Temperature Distribution for Billet Group No:8

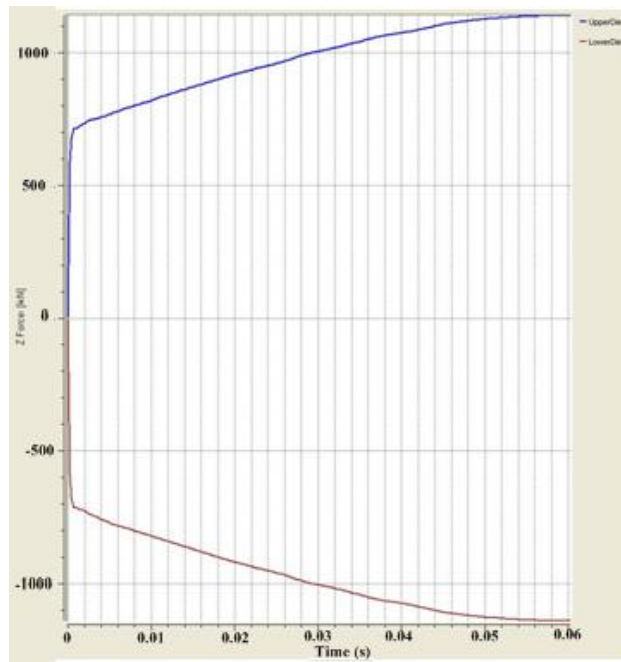


Figure 5.31 Variation of Die Force with Respect to Time for Billet Group No: 9

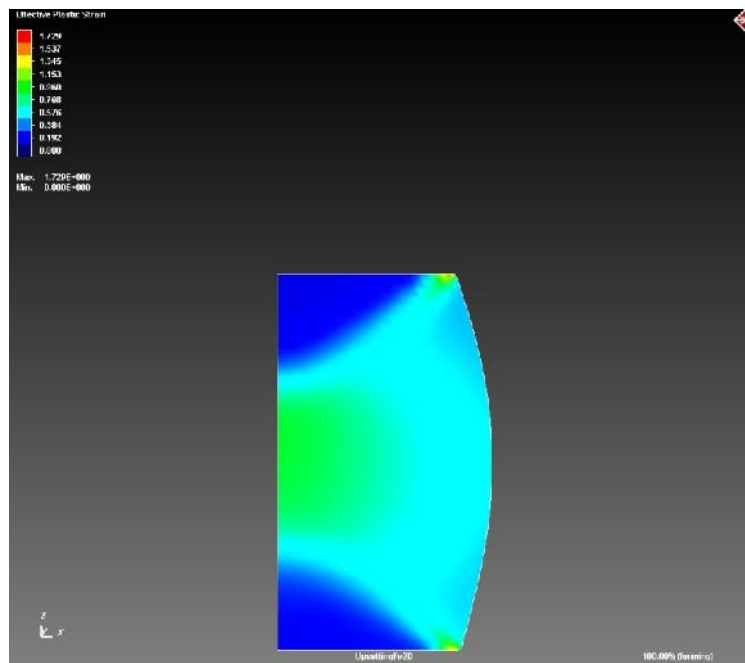


Figure 5.32 Effective Plastic Strain for Billet Group No:9

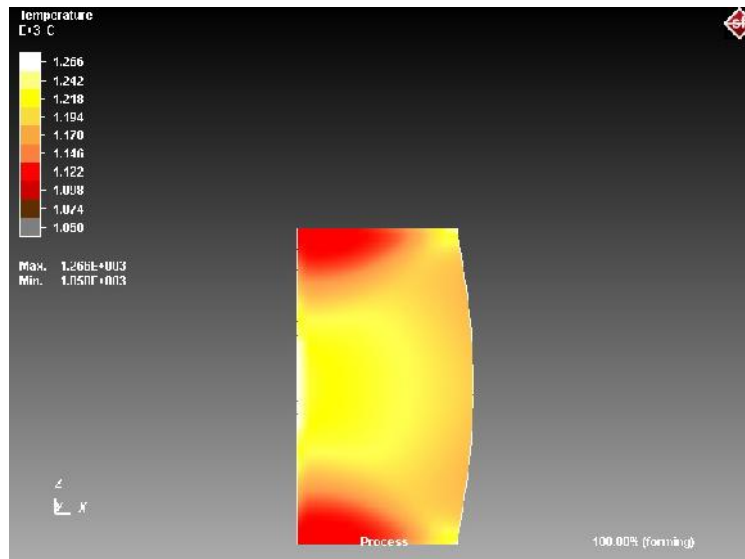


Figure 5.33 Temperature Distribution for Billet Group No:9

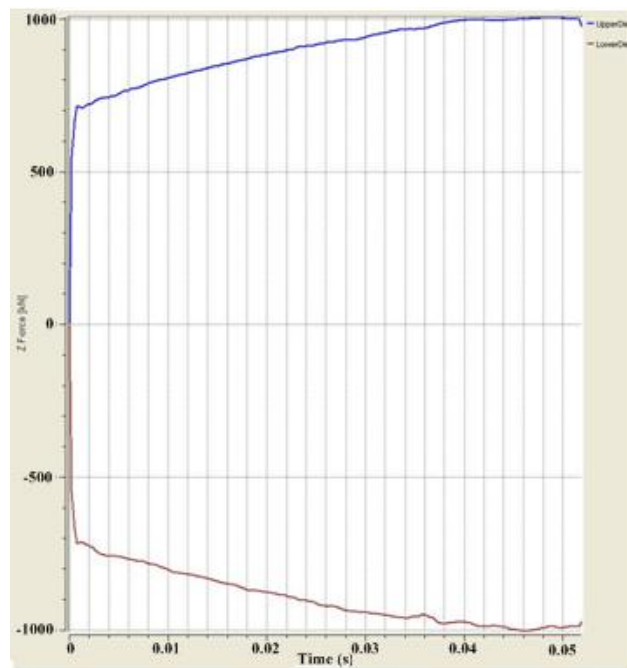


Figure 5.34 Variation of Die Force with Respect to Time for Billet Group No: 10

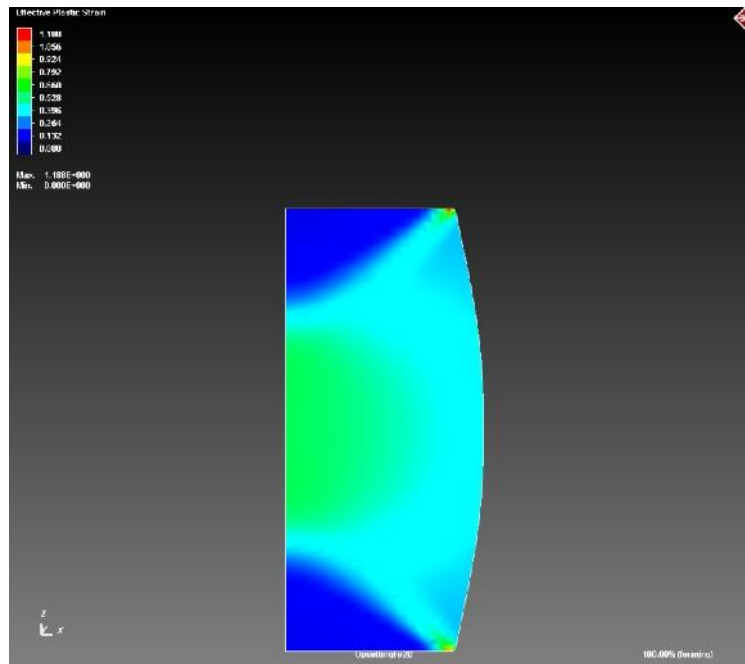


Figure 5.35 Effective Plastic Strain for Billet Group No:10

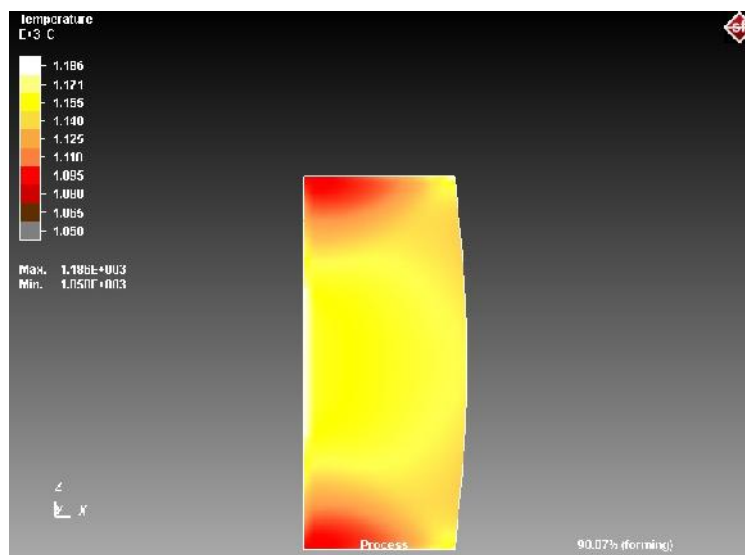


Figure 5.36 Temperature Distribution for Billet Group No:10

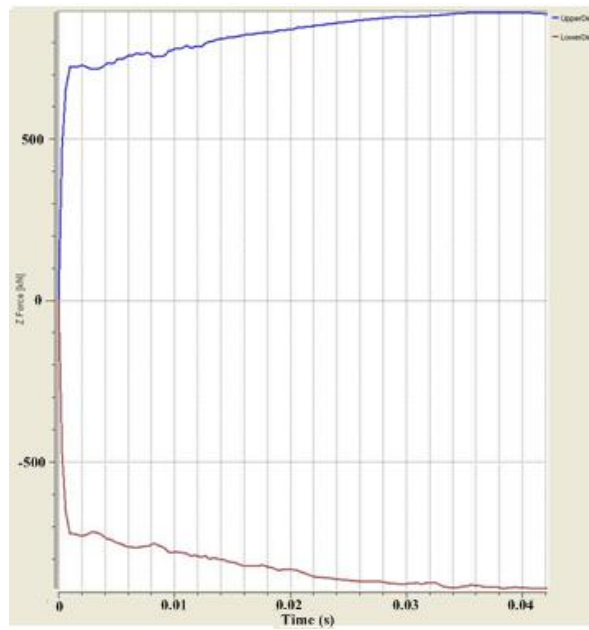


Figure 5.37 Variation of Die Force with Respect to Time for Billet Group No: 11

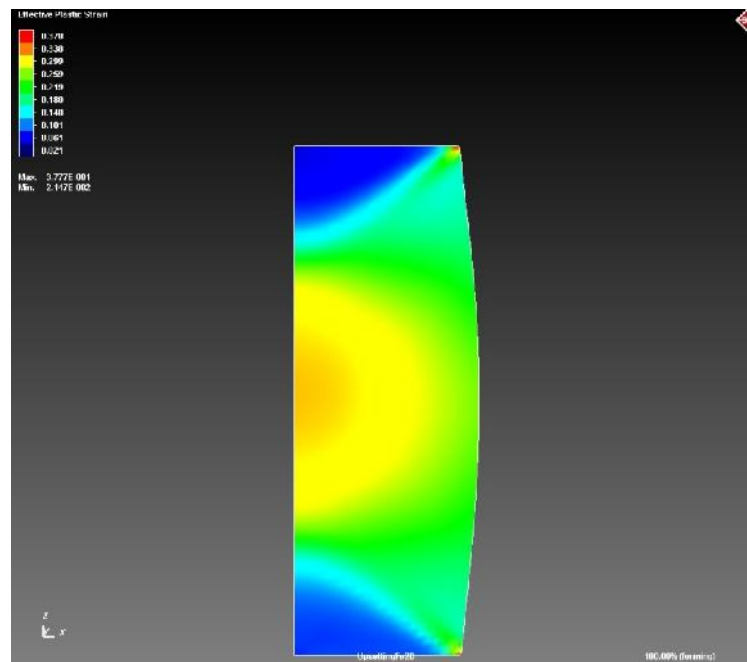


Figure 5.38 Effective Plastic Strain for Billet Group No:11

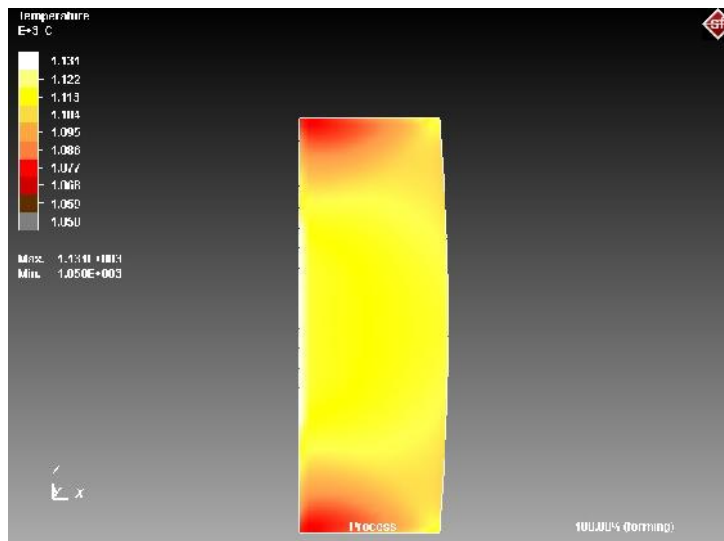


Figure 5.39 Temperature Distribution for Billet Group No:11

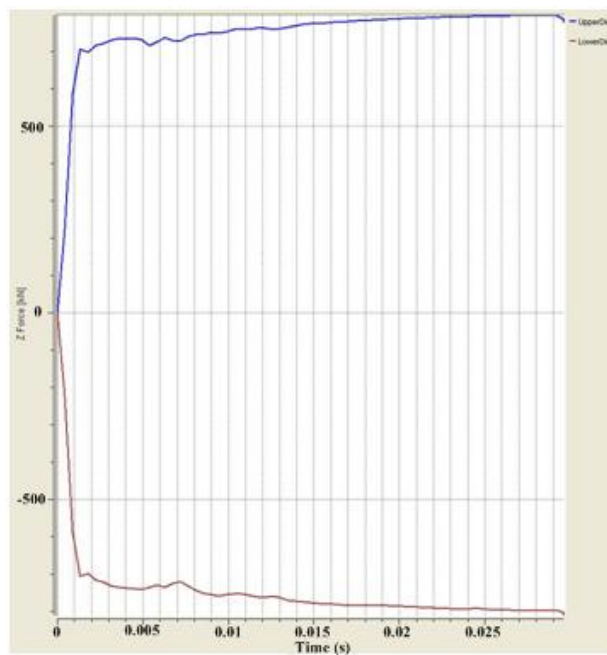


Figure 5.40 Variation of Die Force with Respect to Time for Billet Group No: 12

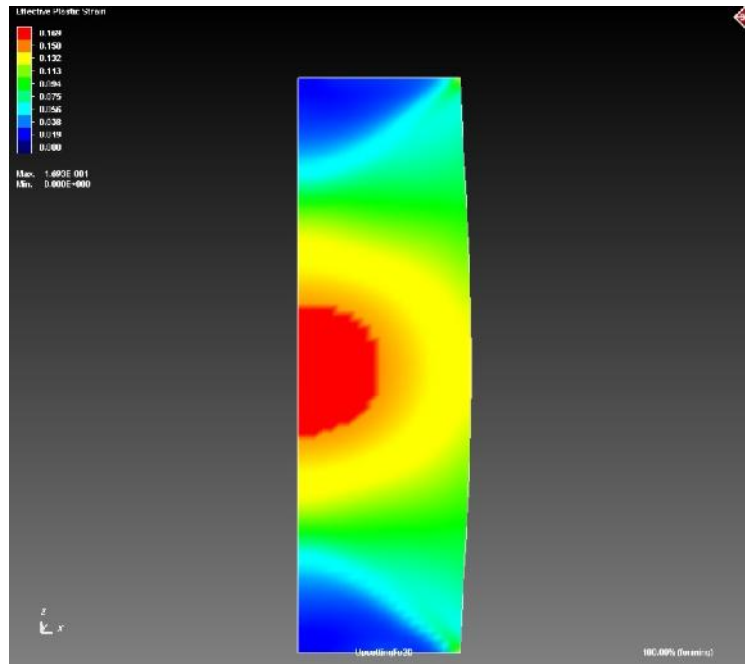


Figure 5.41 Effective Plastic Strain for Billet Group No:12

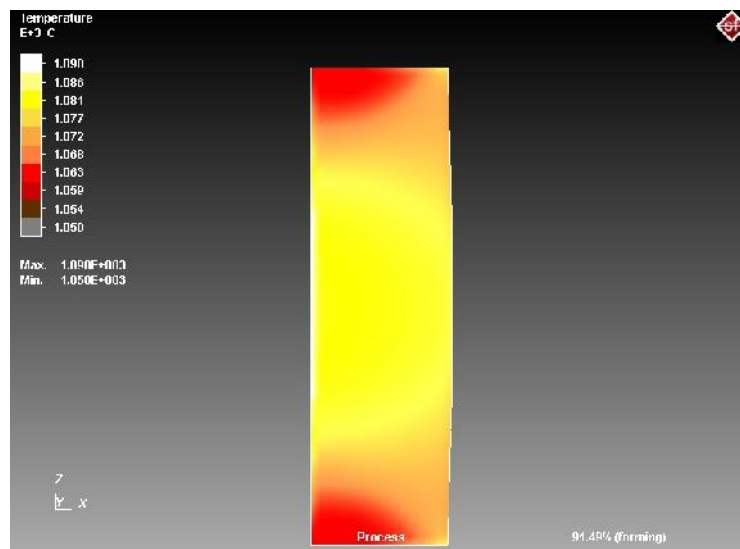


Figure 5.42 Temperature Distribution for Billet Group No:12

CHAPTER 6

MANUFACTURING OF TOOL STEEL SHEAR BLADE SPECIMENS AND FORGING PROCESS

6.1. Introduction

In Chapter 5, the design of the upsetting dies and the billets have been described and the finite element analyses have been conducted in Chapter 4. It has been found that the maximum forces required for forging are lower than the capacity of the forging press available in METU-BILTIR Center Forging Research and Application Laboratory for all billets. The technical information about the 10 MN SMERAL mechanical press is given in Appendix A. Hence, the press is capable of conducting the experiments. In this chapter, firstly the preparation for the billets to the experiment will be explained and then the forging operation of X48CrMoV8-1 billets will be explained.

6.2. Preparation for the Forging Operation

As mentioned in the previous chapters, the billets have been poured and heat-treated. For the consistency of the experiments, 3 billets were produced from each billet group. Since there are 12 groups of billets, in total there will be 36 billets.

At this stage, to remove the excessive material and to obtain a smooth surface, all of the billets were machined by a conventional lathe as shown in Figure 6.1. The dimensions after machining are tabulated in Table 6.1. The turned billets are shown in Figure 6.2.



Figure 6.1 Turning Operation of the Specimens



Figure 6.2 Turned Specimens

Table 6.1 Billet Dimensions After Turning

Billet Id No	Specimen Diameter d_0 (mm)	Specimen Height h_0 (mm)
1	30,03	15,20
2	30,10	15,10
3	30,06	15,06
4	30,03	15,08
5	30,00	30,10
6	29,98	29,96
7	30,05	30,03
8	30,10	30,05
9	30,05	60,20
10	30,02	60,12
11	30,05	59,87
12	30,10	60,02
13	30,05	15,12
14	30,02	15,08
15	30,04	14,96
16	30,06	15,01
17	30,03	30,02
18	30,10	30,10
19	30,05	30,06
20	30,10	30,12
21	30,02	60,02
22	30,04	60,18
23	30,06	60,06
24	30,06	60,05
25	30,03	15,11
26	30,10	15,13
27	30,06	14,99
28	30,03	15,00
29	30,03	30,02
30	30,10	30,14
31	29,99	30,07
32	30,05	30,02
33	30,10	60,19

Table 6.1 Billet Dimensions After Turning (Cont'd)

Billet Id No	Specimen Diameter d_0 (mm)	Specimen Height h_0 (mm)
34	30,05	59,79
35	30,04	60,02
36	30,06	60,12

6.3. Experimentation of the Tool Steel Forging Process

In this study 1000 ton forging press in METU-BILTIR Center Forging Research and Application Laboratory was used. To deform the billets with different strain ratios, a modular die set was required. On both lower and upper dies, the dimensions of the circular die housings are the same. The upper die holder was assembled on the ram. The lower die holder consists of die housing and clamping elements on anvil. The complete configuration of the lower die design set is shown in Figure 6.3.

In the experiment, firstly the billets were heated to 1050°C . For this purpose, KVA-3000 Hz induction heater, which is available in METU-BILTIR Center Forging Research and Application Laboratory, was used. The temperatures of the billets were measured before and after the forging operation. In Figure 6.4, the temperature measurement is shown prior to forging. In the mean time, the dies were also preheated by means of the flame gun of an LPG tube which is shown in Figure 6.5. Portable optical pyrometer was used to measure the temperatures of the dies.



Figure 6.3 Lower Die Assembly of the Forging Press



(a)



(b)

Figure 6.4 a) Billet at the Output of Furnace b) The Temperature Measurement of the Billet

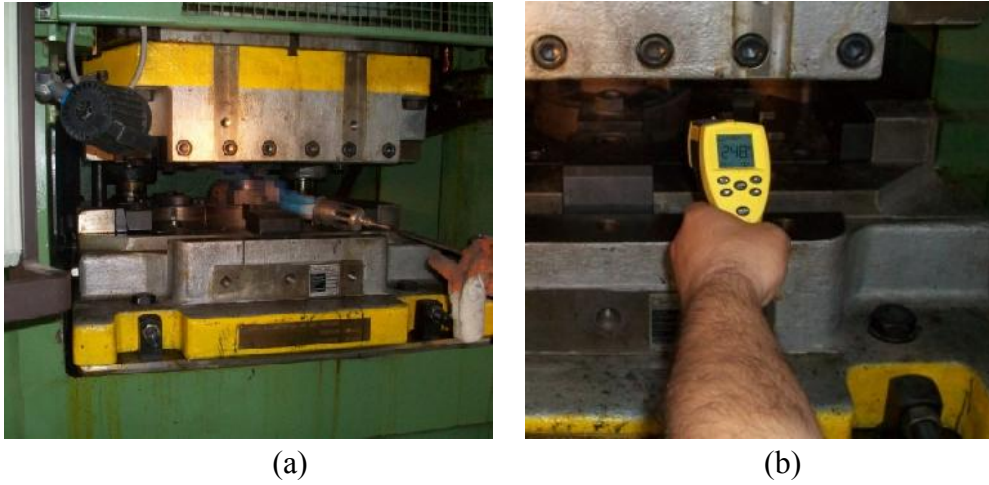


Figure 6.5 a) Preheating of the Dies b) The Temperature Measurement of the Dies

When the billets come out of the induction heater, their temperatures were measured first by the pyrometer. Then, the billets were placed on the lower die.

The heated billets were hold with the tong and their temperatures were measured by the pyrometer before upsetting and the observed temperature values were recorded. The billets were placed on the lower die of the press as shown in Figure 6.6.

As shown in Figure 6.7, the forged pieces were group on the floor after forging. When the billets cool down, they were cleaned first and finally their heights were measured.

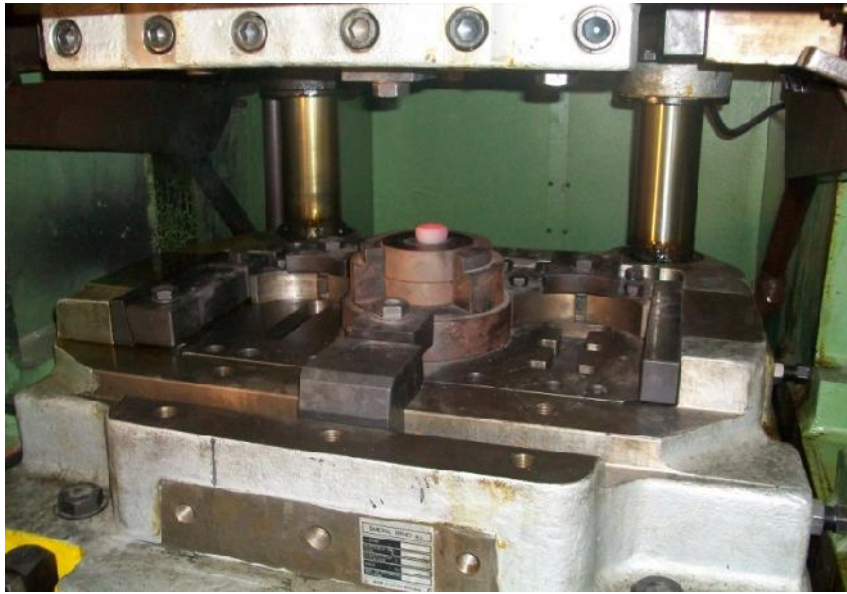


Figure 6.6 Billet Just After Forging



Figure 6.7 Grouped Billets After Forging

6.4. Results of the Experiments

The initial and final dimensions of the billets and temperature of billet and die are tabulated in Table 6.2.

Table 6.2 Measures of the Forging Process

Billet Group No	Specimen ID No	Initial Height (h ₀)	Final Height (h _f)	Temperature of Billet (°C)	Temperature of Die (°C)
1	1	15,2	9,03	1033	237
	13	15,12	9,05	1036	236
	25	15,11	9,07	1045	240
2	2	15,1	10,52	1038	255
	14	15,08	10,54	1040	260
	26	15,13	10,57	1046	270
3	3	15,06	12,03	1055	268
	15	14,96	12,06	1048	244
	27	14,99	12,01	1053	251
4	4	15,08	13,05	1041	260
	16	15,01	13,09	1034	238
	28	15	13,02	1045	254
5	5	30,1	18,04	1055	274
	17	30,02	18,08	1037	245
	29	30,02	18,02	1032	244

Table 6.2 Measures of the Forging Process (Cont'd)

Billet Group No	Specimen ID No	Initial Height (h ₀)	Final Height (h _f)	Temperature of Billet (°C)	Temperature of Die (°C)
6	6	29,96	21,01	1040	260
	18	30,1	21,07	1046	270
	30	30,14	21,03	1050	265
7	7	30,03	24,06	1039	275
	19	30,06	24,03	1042	269
	31	30,07	24,09	1047	264
8	8	30,05	27,01	1041	238
	20	30,12	27,04	1050	342
	32	30,02	27,07	1051	260
9	9	60,2	36,05	1037	244
	21	60,02	36,02	1055	251
	33	60,19	36,09	1059	261
10	10	60,12	42,02	1065	266
	22	60,18	42,08	1062	284
	34	59,79	42,06	1043	269
11	11	59,87	48,04	1041	258
	23	60,06	48,01	1037	254
	35	60,02	48,07	1043	272
12	12	60,02	54,06	1048	275
	24	60,05	54,09	1050	260
	36	60,12	54,03	1055	240

6.5. Quenching and Tempering of the Billets

Cold-work steels are mostly quenched to minimize the presence of grain boundary carbides or to improve the ferrite distribution. Additionally, cold-work steels are quenched to produce controlled amounts of martensite in the microstructure. Successful hardening usually means achieving the required microstructure, hardness, strength, or toughness while minimizing residual stress, distortion, and the possibility of cracking.

The iron lattice is distorted by the carbon atoms in martensite phase. Therefore, quenched parts are excessively brittle. Tempering is a heat treatment process, which is done after quenching. This brittleness of quenching is removed by tempering. Tempering results in a desired combination of hardness, ductility, toughness, strength, and structural stability [32].

Quenching process is mainly cooling steel from the austenitizing temperature rapidly to form the desired microstructural phases, sometimes bainite but more often martensite. The basic function of the quenchant media is to control the rate of heat transfer from the surface of the part being quenched. The liquid quenchant commonly used include [32] ;

- Oil that may contain a variety of additives
- Water
- Aqueous polymer solutions
- Water that may contain salt or caustic additives

Continuous cooling transformation diagrams, as known as CCT diagrams contain a family of curves representing the cooling rates and the final phases corresponding to these cooling rates. These diagrams are useful to estimate the influence of cooling rate on the structure of steel. The CCT diagram for X48CrMoV8-1 is shown in Figure 6.8. For different austenitizing temperatures, holding times and corresponding hardness values after quenching are given in Table 6.3 .

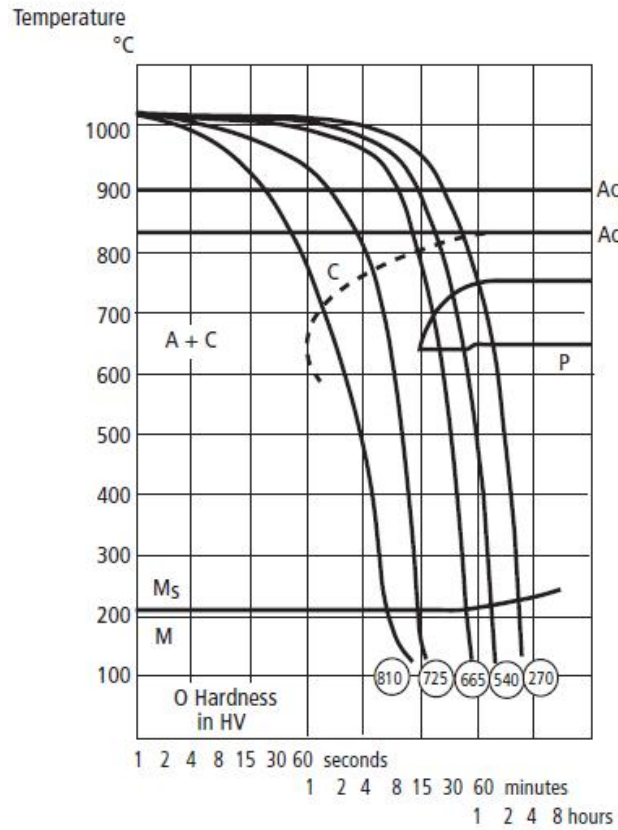


Figure 6.8 CCT Diagram for X48CrMoV8-1 [24]

Table 6.3 Approximate Hardness Values Before Tempering of X48CrMoV8-1 for Different Austenitizing Temperatures [24]

Temperature °C	Holding time minutes	Hardness before tempering (approx.)
980	40	57 HRC
1010	30	60 HRC
1050	20	60 HRC

In this study, the forged billets were firstly heated to 650°C and hold for 2hours. Then, they were heated to 1050°C. These billets were hold at 1050°C for 20 minutes. Finally, the billets were quenched in oil as shown in Figure 6.9



Figure 6.9 Oil Quenching of the Forged Billets

The temperatures of the billets were dropped below 100°C by oil quenching less than 5 minutes. Therefore, according to Figure and Table, the theoretical hardness value of the billets should be at least 62HRC (i.e. 810 HV) before tempering.

The quenching was immediately followed by double tempering at 300°C with one hour for each tempering process. According to the Figure 6.10, the theoretical hardness value after tempering should be around 58HRC.

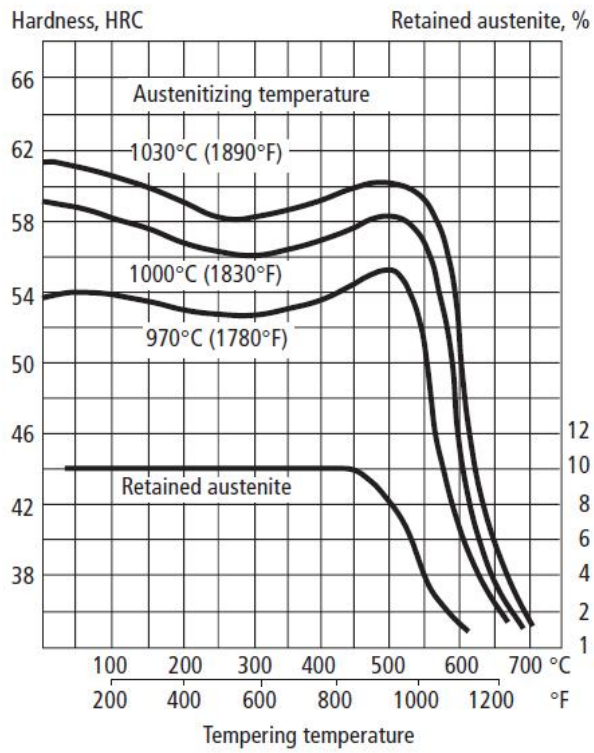


Figure 6.10 Variation of Hardness with Tempering Temperature for X48CrMoV8-1

CHAPTER 7

MECHANICAL TESTS AND MICROSTRUCTURAL ANALYSIS

In previous chapters, the processes related to the production of forced tool steel shear blade is explained. In this chapter, the mechanical properties and microstructure of the produced shear blades will be examined. Moreover, these results will be compared with the results of a commercially available shear blade sample.

7.1. Mechanical Tests

7.1.1. Hardness Test

Hardness testing is one of the methods of mechanically characterizing a material. For tool steels, hardness testing is used very extensively. Since this method does not require an elaborate specimen preparation. Besides, due to the high hardness of the tool steels, it is really hard to prepare specimens. Therefore, in tool steel specifications [24] the mechanical properties of tool steels are mostly based on their hardness values.

In this study, the aim of hardness measurement is to investigate the influence of the critical steps of production on the mechanical properties of cold-work tool steel shear blade. The samples were tested in as annealed, forged and tempered conditions.

Rockwell C hardness test was used, since it is suitable for medium to high hardness [33]. The hardness was measured from 5 point for each specimen by the device shown in Figure 7.1 and the mean value was calculated. As shown in Figure 7.2, the positions of the indentations were arranged according to ISO 6508-1:2005. In the standard, it is stated that “The distance between the centres of two adjacent indentations shall be at least four times the diameter of the indentation” The results are given in Table 7.1.



Figure 7.1 Rockwell Hardness Tester

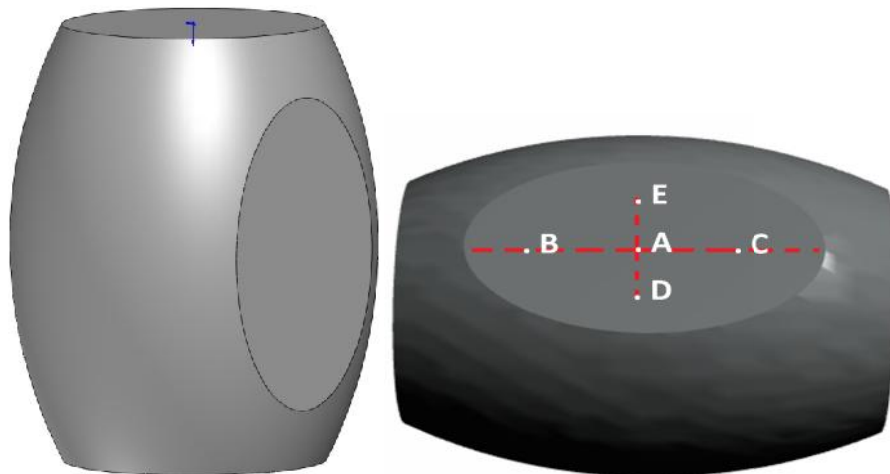


Figure 7.2 Positions of the Indentations from the Ground Side of the Billet

Table 7.1 Hardness of Billets

Type of Specimen	Specimen ID No	Hardness (HRC) at Test Point					Average Hardness (HRC)
		A	B	C	D	E	
Annealed	37	10	12	9	10	11	10,47
	38	11	11	10	9	12	
	39	11	10	10	10	11	
Forged (10% Reduction Ratio)	4	59	58	58	59	58	58,67
	8	58	56	57	60	60	
	12	59	60	59	60	59	
Forged (40% Reduction Ratio)	1	59	60	56	60	61	58,87
	5	58	60	59	59	60	
	9	60	55	60	58	58	
Quenched, Tempered (10% Reduction Ratio)	4	55	56	56	57	58	56,00
	8	56	57	54	58	56	
	12	55	57	56	55	54	
Quenched, Tempered (40% Reduction Ratio)	1	56	55	56	56	57	56,40
	5	55	55	58	54	58	
	9	58	57	58	56	57	

According to the Figure 6.10, the theoretical hardness value for the followed quenching and tempering procedure is 58HRC. Therefore the test results are in accordance with the theoretical results. The tests have shown that, the hardness of the specimens was increased very significantly with forging operation and the heat treatment slightly reduced the hardness.

7.1.2. Charpy Impact Test

The energy needed for the fracturing of the specimen is measured by Charpy impact test. The change in potential energy of the impacting head is measured with a calibrated dial that measures the total energy absorbed in breaking the specimen. [33]

In this study, the notch geometry was prepared according to ASTM E 23 where, the specimen has a V-notch at base of notch as shown in Figure 7.3.

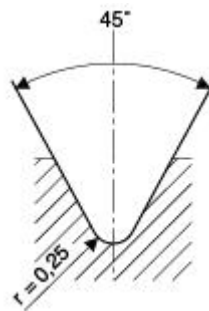


Figure 7.3 V- Notch Geometry

Geometric precision of specimens is crucial for consistent and reproducible test results. The hardness of the cold-work tool steel is around 60 HRC, therefore it is too hard to be machined by conventional tools. That's why; electrical discharge machining was used to machine the specimens as shown in Figure 7.4 and the final shape of the specimens are shown in Figure 7.5



Figure 7.4 V- Notch Machining by Electrical Discharge Machining



Figure 7.5 Charpy V- Notch Specimen

The variation of the impact toughness during the production was investigated by 5 groups of specimens. The first group was annealed specimens. This group is representing the toughness of the shear blades after annealing heat treatment which has been mentioned in Chapter 4. Two types of forged specimens were prepared with different reduction ratios. By this way the influence of the variation of the reduction ratio on the toughness of the shear blade has been investigated. The last two groups are representing the toughness of these two groups of forged samples after quenching and tempering which has been mentioned in Chapter 6. The results of the Charpy impact tests are given in Table 7.2.

Table 7.2 Hardness of Billets as Annealed Condition

Types of Specimens	U-Notch Charpy Impact Test Results (Joule)			
	Test 1	Test 2	Test 3	Average
Annealed	3	4	4	3,7
Forged (10% Reduction Ratio)	3	3	3	3,0
Forged (40% Reduction Ratio)	3	3	4	3,3
Forged, Quenched, Tempered (10% Reduction Ratio)	4	4	4	4,0
Forged, Quenched, Tempered (40% Reduction Ratio)	5	4	4	4,3

7.2. Microstructural Analysis

Cold-work tool steels can be prepared for microscopic examination by using the same basic principles of carbon and alloy steels. On the other hand, cold-work tool steels are high alloyed and they are heat treated to higher hardness as oppose to most carbon and alloy steels. It was difficult to cut the billets, even as annealed condition. This mainly because of the massive carbide particles present in the microstructure.

In this part of the study, the microstructure of shear blade made of X48CrMoV8-1-1 has been examined. Firstly, the billets were grinded slowly and by the help of coolant to avoid overheating and breaking carbide particles. Secondly, the billets have been grinded and polished in several steps. Motor driven disk grinders have been used with 240,320,400,600 and 1200 grit grinding papers. These grinding and polishing steps have been conducted until a shiny and scratch free surface obtained. Finally, the microstructural analysis has been conducted as annealed, as forged with different reduction ratios and as tempered conditions. Additionally, these microstructures have been compared with the microstructures in the literature [33, 34].

7.2.1. As Annealed Microstructure

Hardness of the cold-work tool steel is directly influenced by the morphology of carbides. Therefore, it is important to control the morphology of carbides during annealing. Spheroidal morphology of carbide is preferred to maximize machinability and formability.

As mention in Section 4.4, the billets were annealed at 880°C [24]. The microstructures of the billets were examined after annealing. It has been found that the structure consists of a ferrite matrix and spheroidal cementite as shown in Figure 7.6 and Figure 7.7. In Figure 7.7, it was observed that the transformation from dendritic to spheroidal morphology hasn't been completed yet. Some dendrites still exist in the microstructure. On the other hand, there was no lamellar constituent present in this microstructure. As discussed in Section 7.1.1, after annealing process the hardness drops from 60HRC to 10HRC. The ferritic matrix formation due to annealing is the reason behind the reduction of the hardness. As understood from the

hardness, the annealing process has been carried out successfully to reduce the hardness and to increase the formability.

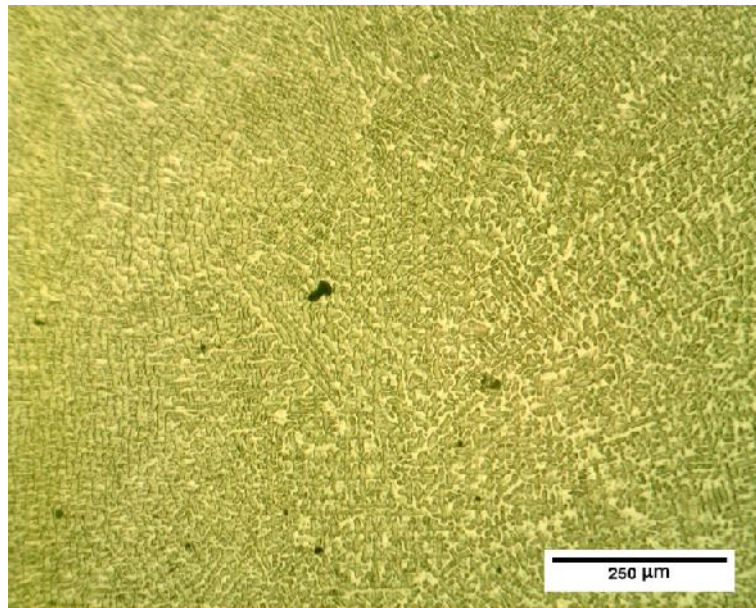


Figure 7.6 X48CrMoV8-1, Annealed, 10% Nital, x100

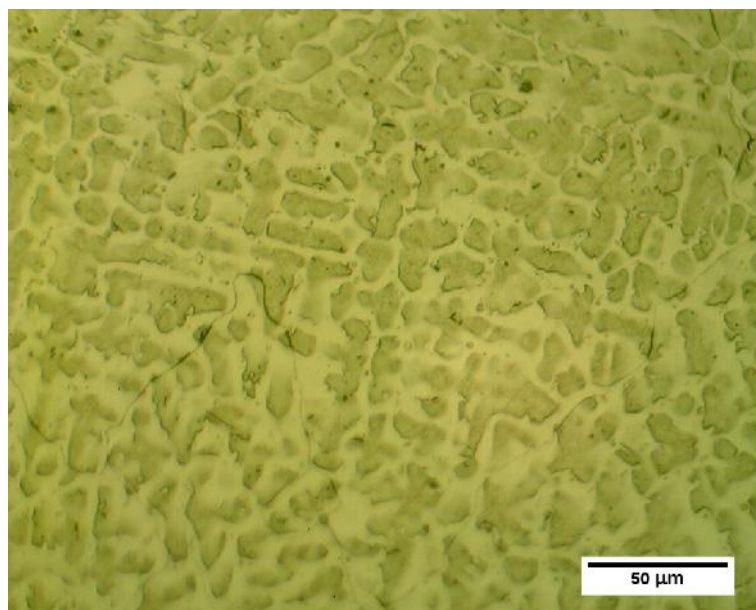


Figure 7.7 X48CrMoV8-1, Annealed, 10% Nital, x400

Another microstructure is shown in Figure 7.8. Although this tool steel does not have a similar composition, the microstructure is very similar after annealing. The formation of spheroidal cementite can be observed in most of the tool steels with correct annealing process.

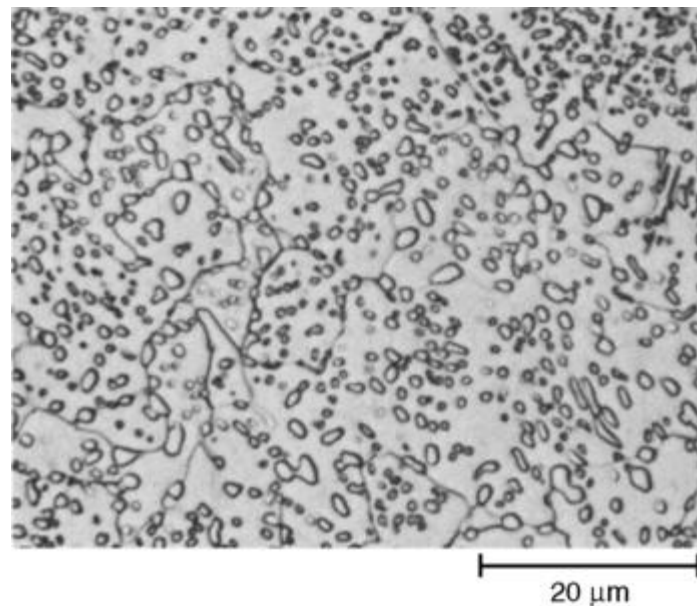


Figure 7.8 AISI W4 water-hardening tool steel, annealed, 4% picral. 1000× [34]

7.2.2. As Forged Microstructure

As mentioned in Chapter 6, the cold-work tool steel was subjected to hot forging around 1050°C. After forging process, the samples were investigated with optical microscope. The microstructure is shown in Figure 7.9 and Figure 7.10 . Unlike the microstructure of annealed samples given in Figure 7.6 and Figure 7.7, the spheroidal cementite was totally eliminated by forging process.

The composition of samples (i.e.) includes 7% chromium. Formation of carbide networks at the prior-austenite grain boundaries is observed in Figure 7.7. In literature [34], the formation of the carbide networks is explained with the 7% chromium in X48CrMoV8-1. These carbide networks occur during the plastic deformation. [34] This morphology reduces the toughness of the tool steel. Therefore, it is important to eliminate it during the further processes. As an example from the literature [34], a microstructure of rolled tool steel with carbide network formation is shown in Figure 7.11.

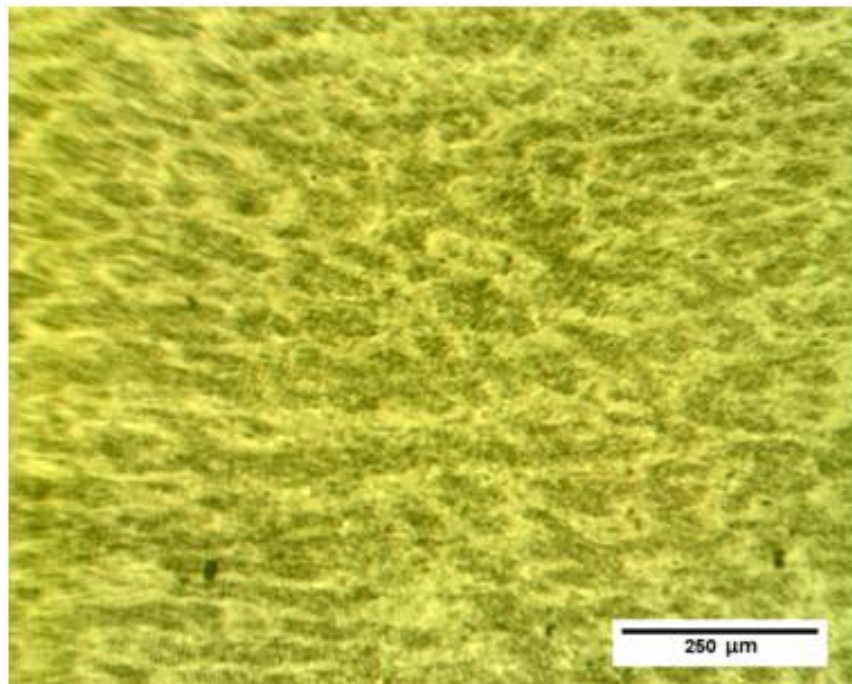


Figure 7.9 X48CrMoV8-1, Forged, 10% Nital, x100

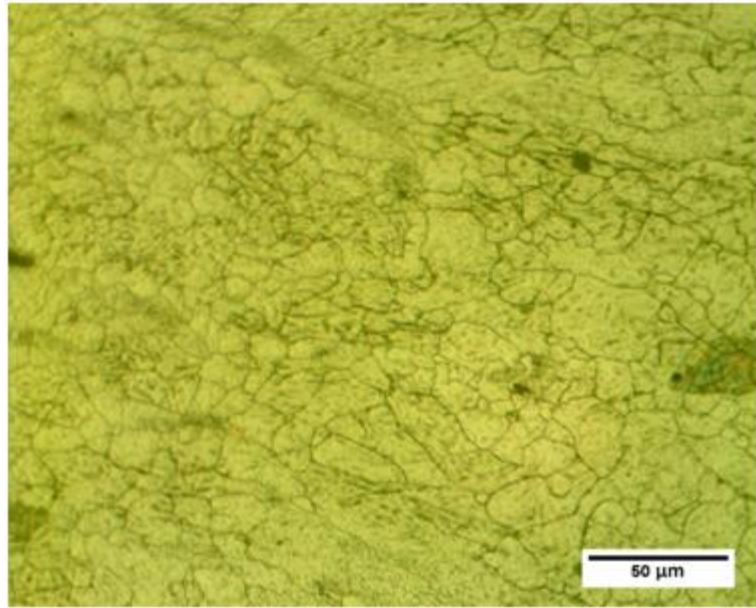


Figure 7.10 X48CrMoV8-1, Forged, 10% Nital, x200

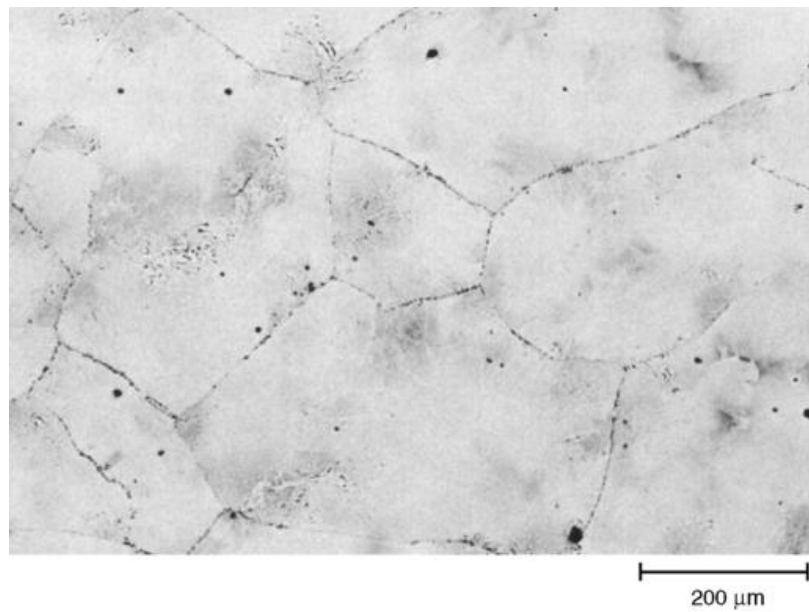


Figure 7.11 AISI L1, As-Rolled, Containing Pearlite and a Grain-Boundary Cementite Network. Boiling Alkaline Sodium Picrate. X100 [34]

7.2.3. As Quenched and Tempered Microstructure

Figure 7.12 and 7.13 shows the optical micrograph for X48CrMoV8-1 that was heat treated at 1050°C, oil quenched and double tempered at 300°C. The microstructure reveals tempered martensite and coarse carbides which do not dissolve during austenitizing. Hardening followed by tempering resulted in coarsening of the martensitic structure and increased dissolution of primary carbides as in Figure 7.12. The carbides are expected to be M_7C_3 (chromium carbides), M_2C (molybdenum carbides) and MC (vanadium carbides).

After forging, cementite network on the grain-boundary was observed as shown in 7.8 and 7.9. The cementite morphology is not observed after quenching and tempering. The change of the morphology of cementite has improved the toughness of the cold-work tool shear blade which is mentioned in Section 7.1.2.

The same heat treatment has been carried on a rolled commercially available shear blade sample as shown in Figure 7.14. Although the sizes of the carbides are smaller than the forged samples the morphologies are the same. The reason of the finer carbide formation is, the thinner wall thickness of the rolled specimen in this study. As mentioned before, the diameter of the forged billets are more than 30mms, but rolled specimen has a thickness of 5mms. Hence, during quenching rolled specimen cools more rapidly than the forged billets. As a consequence, finer carbides are observed in rolled specimen.

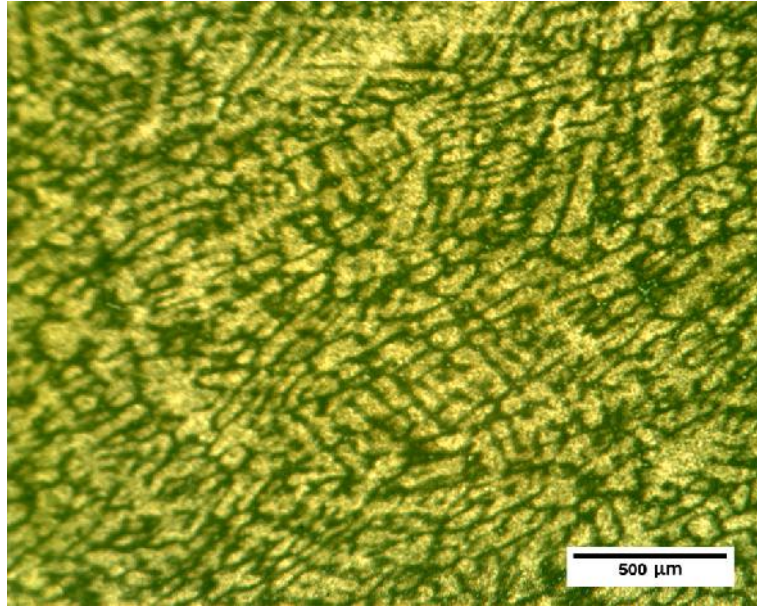


Figure 7.12 X48CrMoV8-1, Quenched and Tempered, 15% HCl and then 10% Nital, x50

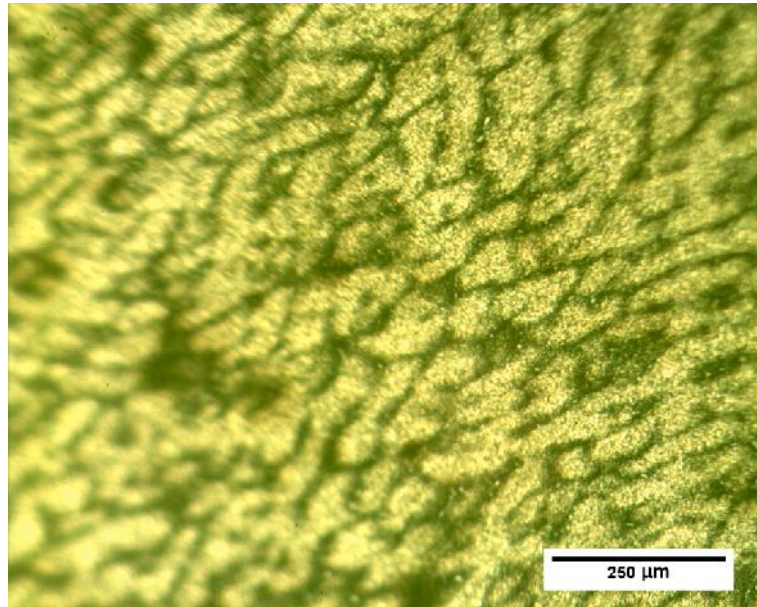


Figure 7.13 X48CrMoV8-1, Quenched and Tempered, 15% HCl and then 10% Nital, x100

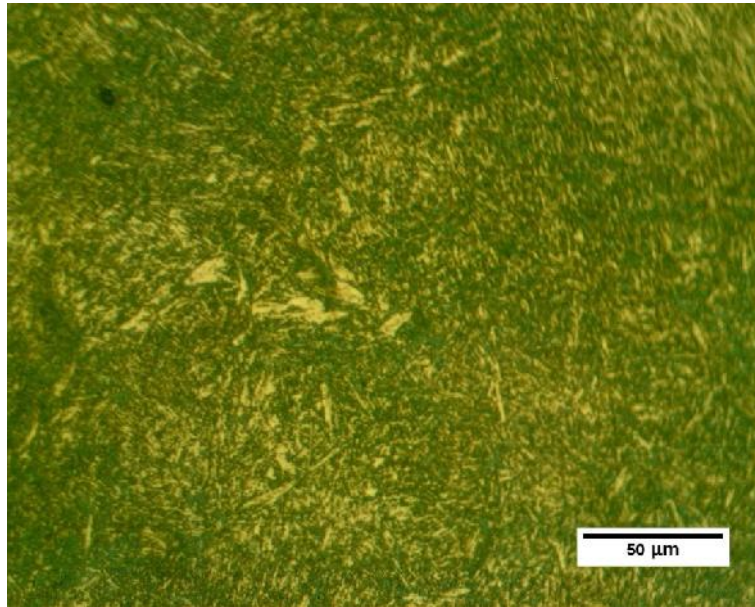


Figure 7.14 Uddeholm Viking Rolled Sample, As Quenched and Tempered, 15% HCl and then 10% Nital, x400

CHAPTER 8

CONCLUSIONS AND FUTURE WORK

8.1. General Conclusions

In this study, design and analysis for cold-work tool steel shear blade production for both casting and forging processes have been realized. Then, real life experiments have been conducted. Finally, the tests and analysis have been performed for both samples and a commercially available shear blade sample which is manufactured by rolling. The following conclusions have been reached;

- To minimize the amount of casting defects, finite volume analysis simulations have been conducted. Simulations results' have shown that, there were minor defect indications. However, during turning process, these defects would be machined. Therefore, the design has been left as it is. As a result, sound castings have been produced by the help of the finite volume analysis simulation.
- During the sand casting experiments, it has been observed that the alloying stage for X48CrMoV8-1 is challenging. Due to high alloy content of the steel, the desired composition is achieved by several alloying stages.
- By the experiment, it has been shown that, the simulation results were exactly the same as the experiment results. The positions of the defects have been predicted correctly and these defects are completely eliminated after machining.
- The simulation results have shown that, all forging operations were safe in terms of the capacity of the SMERAL mechanical press allocated in METU-BILTIR Center Forging Research and Application Laboratory.
- The microstructural analysis have shown that microstructure of the final samples are all tempered martensite likewise the commercially available shear blade sample which is manufactured by rolling.

- The quenching and tempering heat-treatments were conducted for a target hardness value, which was between 52-58 HRC. The measurements have shown that the hardness of all samples were in this hardness band.
- The mechanical properties are compared with tool steel with a brand name Uddeholm Viking which is a rolled product with the very similar composition. The hardness was measured as 58HRC as rolled and 56 HRC as forged. Besides, the toughness values were also compared. The rolled product's toughness is 5 Joules and forged product after 40% reduction is found as 4.3 Joules.
- The toughness tests have shown that, as the reduction ratio increases the toughness of the products also increases. This variation in the toughness can be explained by the reduction of the carbide size by means of plastic deformation. The fine carbide distribution increases both hardness and toughness at the same time.
- As mentioned in Chapter 2, the high alloy content of the tool steel, causes excessive carbide formation. As expected, the final heat treatment followed after forging operation has reduced the hardness of the samples. The reduction of the carbide size has increased the toughness of the shear blade samples.

8.2. Future Works

The possible future works can be suggested as follows;

- The same tests and analyses can be performed to observe the influence of diameter variation.
- Alternative cold-work tool steel compositions can be used to analyze and produce the shear blades
- Cold forging can be performed to see the effect on the microstructure.

- The desired final geometry of the shear blade can be obtained by means of forging.
- The types and the morphology of the carbides can be investigated by means of Scanning Electron Microscopy.

REFERENCES

- 1) DeGarmo, P., Black, J.T., Kohser, Materials and Processes in Manufacturing, 10th Edition
- 2) Copkogroup [On-Line], Available at, <http://www.copkogroup.com/Steel-Shearing-Machine.html>, last accessed; August 2012
- 3) Cnblade [On-Line], Available at, <http://www.cnblade.com/product/type/>, last accessed; August 2012
- 4) Sully L.J.D., Die Casting, ASM Handbook, Vol. 15: Casting, ASM International, Cleveland, 1998
- 5) George Adam Roberts, George Krauss, Richard L. Kennedy, Tool steels p.1
- 6) M. Forejt, M. Jopek, J. Krejci, Effect of Deformation Changes on Microstructure of Forming Steels, Istanbul, 2001
- 7) B. Johansson, R. Jervis, L.A. Norström, “Toughness of Tool Steel”, Proceedings of the International Seminar on Tool Steels for Moulds and Dies, 2000
- 8) S. Karagöz, A. Yılmaz, ‘Cast High Speed Tool Steels with Niobium Additions’, 66. World Foundry Congress, Istanbul, (Sepr. 2004) 1103-1
- 9) N.T. Switznera, C.J. Van Tyneb, M.C. Matayab, “Effect of forging strain rate and deformation temperature on the mechanical properties of warm-worked 304L stainless steel”, 2000
- 10) S. Karagoz, H.I. Unal, F. Kahrıman, F. G. Demircan, Segregation in Steels and Their Influence 2009
- 11) G. Bicer, “Experimental and Numerical Analysis of Compression on a Forging Press”, 2009
- 12) Flemings M.C., *Solidification Process*.1974, McGraw-Hill.
- 13) Chvorinov N., *Giesserei*, 1940. 27: p. 201-208
- 14) Trbizan K., *Casting Simulation*. World Foundry Organization, 2001. paper 4: p. 83-97.

- 15) Gori F., Corasaniti S., *Theoretical Prediction of Soil Thermal Conductivity at Moderately High Temperatures*. Journal of Heat Transfer, 2002. 124: p. 1001-1008.
- 16) Reed-Hill R.E., Abbaschian R., *Physical Metallurgy Principles*.1994, Boston: 3rd ed., PWS Publishing.
- 17) Semiatin, S.M., “Forming and Forging Volume 14-9th Edition Metals Handbook”, ASM International, 1988, pp. 10-58.
- 18) Thomas S. Piwonka, University of Alabama, Classification of Processes and Flow Chart of Foundry Operations, ASM Handbook, Vol. 15: Casting, ASM International, Cleveland, 1998, p.441 – 737
- 19) Altan, T., Boulger, F. W., Becker, J. R., Akgerman, N., Henning, H. J., Forging Equipment, Materials and Practices, Batelle Columbus Laboratories Metalworking Division, Ohio, 1973.
- 20) L. Stonecypher, “Drop Forging - How a Forging Hammer Works”, (2010)
- 21) Special Steels and Metals Limited [On-Line], Available at, <http://www.ssm.co.nz/products/cold-work-tool-steel.cfm> ;last accessed; August 2012
- 22) MagmaSoft 5.3
- 23) Simufact Forming 10.0
- 24) Uddeholm Viking, Edition 3, Jan. 2010
- 25) T. Altan, F. W. Boulger, J. R. Becker, N. Akgerman, H. J. Henning, “Forging Equipment, Materials and Practices”, Air Force Materials Laboratory, October 1973.
- 26) M. Halisçelik, “Elastic-plastic finite element analysis of semi-hot forging dies”, 2010
- 27) L. Stonecypher , “Mechanical Forging Press Machine – How It Works”, (2010)

- 28) C.J. Van Tyne, J. Walters, Understanding Geometrical Forging Defects, 2007
- 29) Campbell J., *Castings*.2003, Oxford: 2nd ed., Butterworth-Heinemann.
- 30) Instruction Manual of Smeral Brno® LZK 1000
- 31) H. Ozturk, “Analysis and Design for Aluminum Forging Process”, Dec. 2008
- 32) Charles E. Bates, Quenching of Steel, ASM Handbook, Vol. 4: Heat Treating, ASM International, Cleveland, 1991
- 33) John D. Verhoeven, Metallurgy of Steel for Bladesmiths & Others who Heat Treat and Forge Steel, March 2005
- 34) George F. Vander Voort, Metallographic Techniques for Tool Steels, ASM Handbook, Vol 9, ASM International, Cleveland, 2004
- 35) Christian Højerslev, Tool Steels, Jan 2001
- 36) T. Altan, F. W. Boulger, J. R. Becker, N. Akgerman, H. J. Henning, “Forging Equipment, Materials and Practices”, Air Force Materials Laboratory, October 1973.

APPENDIX A

TECHNICAL INFORMATION OF 10 MN (1000 TON) SMERAL MECHANICAL PRESS

The press used in the experimental study is shown in Figure A.1.



Figure A.1 Smeral 10 MN Mechanical Press in METU-BILTIR Center Forging Research and Application Laboratory

The technical information of the press is given as follows:

Nominal Forming Force: 10 MN

Ram Stroke : 220 mm

Shut Height : 620 mm

Ram Resetting : 10 mm

Rod Length: 750 mm

Crank Radius: 110 mm

Number of Strokes at Continuous Run: 100 min⁻¹

Press Height: 4840 mm

Press Height above Floor: 4600 mm

Press Width: 2540 mm

Press Depth: 3240 mm

Press Weight: 48000 kg

Die Holder Weight: 3000 kg

Main Motor Input: 55 kW

Max. Stroke of the Upper Ejector : 40mm

Max. Stroke of the Lower Ejector: 50 mm

Max. Force of the Upper Ejector: 60 kN

Max. Force of the Lower Ejector: 150 kN

APPENDIX B

TECHNICAL DRAWING OF THE PATTERN

The technical drawing of the pattern is shown in Figure B1;

APPENDIX C

TECHNICAL DRAWINGS OF THE DIE SET

The technical drawings of the Upper Die, Lower Die and the Inserts are given in Figures C1-C6; [11]

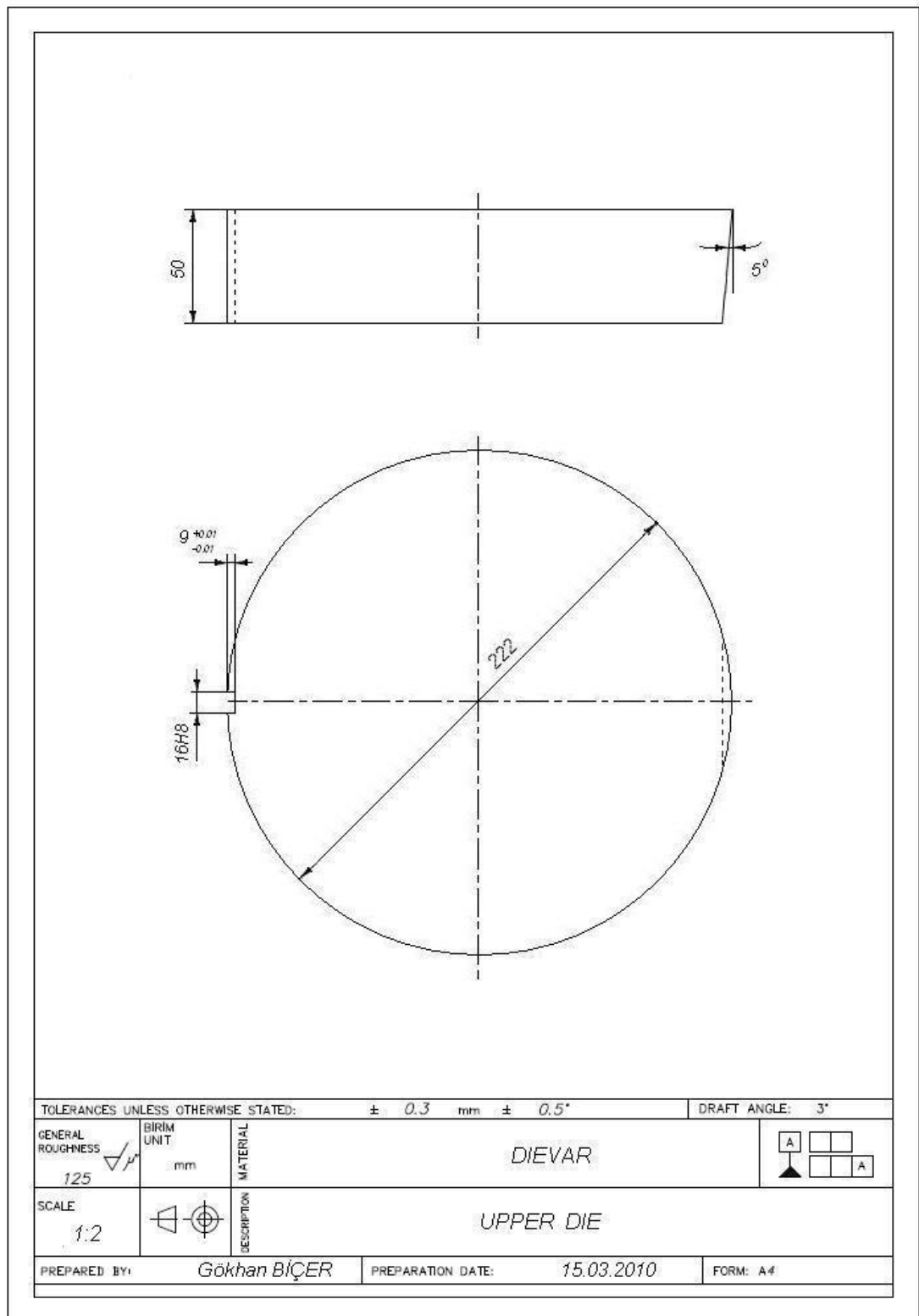


Figure C.1 Technical Drawing of the Upper Die

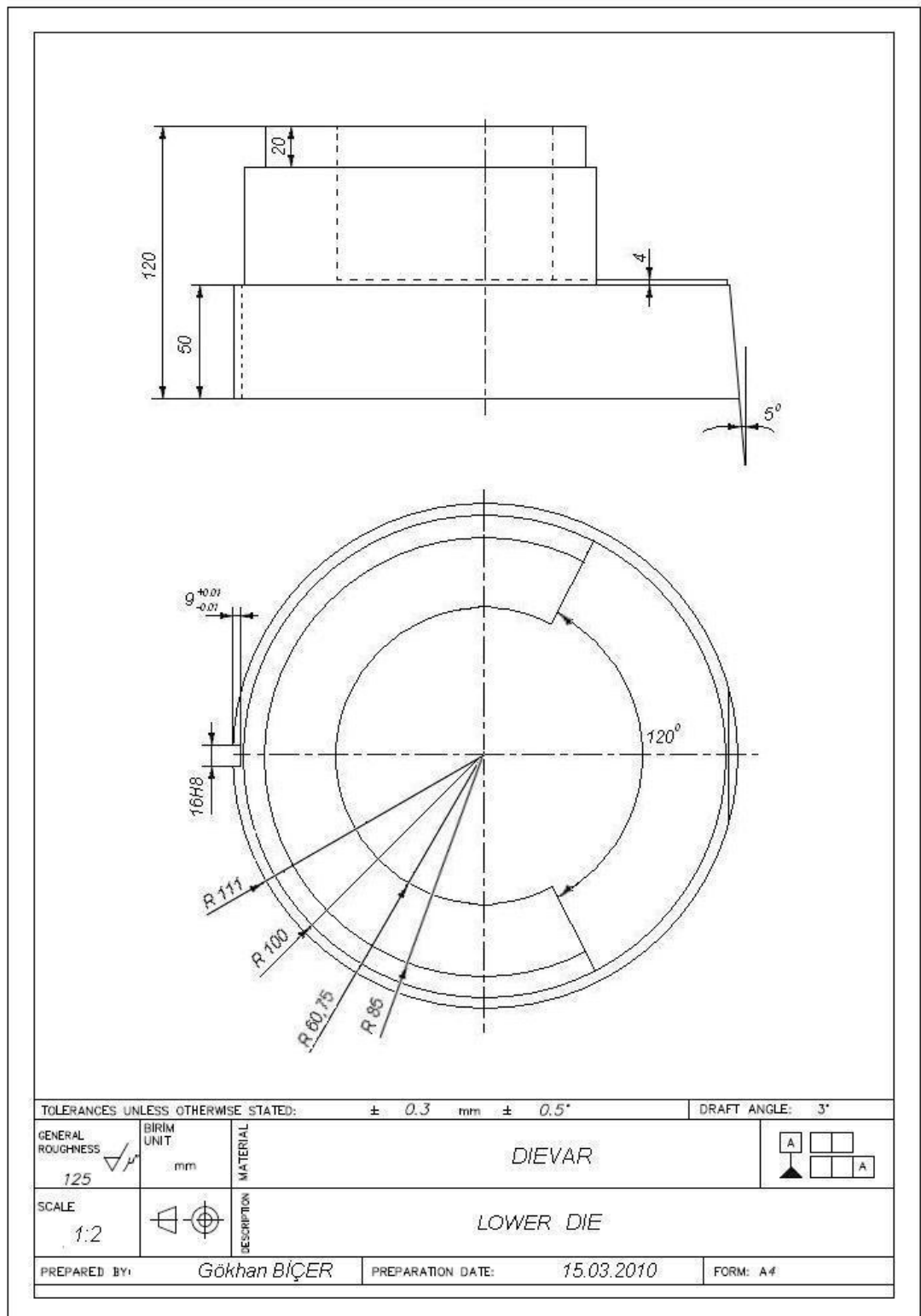


Figure C.2 Technical Drawing of the Lower Die

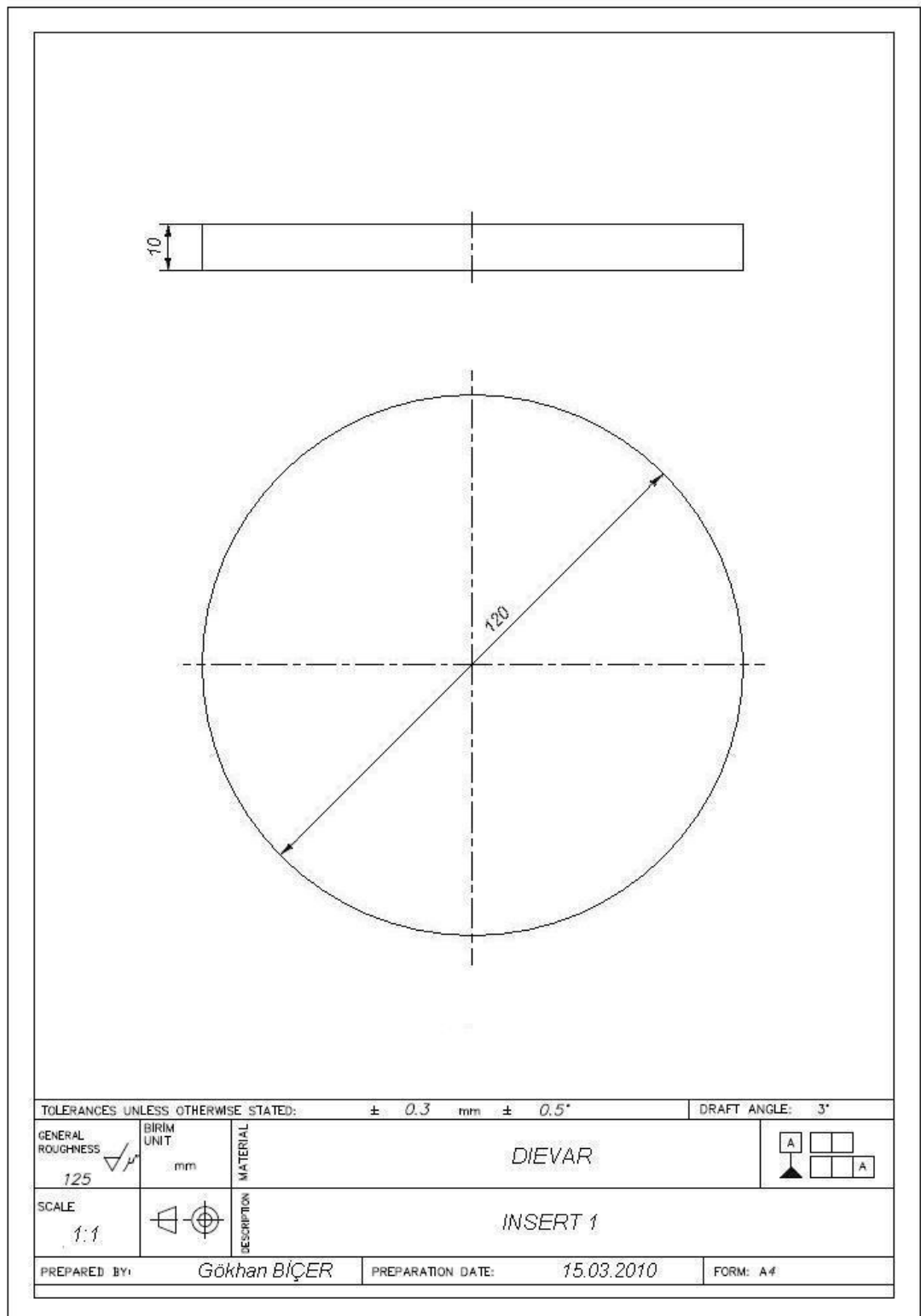


Figure C.3 Technical Drawing of the Insert with 10 mm Height

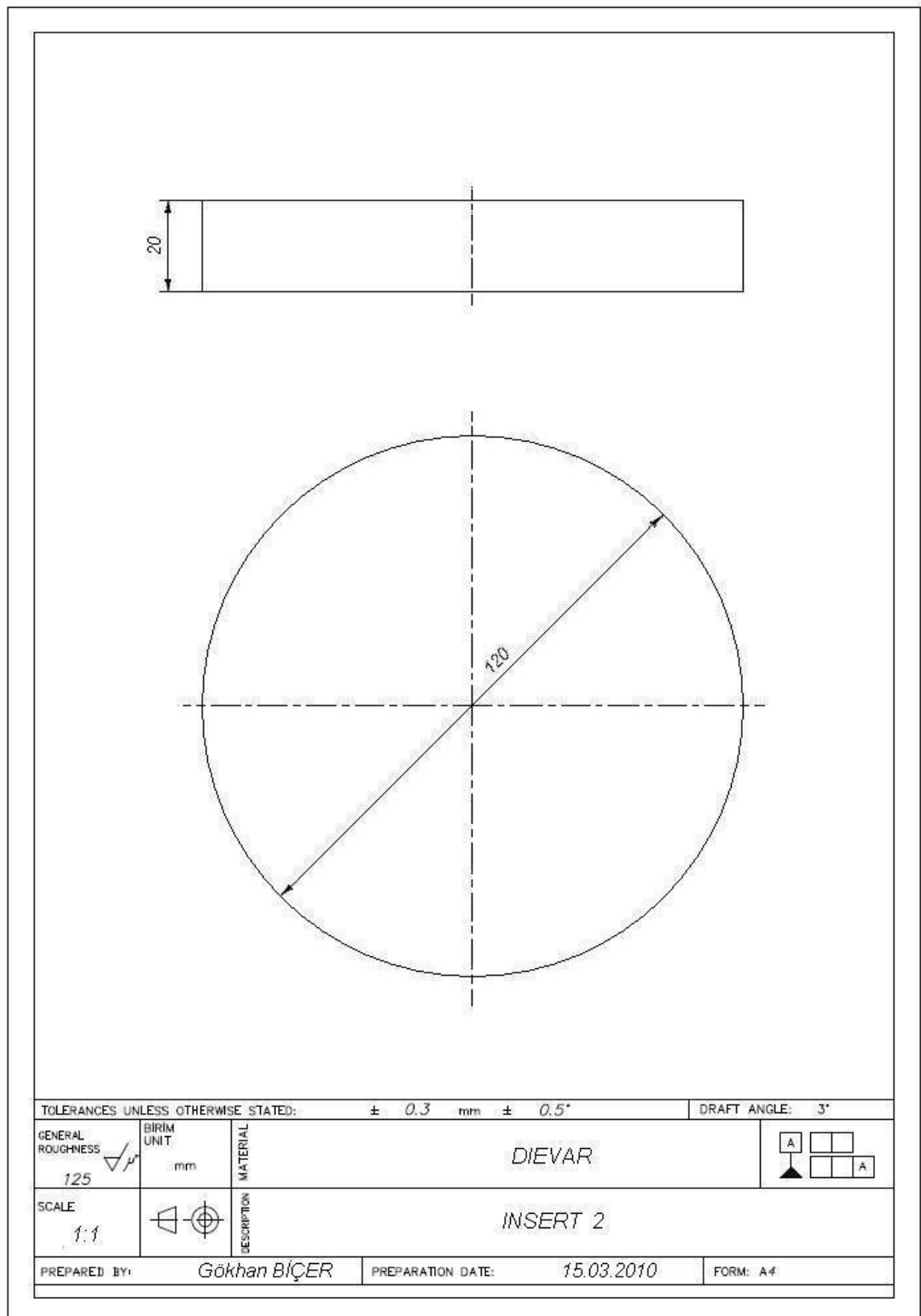


Figure C.4 Technical Drawing of the Insert with 20 mm Height

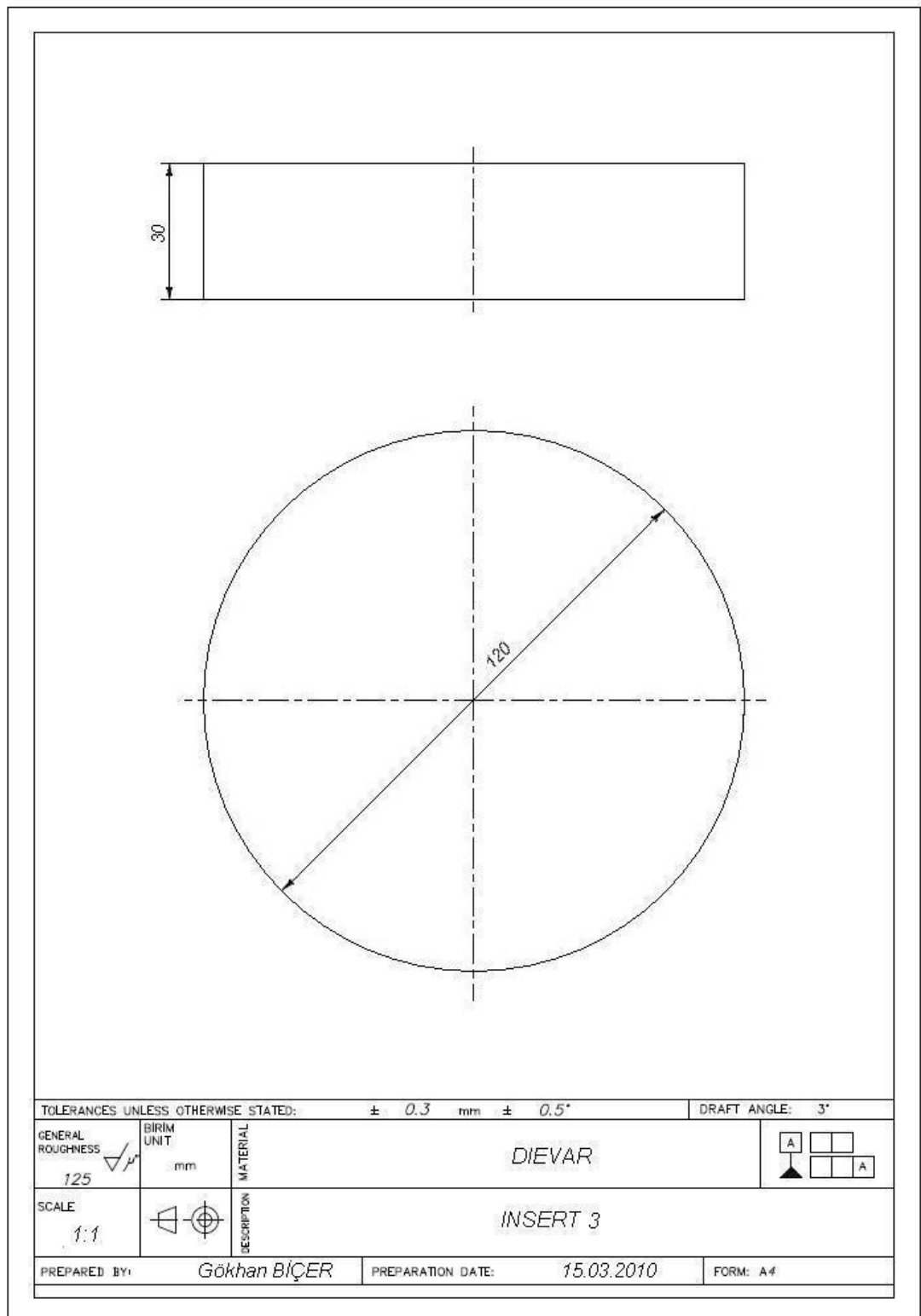


Figure C.5 Technical Drawing of the Insert with 30 mm Height

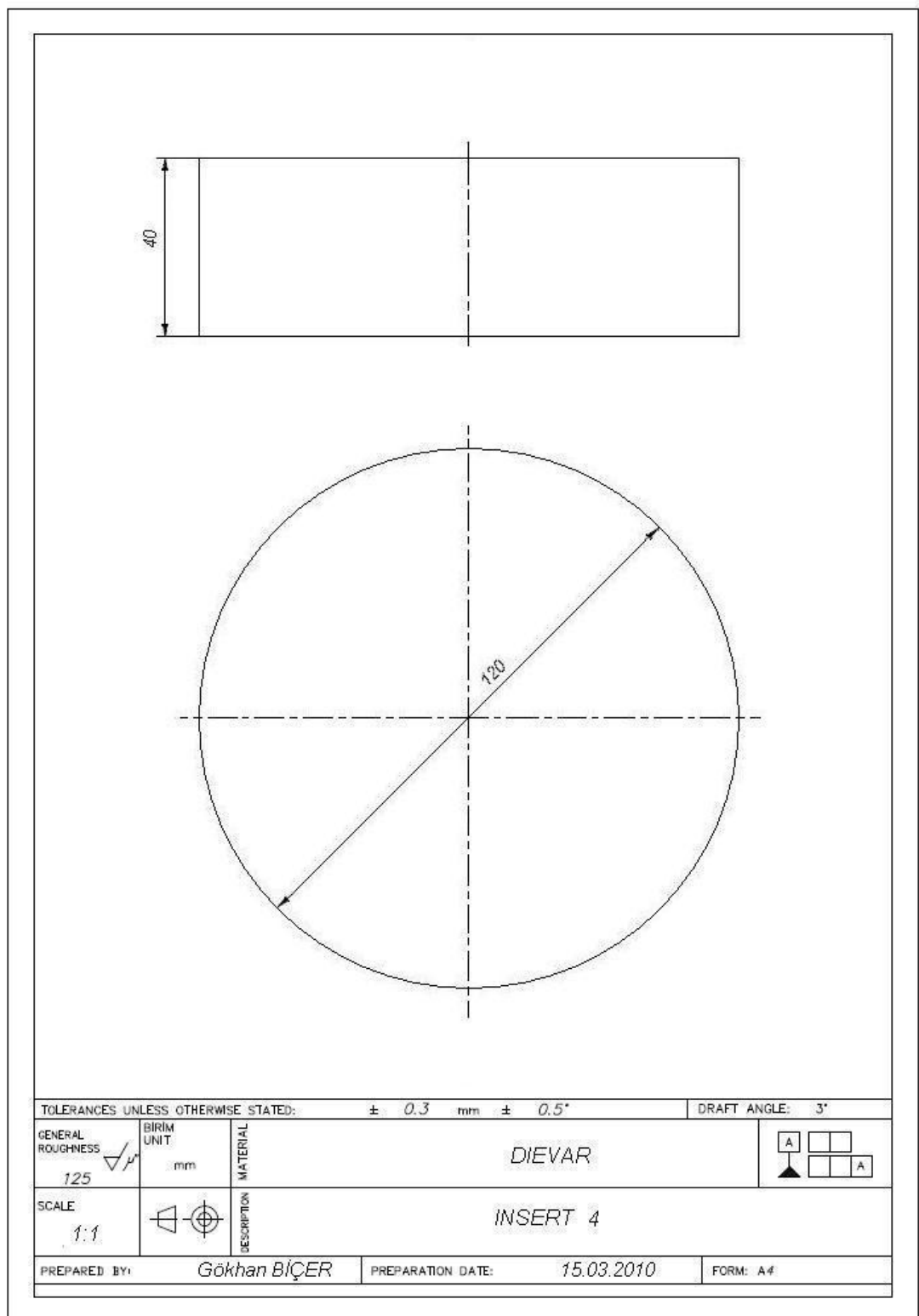


Figure C.6 Technical Drawing of the Insert with 40 mm Height